The Development and Evaluation of a Method for the Quantitative Determination of a Monoclonal Antibody using Capillary Electrophoresis-High Resolution Mass Spectrometry

Thesis submitted to the University of Strathclyde in fulfilment of the for the degree of Master of Philosophy

By

Richard Snell

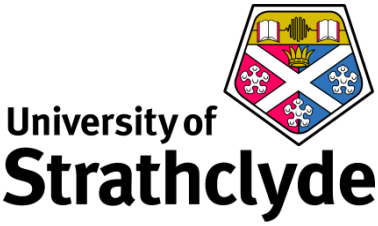

Department of Pure and Applied Chemistry
University of Strathclyde
Thomas Graham Building
295 Cathedral Street
Glasgow
G1 1XL
Jun 2020

Declaration of authenticity and authors rights

This Thesis is the results of the author's original research. It has been composed by the author and has not been previously submitted for examination which has led to the award of a degree.

Signed: Date:

Table of Contents

Abstract

Biotherapeutics are becoming of greater importance within the pharmaceutical industry, with companies expanding their portfolios into this area and an increasing number of biotherapeutic regulatory submissions and approvals. As a result of this move away from traditional small molecules progresses the methods used to support the data for the submissions have to evolve and new techniques explored to ensure the quality of data and meet the analytical challenges that this shift in strategy presents. LC-MS has been the main technique involved in the production of toxicokinetic (TK) and pharmacokinetic (PK) data for a number of years and has been reliable for quantification of small molecules. LC-MS using a 'bottom-up' approached based on enzyme digestion and surrogates' peptides along with plate-based techniques such as enzyme linked immunosorbent assay (ELISA) have been used for quantification of biotherapeutics however these techniques both have restrictions and limitations. This work looked to develop a method that could fill these gaps for the quantification of monoclonal antibodies (mAbs) using capillary electrophoresis-high resolution mass spectrometry (CE-HRMS).

The final method that was developed for quantification was based on reduction to the light and heavy chains and used a capillary electrophoresis (CE) separation with a discontinuous buffer system and two stage application of pressure to achieve a method that produces good peak shape; analyte response (in terms of peak intensity) and reasonable run times. The method used electrokinetic injection as a means of introducing the sample to the capillary. The data are greatly improved by the used of an internal standard to counteract the variation that is introduced as an artefact of the electrokinetic injection. The CE-MS method had a low limit of quantification for the mAb of 50 ng/mL in human plasma and achieved partial resolution of the mAb light and heavy chains in a run time of 15 minutes.

This work shows that CE-MS has the potential to be used to produce PK and TK data based on a ‘middle-up’ approach, that is more representative of the circulating levels of the intact unmodified mAb.

Abbreviations and Definitions

Term	Definition
ADA	Anti-drug antibody
ADC	antibody-drug conjugate
ADCC	antibody dependant cellular cytotoxicity
APCI	Atmospheric pressure chemical ionisation
aTTP	acquired thrombotic thrombocytopenic purpura
BGE	Background electrolyte
Bioanalytical/bioanalysis	Bioanalysis is the quantitative measurement of a drug and/or their metabolites in a biological matrix typically blood, plasma, serum, urine or tissue
BiTE	bispecific t-cell engager
Bottom up	Analysis of a protein (or similar) based on a signature or surrogate peptide, often after enzymatic digestion
BSA	Bovine serum albumin
BsAb	Bispecific antibody
C	Centigrade
C_{18}	Octadecyl carbon chain
Calibration curve	Comparison of a set of standard samples of known concentration against samples with unknown concentrations to determine their concentration
CDR	Complementary determining region
CE	Capillary electrophoresis
CESI 8000	Capillary electrophoresis instrument
CI	Chemical impact

CID	collision-induced dissociation
cpAb	chemically programmed antibody
CV	Coefficient of variance
CZE	capillary zone electrophoresis
dAb	domain antibody
DART	Dual-affinity retargeting bispecific antibody
DC	Direct current
Deconvoluted spectra	Reconstructed from the mass spectra to show the mass of a molecule as opposed to the *m/z*
DTT	Dithiothreitol
DVD-Ig	Dual variable domain- immunoglobulin
EI	Electron impact
ELISA	enzyme linked immunosorbent assay
EK	Electrokinetic
EOF	Electroosmotic flow
EOM	Electrophoretic mobility (μ_{ep})
ESI	Electrospray ionisation
EU	European Union
Fab	Fragment antigen binding
Fc	Fragment crystallisable region of an antibody
FcRn	Neonatal Fc receptor
Fd	Heavy chain portion of the Fab region
FDA	Food and Drug Administration
FT Orbitrap	Fourier transform Orbitrap

FT-ICR-MS	Fourier transform-ion cyclotron resonance-mass spectrometer
Hc	Heavy chain of an antibody
HcAb	heavy chain only antibody
HCl	Hydrochloric acid
HILIC	Hydrophilic interaction chromatography
HPLC	High performance liquid chromatography
HRMS	High resolution mass spectrometry
HVPS	High voltage power supply
IC	Immunocytokine
IdeZ	Immunoglobulin degrading enzyme
IgG	Immunoglobulin G
IL	Interleukin
ISV	Ion spray voltage
IT-TOF	ion trap time of flight
LBAs	Ligand binding assays
Lc	Light chain of an antibody
LC	Liquid chromatography
LLQ (s)	Lower limit of quantification; lowest concentration at which the analyte can be detected with predefined bias and precision
K’	Capacity factor
m/z	Mass to charge ratio
mAb	Monoclonal antibody
MALDI	Matrix-assisted laser desorption/ionisation
MEW	Mass extraction window

Middle down	Analysis of a protein (or similar) based on the protein fragment or sub-unit e.g. Fc, Fd, Lc or Hc
MRM	Multiple reaction monitoring
MS	Mass Spectrometry
MS/MS	Tandem mass spectrometry
N	Theoretical plates
N_2	Nitrogen
NCE	New chemical entity
OptiMS Cartridge	Combined separation capillary and MS interface for use with the CESI 8000
PEI	Polyethyleneimine
PFP	Pentafluorophenyl
PK	Pharmacokinetics - study of the time course of drug absorption, distribution, metabolism, and excretion – described through mathematical models
PTM	Post-translational modification
Q1	Quadrupole 1
Q2	Quadrupole 2
Q3	Quadrupole 3
Q-TOF	quadrupole time of flight
Q-trap	quadrupole ion trap
Rf	Radio frequency
TandAb	Tetravalent bispecific tandem diabody
THRMS	tandem high-resolution mass spectrometry
TK	Toxicokinetics - the study of PK at high doses using toxicology studies where absorption and clearance mechanisms

	may be saturated
TOF	Time of flight
Top down	Analysis of a protein (or similar) based on the intact molecule
TripleTOF 6600™	Sciex Q-TOF mass spectrometer
US	United States
VH	Variable region of heavy chain
VHH	Variable region of a heavy chain only antibody
VL	Variable region of light chain

1 Introduction

1.1 A Shift in Paradigm Within the Pharmaceutical Industry

In recent years there has been a steady increase in the rise of the class of therapies known as biologics or biotherapeutics. In 2018 the Food and Drug Administration (FDA) approved a total of 59 new drugs, 42 of which were new chemical entities (NCEs) and 17 were biotherapeutics; this was a new record for biotherapeutic drug approval. There has been a steady rise in the approval of biotherapeutic drugs; in 1996 out of a total of 53 approved drugs, only 6 were biotherapeutics, in 2015 and 2017, this increased to 12 and in 2018, 17 biotherapeutics were approved, as shown in Table 1. Of the 17 biotherapeutics approved in 2018, 12 were monoclonal antibodies (mAbs), 3 were pegylated enzymes, one was protein-based and one was a fusion protein [1].

Until the first mAb, Orthoclone OKT3, was approved for use in 1986, followed by daclizumab in 1997, the drug development process was completely focussed on taking a NCE to market, from hit to lead screening through to pre-clinical development [2]. The development of new biotherapeutic drugs also represented a shift in the approach taken to the drug receptor interaction. Biotherapeutics are raised against a given antigen and the mechanism is usually known in advance, whereas previously with NCE development the mechanism was unknown and had to be determined as part of a high throughput screening programme. Biotherapeutics offer other advantages such as favourable attrition rates, limited toxicological issues, highly specific to the target, and the ability to augment the body's own immune system [3].

The production of biotherapeutics on an industrial scale was more complex than for NCEs. As a consequence, production costs were higher which meant discovery and development of small molecules remained the dominant focus of the pharmaceutical industry. The rise

in the interest of biotherapeutics in the mid-1990s was driven by different, emerging companies to those pursuing traditional NCEs, however today the two streams of drug target are far more aligned. The molecular complexity of the generics market for biotherapeutics is far more challenging relative to NCEs. The exact molecular structure of an NCE can be copied exactly whereas for biotherapeutics the term 'biosimilars' has emerged which reflects the fact that certain attributes (such as glycosylation patterns) cannot be replicated in different manufacturing processes. This means biosimilars must undergo a certain amount of additional characterisation work to determine if these deviations from the original biological construct have an impact on the efficacy, pharmacokinetics (PK) or safety of the therapeutic original drug [2, 4, 5].

Table 1 Number of NCE and biologic drug approvals by the FDA in the last 19 years [1].

Year	Number of NCE approvals	Number of biotherapeutics approved
1999	35	3
2000	27	2
2001	24	5
2002	17	7
2003	21	6
2004	31	5
2005	18	2
2006	18	4
2007	16	2
2008	21	3
2009	19	6
2010	15	6
2011	24	6
2012	33	6
2013	25	2
2014	30	11
2015	33	12
2016	15	7
2017	34	12
2018	42	17

1.2 Classes of Biotherapeutics

Biotherapeutics, or biologics, are treatments derived from or involve living cells. Biotherapeutics can be produced from a variety of cell types such as mammalian, viruses or bacteria. In broad terms biotherapeutics operate in two ways; either acting on a specific target (in plasma or cells) or by manipulating the immune system to act [6, 7]. As shown in section 1.1 the number of biotherapies coming to the market is increasing and with pharmaceutical companies diversifying their portfolios the number is expected to increase [8], especially in key areas such as oncology and autoimmune diseases (e.g. Crohn's Disease and Ulcerative Colitis [7, 9]) but also in other areas, with drugs like Erenumab, Fremanexumab and Galcanezumab, all being approved in the last year for migraine prevention [1]. The diversity in biotherapeutics is also increasing with different types of molecules being developed. These include mAbs (Figure 1), immunoconjugates, immunoglobulin (Ig)-like scaffolds and peptides, many of which have further sub categories [10], these categories of biotherapeutics will be described in the following sections.

1.2.1 Monoclonal antibodies

The most common type of biotherapeutics currently approved are mAbs, based on an Immunoglobulin G (IgG). mAbs often provide a rapid route to proof of concept for new targets, and this coupled with generally good tolerability meaning the risk of unexpected safety issues is generally low, means that mAbs offer shorter development times [11]. The first drugs developed were based on murine mAbs, but mAbs have progressed through humanised, and now onto fully human mAbs [12]. The main drive behind this progression was that application of the early murine mAbs were limited due to immunogenicity (the ability of a substance to cause an immune response) observed in the clinic. In such cases

the production of anti-drug antibodies (ADAs) to the 'foreign' mAbs caused reduced efficacy or adverse events [13].

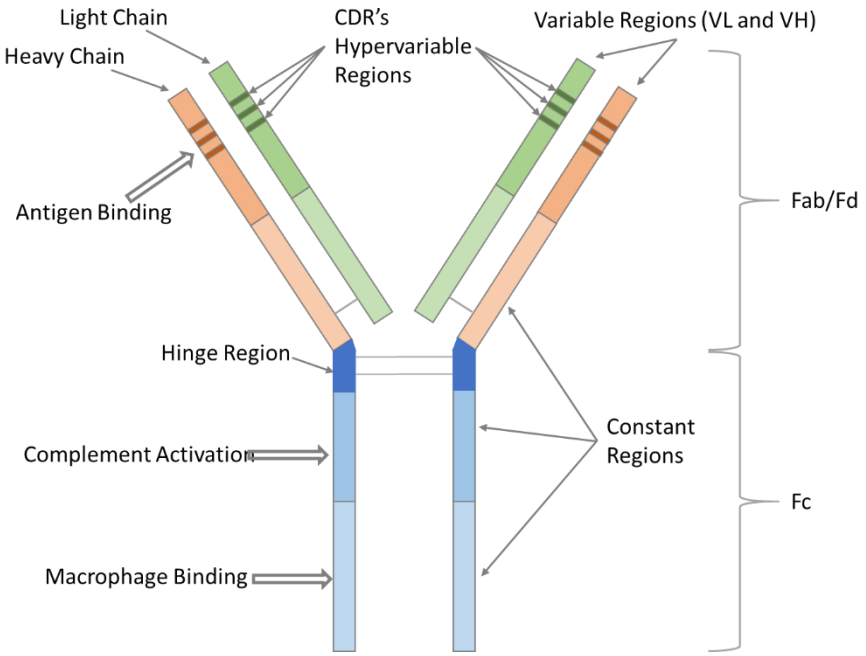

Figure 1 Representative structure of a mAb showing the constituent regions that make up the structure, with the complementary determining regions (CDRs), variable regions of the light and heavy chains (VL and VH, respectively) constant regions, hinge region, light and heavy chains and where antigen and macrophage binding occurs, also where these are located on the fragment antigen binding (Fab), including the heavy chain portion of the Fab (Fd) and fragment crystallisable (Fc).

The development of chimeric mAbs went some way to negate this observed immunogenicity. With chimeric mAbs the variable domains remain murine (to maintain binding activity) and are fused with human constant regions resulting in a mAb that is approximately 70% human. Chimeric mAbs provided a stepping stone to fully humanised mAbs, in which the constant domain is human while retaining portions of the murine variable regions resulting 85 to 90% human (Figure 2) [14, 15]. Humanised mAbs are even more successful than chimeric in reducing adverse events.

mAbs can be designed to function in one of two ways; either to produce a cell mediated immune response, otherwise known as antibody dependant cellular cytotoxicity (ADCC)

(Figure 3), or to block a protein binding to its receptor. Both mechanisms are achieved by designing the mAb to bind to a specific target which can be soluble or membrane bound [3].

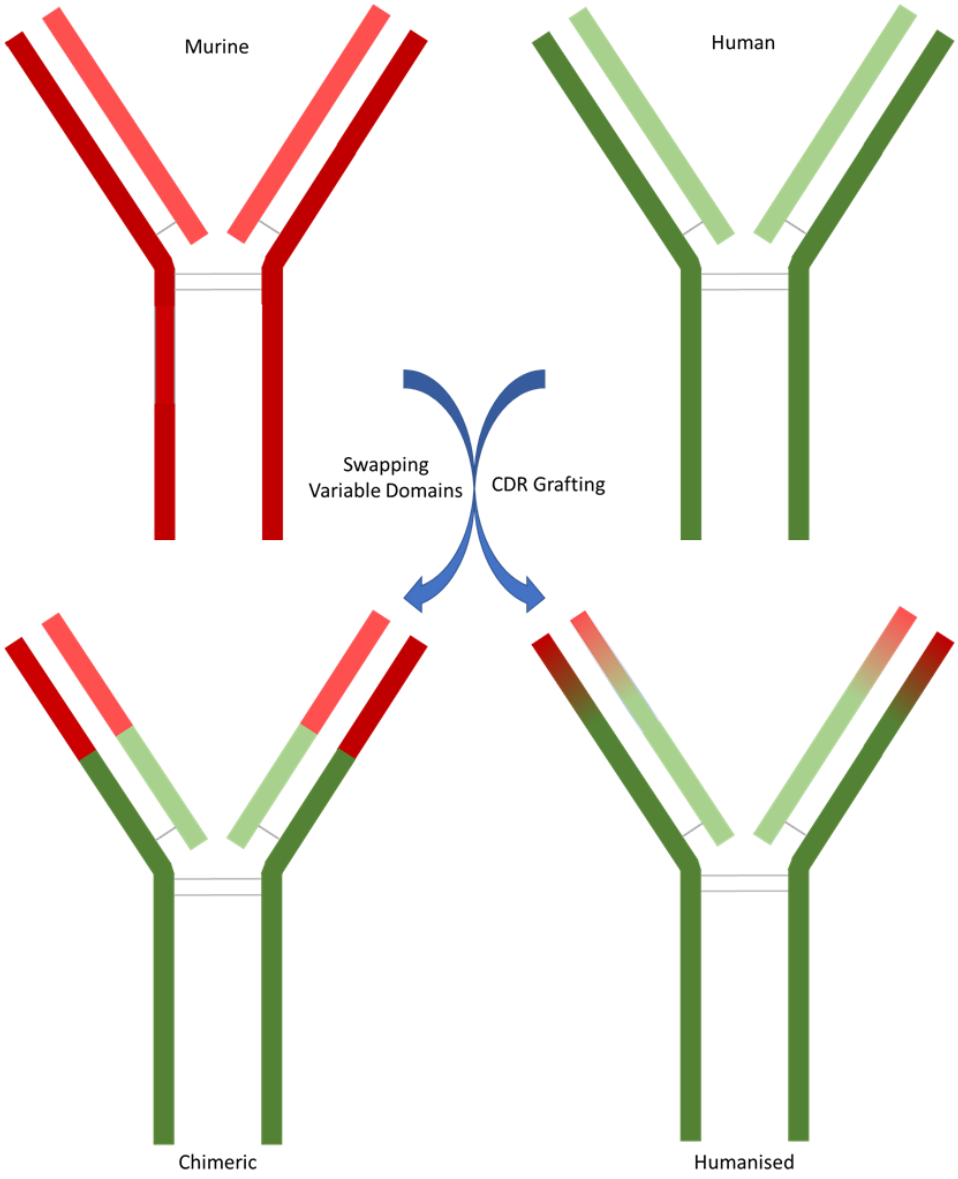

Figure 2 Depiction of the evolution of mAbs. combining fully murine and human mAbs, through the swapping of variable regions and grafting of the complementary determining regions (CDRs) to produce chimeric and humised mAbs, respectively. Murine sequences in red, human in green with light colours signalling light chains and dark colours signalling heavy chains.

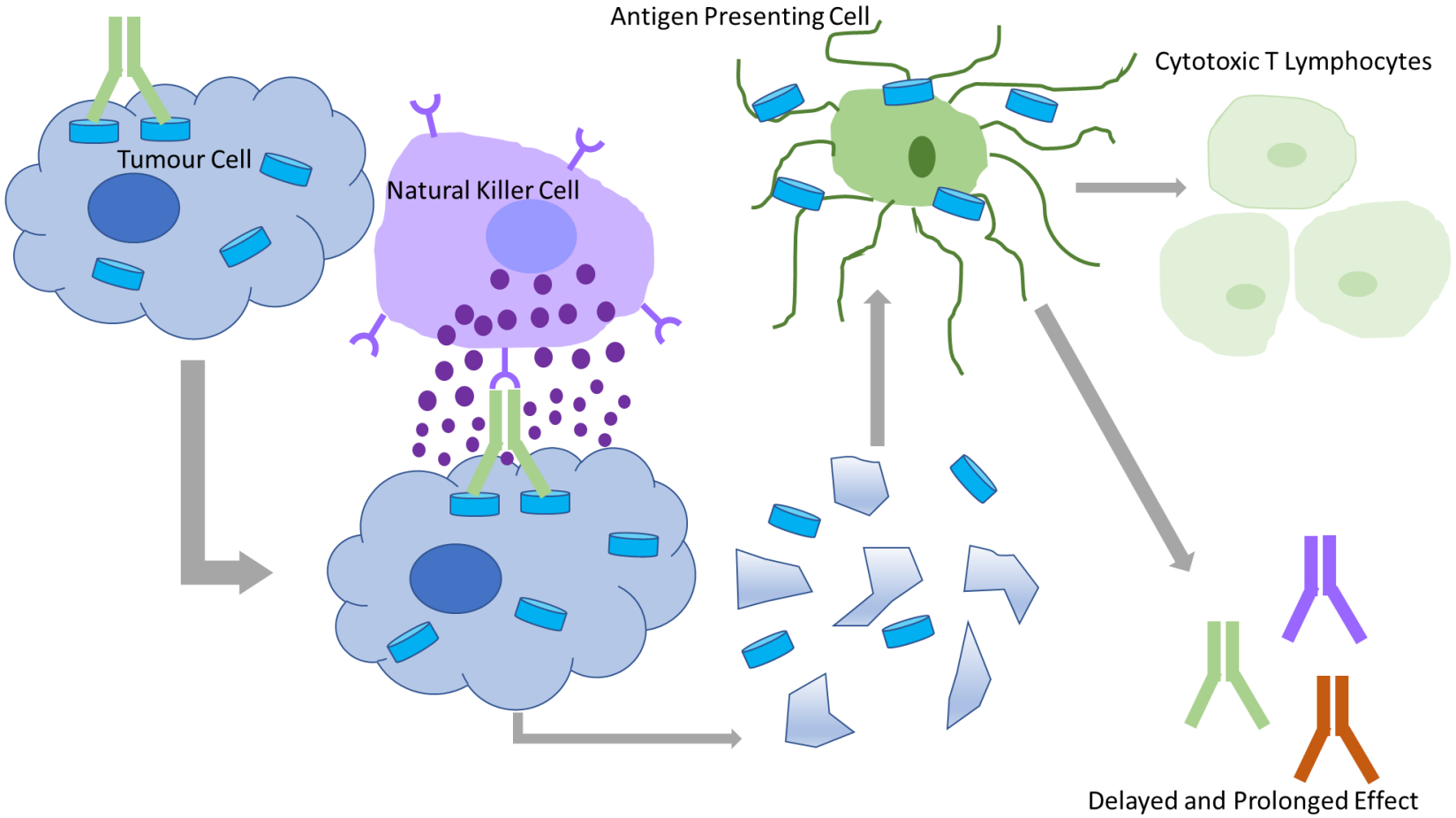

Figure 3 Example of a mechanism of antibody dependent cellular cytotoxicity (ADCC) on a tumour cell, mAb binding to an antigen on the tumour cell acting as a target for natural killer cells leading to lysis of the tumour cell, the debris is then 'mopped up' by antigen presenting cells which in turn leads to the release of antibodies with specific epitopes for target antigens and cytotoxic T lymphocytes that are capable of recognising and killing cells that express the target antigen [14].

1.2.2 Immunoconjugates

A second group of biotherapeutics are immunoconjugates these molecules are antibodies that carry an attachment such as an NCE, toxin, enzyme or radionucleotide, where the antibody is essentially a vehicle for delivering one of these cytotoxic payloads [10]. Biotherapies that combine an NCE are known as antibody-drug conjugates (ADCs) and one example of such a drug is brentuximab vedotin. The antibody and active drug are connected by a chemical linker where the conjugate can be viewed as the deactivated form needed to transfer the small molecule drug to the target cell. Once at the target site the 'payload' can be released (via cleavage of the chemical linker) causing rapid cell death [16], the net result of this type of delivery is the reduction of off-target toxicity [17]. In 2000, the first ADC to gain approval was Gentuzumab ozogamicin which was approved for the treatment of acute myeloid leukaemia. Gentuzumab ozogamicin is a construct of calicheamicin, a cytotoxic antibiotic linked to a humanised anti-CD33 mAb [18]. Currently there are four ADCs approved all for treatment of hematologic malignancies, as opposed to solid tumours which are more inaccessible to ADCs. The ADC approach is gaining in popularity with over 60 currently in clinical trials, making this class being one the most proactive research areas in the oncology arena [17].

A sub group of immunoconjugates are immunocytokines (ICs). Cytokines, alone work by boosting the body's immune response to tumours and as such have been long pursued as an oncology therapy. However the development of cytokine-based therapies have been limited by their high levels of toxicity [19]. Attempts to alleviate off-target effects has involved targeted delivery of cytokines to the site of action such as, by fusing with a mAb or antibody fragment as with ADCs, which have come to be known as ICs [20]. Two types of ICs have been produced based on IgG mAb-based or antibody fragments. The two groups have one main difference, the circulatory half-life, with the full mAb having longer persistence

e.g. IgG-Interleukin-2 (IL-2) fusion protein, (hu14) has a half-life of 4 to 5 h, compared to the diabody (L19) at 2 to 3 h [21], this largely due to reduced renal clearance and neonatal Fc receptor for IgG (FcRn) mediated recycling [22]. However, IgG-based immunocytokines also have reduced efficacy because of their overall size, impacting on vascular evasion and tissue penetration [23]. Therefore, whether to use a full mAb (prolonged exposure) or a fragment (better tissue penetration) comes down to the therapeutic need and location of the target.

A third category of immunoconjugate are radioimmunoconjugates. Similar to ADCs and ICs, these constructs carry radioactive particles as their payload, but unlike the other types radioimmunoconjugates are currently in development for solid tumours [10]. Radioimmunoconjugates have additional advantages over other immune conjugates, in that they can also be used for molecular imaging. As with ICs, radioimmunoconjugates come in a different forms, whole mAbs or a variety of fragments can be used [24]. Chelators e.g. DOTA (1,4,7,10-tetraazacyclododecane-1,4,7,10-tetraacetic acid) act as links between the antibody and the radionuclide, allowing the effect attachment of the payload.

1.2.3 Ig scaffolds

Another group of biotherapies based around IgG fragments are known as Ig scaffolds; these include nanobodies, domain antibodies (dAbs), bispecific scaffolds and chemically programmed antibodies (cpAb) [10]. Naturally occurring antibodies have been discovered in camelids where the light chain (Lc) is absent. This discovery of heavy chain only antibodies (HcAbs) has in turn led to the development of single domain antibodies, also known as VHH or nanobodies (Figure 4) [25, 26]. In 2018 the nanobody caplacizumab (Cablivi™) was approved for the treatment of acquired thrombotic thrombocytopenic purpura (aTTP) in the European Union (EU) [27]. Nanobodies offer advantages over

conventional IgG based antibodies, they have good solubility, good temperature and pH stability as well as an appropriate size that allows them to penetrate tissue with greater ease [25]. A less desirable consequence of their reduced size is that it can lead to a shorter PK half-life [28] compared to full IgGs that are protected from degradation by FcRn; FcRN binds to the Fc region of an IgG in acidic conditions in endosomes. The FcRn is then released at physiological pH and returned to the circulation, allowing the IgG to access its binding site. This has been demonstrated in FcRN deficient mice, which sees the half-life of IgG reduced from 6 - 8 d to 1 d [29]. The renal clearance of a full IgG is also negligible, but lower molecular weight fragments have increased renal clearance [30].

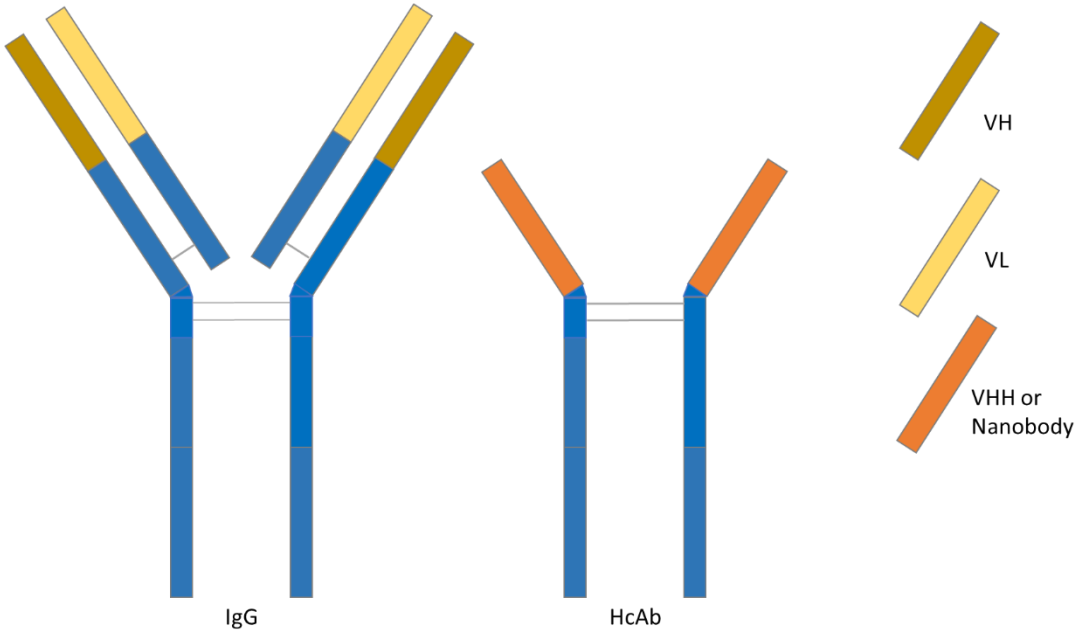

Figure 4 Schematic of the differences between Immunoglobulin G (IgG), camelid or heavy chain only antibodies (HcAb) and resulting variable regions; variable region of the heavy chain (VH), variable region of the light chain (VL) and variable region of a HcAb (VHH), leading to nanobodies that can be used for therapeutic purposes.

The variable domains from human antibodies engineered as a biotherapeutic are called dAbs, these can be derived from either the variable region of the Lc or heavy chain (Hc). dAbs share many of the same attributes as nanobodies, given that they are of similar sizes 11 to 15 kDa [10, 31].

A further class of biotherapeutics that are based around an Ig scaffold are known as bispecific antibodies (BsAb), the premise of these is that they bind to two different antigens, or two different epitopes on the same or different antigens [32]. As with other biotherapeutics the use of BsAbs is on the increase. In 2018, two BsAbs were approved in the EU and the United States (US), with 60 in preclinical development and 30 in clinical trials for a variety of indications [33]. There are multiple BsAb forms, some being relatively small antibody fragments, such as bispecific t-cell engagers (BiTEs), tetravalent bispecific tandem diabody (TandAb) and dual-affinity retargeting bispecific antibodies (DARTs) [34]. Some BsAb are based on full IgG while, with an Fc region e.g Triomabs, CrossMabs, dual variable domain immunoglobulin (DVD-Ig) and 2 in 1-IgG, one further type are chemically conjugated BsAbs (Figure 5) [35]. Apart from the obvious structural differences of size, valence and presence of Fc region (or lack of), BsAb also exhibit differences in, PK, half-life and their ability to penetrate tumours (solid) [33].

1.2.4 Therapeutic peptides

Therapeutic peptides form a final group of biotherapeutics, made up of relatively short amino acid sequences that can be a drug, or also a method of delivery similar to ADCs [36]. One thing that stands therapeutic peptides apart from other biotherapeutics is that they can either be naturally or chemically produced [10]. The use of peptides as pharmaceuticals dates back a long way, with insulin being developed in the 1920s, while today, there are over 60 marketed products for the treatment of cancers, diabetes and cardiovascular disease. Peptides are not without their problems, short half-lives and poor oral bioavailability have hindered their development. However, recent advances in synthesis techniques and injection (versus oral dosing) no longer being seen as an inferior route of administration has allowed for the PK profiles and stability of peptides to be improved [37].

When this is taken into consideration with the low toxicity peptides become a viable option as a developable therapy [38].

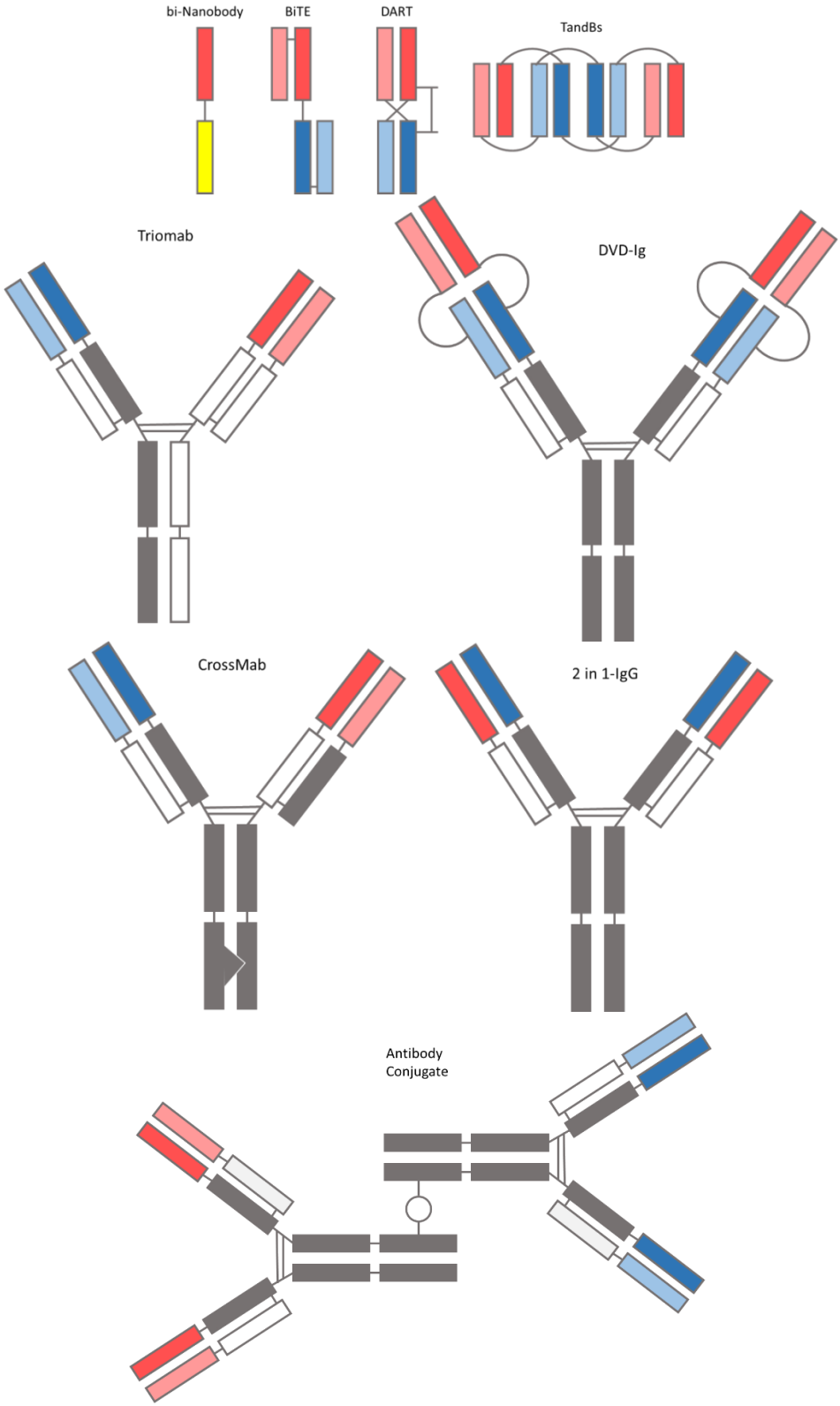

Figure 5 Schematics showing the general make-up of some of the common bispecific antibodies (bsAbs) types, with Triomabs, dual variable domain- immunoglobulins (DVD-Ig), CrossMabs, 2 in 1-IgGs, and antibody conjugates forming the group IgG based bsAbs type and bi-Nanobodies, bispecific t-cell engagers (BiTEs), tetravalent bispecific tandem diabody (TandAb) and dual-affinity retargeting bispecific antibodies (DARTs) which are fragment based bsAbs all depicted.

1.3 Current Approaches to Bioanalysis of Biotherapeutics

The support of toxicokinetic (TK) and PK studies from a bioanalytical point of view has traditionally employed the use of liquid chromatography (LC) followed by tandem mass spectrometry (MS/MS) on triple-quadrupole mass spectrometers [39-41]. The focus of such analyses has been the quantification of intact small molecule therapeutics. This follows from the industry traditionally focussing on novel chemical constructs as therapeutic molecules. However, as discussed in section 1.1, there been a paradigm shift within the pharmaceutical industry towards the use of larger molecules and, in particular, biotherapeutics, the intact analysis of which has been limited to those molecules with lower molecular weights [42-44].

Proteins with higher molecular weights had to be quantified with techniques such as enzyme linked immunosorbent assay (ELISA) [45]. These assays are capable of quantifying both free and bound forms of the molecules and these can both be important in pharmacologic measurements [46-48]. However, a free measurement can be skewed by other types of binding, i.e. not just to the target e.g. the presence ADAs can give an artificially low response [49]. Ligand binding assays (LBAs) also lack specificity when it comes to post-translational modification (PTMs), failing to detect deamidated, isomerised or clipped forms, which can all affect the binding at the target. LBAs also have the disadvantage of requiring generation of specific reagents, which can be problematic, particularly in early development. As a consequence there has significant efforts to transition toward protein quantification by mass spectrometry (MS) [50].

The current state of quantifying proteins by LC followed by MS for bioanalysis largely employs the use of enzymatically derived peptides, referred to as ‘bottom up’ analysis [51].

The use of enzymes like trypsin give reliable and predictable digestions which result in proteins being cleaved at specific amino acids. If the amino acid sequence is known, as for a biotherapeutic, then signature or surrogate peptides can be used with LC-MS detection [52]. However, enzymatic digestion also has its drawbacks for quantitative bioanalysis, particularly by adding to the assay complexity. The protease enzymes such as trypsin are only selective in terms of the cleavage sites and not in terms of the proteins they act on, which leads to generation of vast numbers of peptides from a protein sample, which increases the need for high challenges of selectivity to reduce the impact of endogenous interferences. A move away from the quantitative mass spectrometers (triple quadrupole) to high resolution mass spectrometers such as time of flight (TOF) and orbital trap mass analysers can reduce the impact of these inferences [53]. The digestion of biotherapeutics with a single enzyme can also lead to a loss of information about PTMs, by carrying out multiple digestions with different cleavage site it possible to reconstruct this, however [54].

What is the result of losing information about PTMs when quantification is required and not characterisation the molecule? In terms of quantitation for TK and PK studies, it is the circulating concentration of active drug that is of interest, the key word being active, and so if a PTM affects the activity of a biotherapeutic but does not occur on the signature peptide, then using this approach to infer the concentration of the active molecule is not valid. However, from a proteomics view the production of a peptide map when using a bottom up approach can be very useful [55].

An approach, whereby analysing the intact protein in quantitative bioanalysis can give a more accurate picture, given that it is the often the intact, native form the molecule that is active, therefore it would desirable to quantify the intact, native molecule [56]. The quantitation of the entire molecule is possible by LC-MS and is referred to as the top-down

approach and has been shown to be able to characterise proteins of greater than 200 kDa [57]. This approach to quantitation also has its challenges, such as low sensitivity, high limits of quantification or requiring one or two orders of magnitude more material than a bottom-up approach. Top-down analysis also becomes increasingly more difficult as the complexity of the sample increases, so using this form of quantification for samples generated in TK and PK studies which will be biological matrices the likes of plasma, serum, blood or tissue homogenate will present significant challenges to the analyst [57, 58].

There is an alternative, or compromise approach, which has been termed middle down. This technique uses limited digestion of proteins such that the resulting fragments are far larger in size than those produced in a bottom-up method [59]. Middle down methods have been able to approach the sensitivity of bottom-up methods. With protein being digested into 3 to 20 kDa with the use of microwave-accelerated acid cleavage or endoproteinases e.g. Lys-C or Asp-C [60, 61], although there is some debate over whether this can be termed middle down as the peptides produced are only marginally larger than those generated by tryptic peptides [62]. Recently the use of the IgG degrading enzyme (IdeZ) has gained popularity due to its high specificity. IdeZ cleaves IgG at the hinge region of the four chains (two Lc and two Hc), this then followed by chemical reduction giving rise to 3 sub unit of approximately 25kDa, these are the Lc and two half Hc known as the fragment crystallisable (Fc)/2 and the fragment antigen binding (fab) of the Hc (Fd) fragments [63, 64].

1.4 Aims and Objectives

As explained in the previous sections, the use of biotherapeutics as treatments are gaining in popularity with a significant increase in therapies of this type being approved for use. This presents new analytical challenges to quantification and methods of analysis for the

new biological materials. To ensure the research is fit for purpose the following will be included:

- In Chapter 2 the theory of capillary electrophoresis (CE) (including sample loading, buffer systems and specifically the CE-MS interface) and high resolution mass spectrometry (with a focus on HRMS, but including ionisation techniques and general MS theory) are discussed. These techniques are evaluated in this thesis for the quantification of mAb as an orthogonal approach to high performance liquid chromatography.
- Chapter 3 describes the equipment and materials used to produce a CE-MS method for the identification and quantification of mAbs, as well as the practical methodologies employed to generate samples used during the method development and evaluation. Finally, the CESI 8000 and OptiMS cartridge set up is provided.
- The results presented in chapter 4 focuses on the outcome of experiments to determine the conditions that give best measurement responses (with respect to peak shape and resolution). Conditions assessed include the buffer separation system used and the injection conditions.
- The final chapter discusses the methods developed and assesses the impact that this work could have on the future of quantification of mAbs and further work that follows from this MPhil project.

The aim of this research will be to develop a new method of for the quantification of mAbs using an electrophoretic approach to separation coupled with HRMS. This will allow a middle down approach to quantification to be used rather than the bottom up approach commonly used to generate TK and PK data. Once the method has been developed its

performance will be assessed. The final method will look to achieve maximum sensitivity, in order to achieve the lowest possible limit of quantification, in a run time of less than 20 minutes. Electrophoretic resolution of the fragment peaks would be desirable but is not essential since HRMS will be used giving spectral resolution, peak shape will also be taken into account when selecting the CE conditions for separation. The final method is likely to a balance between the above factors, a compromise to achieve the most suitable method for quantification in a bioanalytical lab.

2 Instrumental Theory and Applications in Industry

In this chapter CE and HRMS, are discussed as techniques being evaluating for the determination and quantification of mAb. High performance liquid chromatography (HPLC), the traditional technique used in this area of research, will also be discussed but to a lesser extent.

2.1 Capillary Electrophoresis

In CE, separation is achieved by exploiting differential migration rates of analytes in an applied electric field [65]. Electrophoretic techniques encompass capillary isoelectric focusing, gel electrophoresis and capillary zone electrophoresis (CZE). CZE is the area of interest in this research and as such shall be discussed in more detail and referred to as CE throughout this thesis.

Electrophoresis is an orthogonal separation technique to HPLC but has traditionally suffered challenges when trying to be coupled with mass spectrometry. From an industry standpoint, the major drawback (until very recently) has been the lack of an 'off the shelf solution' from vendors as well as the challenge of closing the circuit of the high voltage electrical field used in separations [66]. CE can offer exceptional resolving power when compared to HPLC, with peak efficiencies of greater than one million theoretical plates [67]. The operation principle of CE is the movement of charged or polar molecules inside a capillary filled with a conductive fluid under the influence of a uniform electric field (Figure

6) [68].

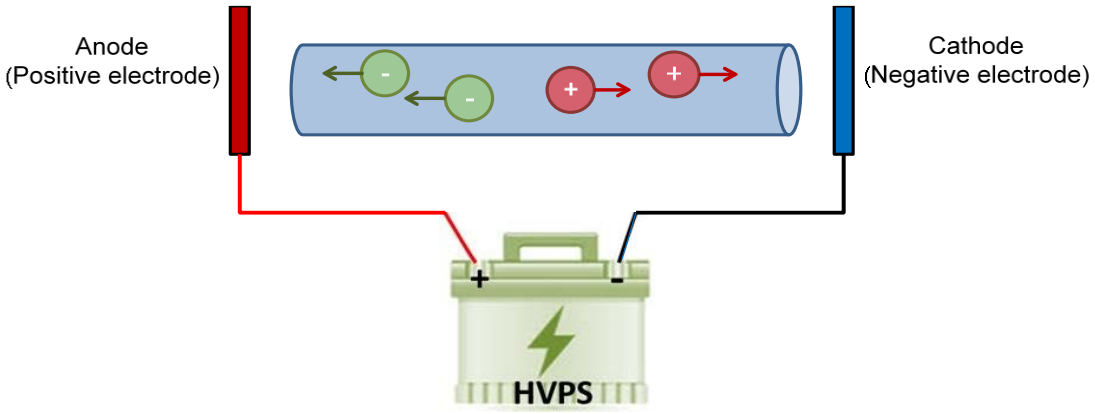

Figure 6 Inside a capillary filled with a conductive fluid under the influence of a uniform electric field supplied by a high voltage power supply (HVPS), charged or polar molecules will migrate, with positively charged molecules migrating towards the cathode and negatively charged species moving towards the anode. This forms the basis of separation in capillary electrophoresis (CE), however it does not take into account other factors such as electroosmotic flow and the application of pressure to the system [67].

The mobility of molecules during CE separation is balanced between the electric force and the viscous drag. Electrophoretic mobility (EOM) (μ_{ep}) is equal to velocity/unit field strength and is described the equation $\mu_{ep} = \frac{q}{6\pi\eta r_{st}}$ (where q = charge, $\boldsymbol{\eta}$ = viscosity of the solution and r_{st} = Stokes radius of the ion) and indicates that mobility is dependent on mass-to-size ratio. The molecule's velocity within the capillary can be calculated using the equation $\nu_{ep} = \mu_{ep}E$ (where μ_{ep} = electrophoretic mobility and $\boldsymbol{E}$ = electrical field) shows that the velocity of the analyte is directly proportional to the magnitude of the electrical field [69]. Another factor to consider in CE is electroosmotic flow (EOF), which manifest itself because of surface charges on the capillary wall, the extent of which is controlled by the pH of the buffer system. The EOF is a net movement of the buffer towards the negative electrode caused by positively charged ions being attracted to the negative charge on the surface of the capillary. This flow varies with pH and is much higher at higher pH. EOF is defined by the equation $\nu_{eo} = \frac{\epsilon\zeta}{4\pi\eta}E$ (where ϵ = Dielectric constant, ζ = Zeta

potential, $\boldsymbol{\eta}$ = Viscosity of the solution and $\boldsymbol{E}$ = electrical field). The zeta potential (ζ) displays an inverse relationship with the charge on the surface area, number of valence electrons and square root of the ionic strength of the electrolyte. As a result of this relationship, increasing the concentration of the background electrolyte (BGE) will decrease the EOF [70-72]. Having control of the EOF is extremely important, and EOF can be used as an advantage allowing for the analysis of negatively charged, positively charged and neutral analytes in a single analytical experiment. At neutral pH and above, the EOF is at its highest, and at low pH (<pH 2.5) the EOF may effectively stop. When using high pH buffers the EOF is stronger than the EOM and therefore all species are carried towards the negative electrode, migrating in the order of cations, neutrals and finally anions.

LC, being pressure driven is subject to frictional forces where the solid surfaces and the liquid meet resulting in a parabolic flow profile. This phenomenon of the flow velocity gradient may lead to band broadening with in the column [73]. With an electrically driven system, like the EOF described here, the flow velocity is far more uniform (see Figure 7) and results in a flat profile which results in the production of narrower peaks [74].

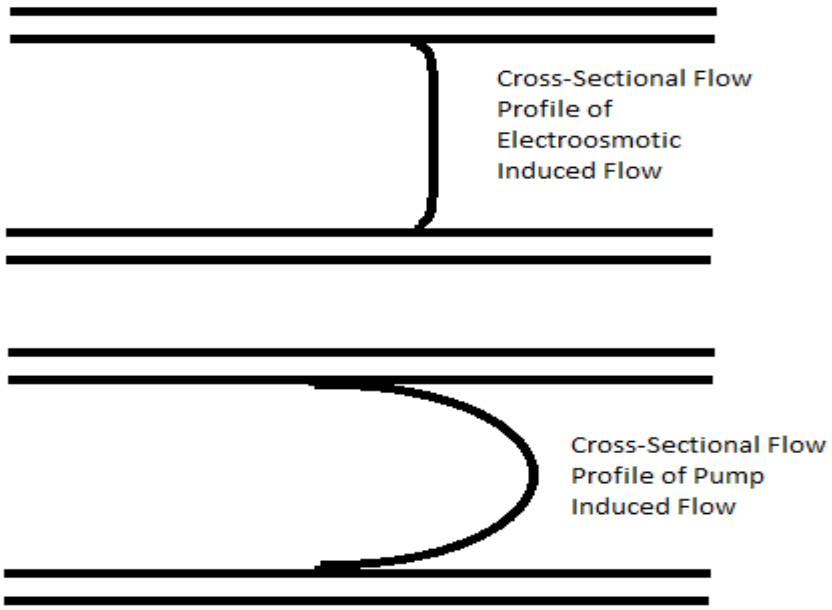

Figure 7 Capillary flow profiles showing the uniform, flat flow profile generated by electroosmotic driven flow (top) and the parabolic flow profile of pressure driven flow (bottom) generated by the frictional forces being exerted on the liquid. The flat profile for electroosmotic driven flow leads to sharper, narrower peaks.

Joule heating is another factor of the system which must be taken into consideration when working with CE. As current passes through a fluid-filled capillary the electrical energy is partially converted to heat, which increases the temperature. The extent of this heating is dependent on the internal diameter of the capillary and the surrounding environment; the net result of which is a radial parabolic temperature gradient, with the temperature at the centre of the capillary being greater than at the edges. Since an increase in temperature is associated with a decrease in viscosity, it follows that a temperature gradient will again lead to a parabolic flow profile analogous to that seen with pump induced flows and consequently band broadening [75]. Thus, narrower capillaries are used to negate this effect for two reasons. First, because the heat is more readily dispersed across a narrower capillary and second, the current that is being passed through the capillary is reduced. Since the temperature increase can be cumulative with continued injections, and analyte mobility increasing by approximately 2 % with every degree Centigrade (C), it is often necessary to control the temperature through the use of an air or liquid cooling system. Other outcomes

of excessive Joule heating can be the production of microbubbles which lead to the detection of false peaks, or in extreme cases the buffer can boil within the capillary resulting in an interruption of conductivity [76-78].

2.1.1 Sample loading in CE

There are several ways to load a sample into a CE capillary, described by hydrodynamic (otherwise known as pneumatic) or electrokinetic (EK) sample introduction as illustrated in Figure 8. Hydrodynamic injections work by applying a pressure differential across the capillary which physically introduces a small amount of sample solution into the capillary. The volume of sample introduced is dependent on a number of variables such as dimensions of the capillary, buffer viscosity and both the amount and duration of pressure applied. Hydrodynamic injections can lead to band broadening as a consequence of the parabolic effect of applying pressure to the system. In addition, the size of the sample plug must also be limited as this can have an impact on separation efficiency and, as a general rule, the plug length should be less than 1 % of the total separation length of the capillary. Alternatively, EK injection can be used where a constant voltage is applied (typically 3 to 5 times lower than the separation voltage). The amount of sample loaded is dependent upon the duration of the voltage step and the voltage applied, the EOM of the analyte, the conductivity of the sample buffer, the BGE and the EOF. This can result in difficulties controlling the amount of sample injected, particularly if there are large variations in the salt content of the samples [79]. The use of EK injection can facilitate a process called sample stacking, *via* a discontinuous buffer system. Applying a plug of buffer with lower conductivity than that of the BGE prior to analyte injection induces a concentrative or stacking effect. This is a result of the electric field in the sample zone being relatively high, causing the analytes to migrate rapidly until the boundary of the two zones are reached

where migration slows causing the band of ions to be compressed [80, 81]. The greater the difference in conductivity between the sample zone and the BGE the greater the focusing.

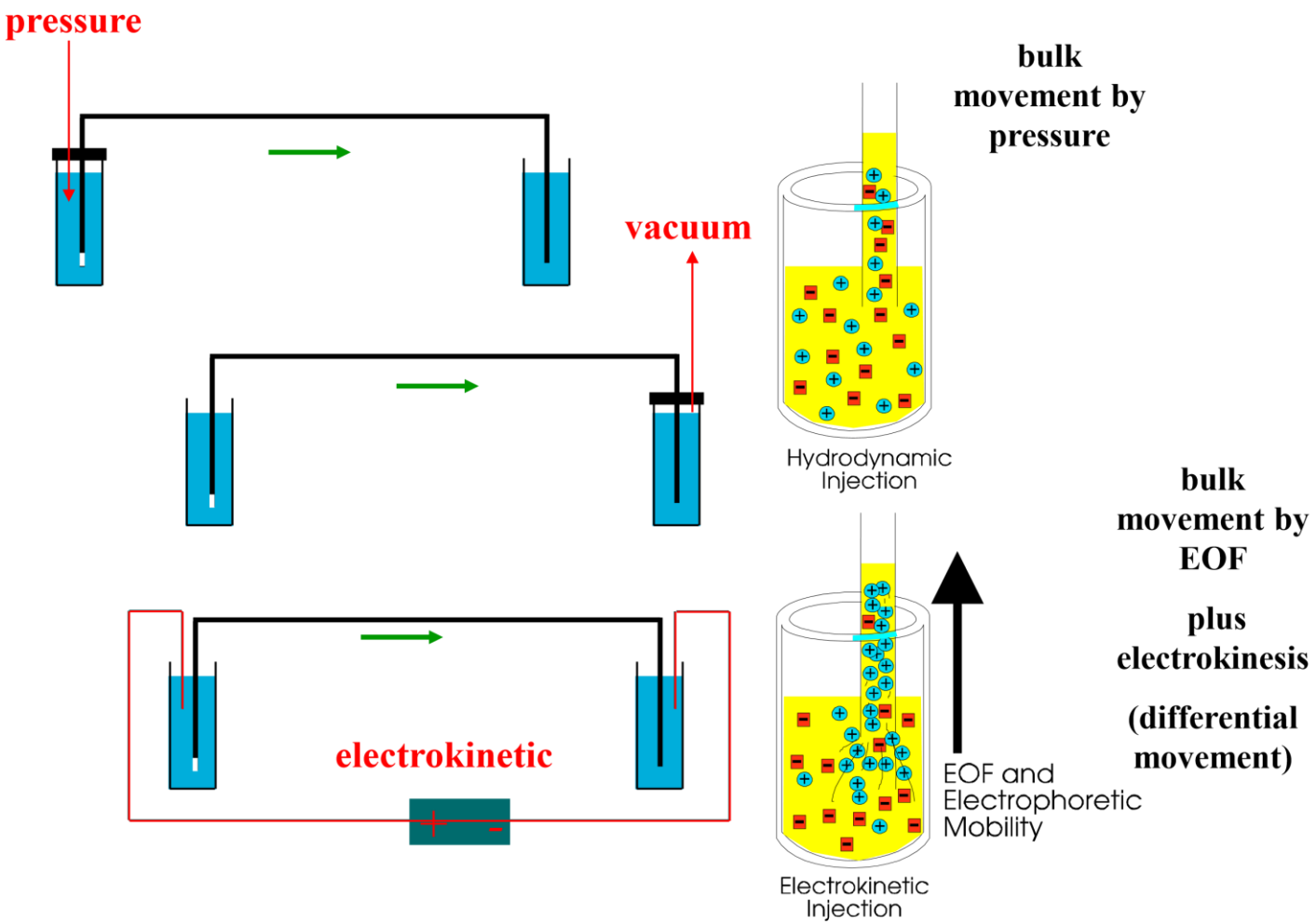

Figure 8 Schematic of CE injection modes. Hydrodynamic injection (pressure and vacuum) results in the bulk movement of sample into the capillary. For electrokinetic injection, the sample migrates in the capillary by means of electrokinesis as well as bulk movement driven by electroosmotic flow (EOF) resulting in differential movement of charged species.

2.1.2 The CE-MS interface

CE-MS is becoming more popular, particularly in the world of proteomics, with CE being successfully coupled with electrospray ionisation (ESI) and matrix-assisted laser desorption/ionisation (MALDI). Coupling CE with MALDI can be less challenging than with ESI as MALDI is frequently employed as an offline technique, but can also result in lower resolution and increased variability and as such the more popular choice is to couple CE to ESI [82]. The CE-MS interface can take two forms, sheath-flow or sheathless (Figure 9) [83, 84], with the former being most commonly used in industry as it offers greater stability. However, with a sheath-flow interface the sample is diluted prior to introduction into the mass spectrometer and there is a higher flow rate comprising detection limits. One interface that takes advantage of the sheathless approach is the CESI 8000, developed by Siex. The CESI 8000 together with an OptiMS cartridge (an integrated unit that fits into the CESI 8000, with fixed lengths of silica for the separation and conductive lines and sprayer housing) that allows for the integration of CE with ESI within the same interface (see Figure 10). The system uses an adapted nano spray source, with the emitter tip integral to OptiMS cartridge (Figure 11), giving a 'plug and play' style set up.

There are several types of capillary available in this cartridge format; bare-fused silica, neutrally coated and polyethyleneimine (PEI) coatings that can be applied by the user. The neutral coating involves covalently bonded acrylamide to the silica surface [85]. Covalantly bonded coatings are very stable and provide good properties, they are ideal for CE-MS as there is very little bleeding of the coating into the mass spectrometer reducing potential contamination by the coating [86]. The purpose of the neutral coating on the capillary is to reduce the EOF increasing the separation window, reducing the interactions of the sample with the surface of the capillary and broadening the pH stability range. These attributes are

suited to the analysis of intact proteins or complex peptide digests and therefore will be used within this project.

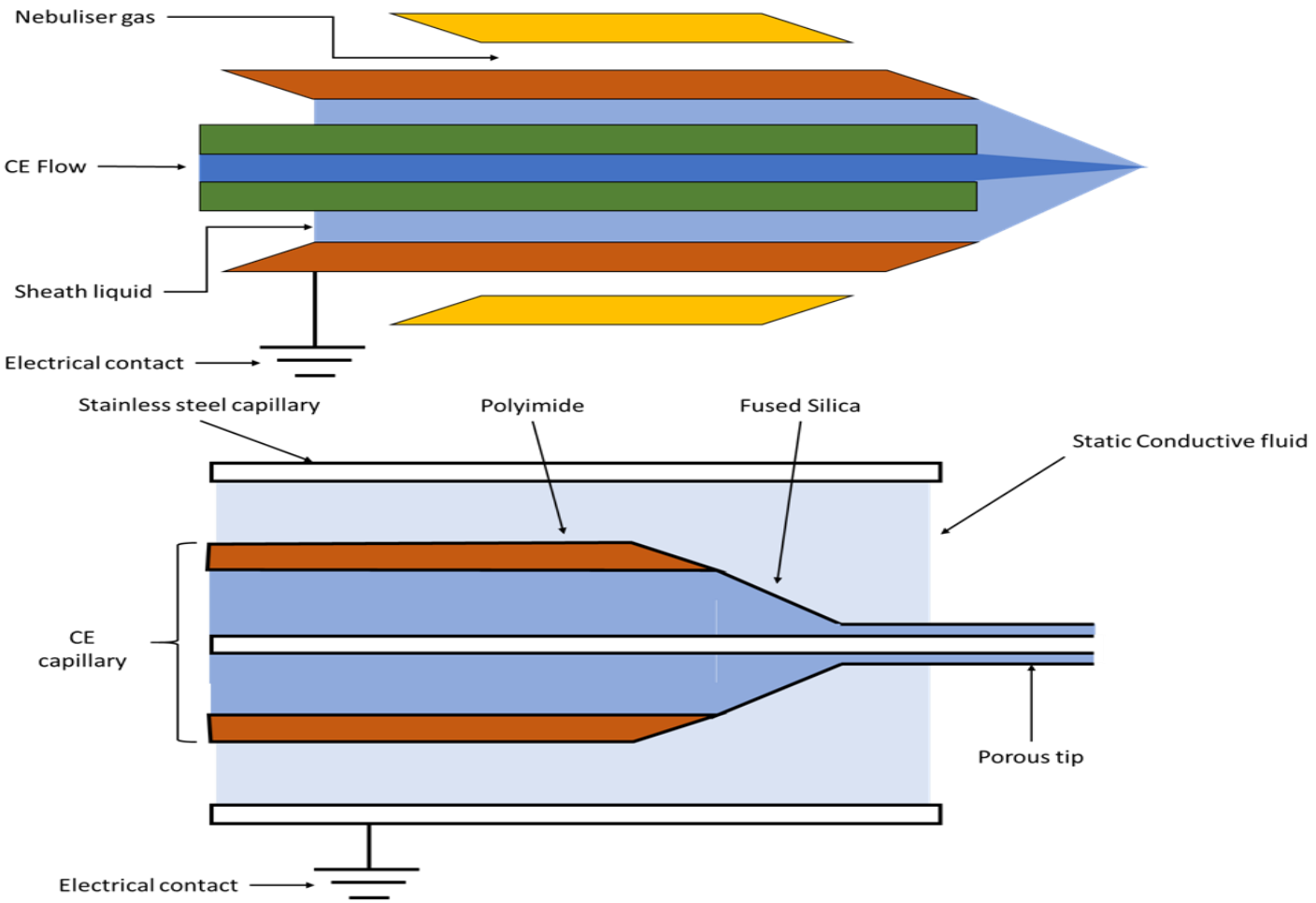

Figure 9 Schematic of electrospray ionisation emitter using sheath-flow (top) and sheathless (bottom). The additional flow used in the sheath-flow design can be seen combining with the capillary electrophoresis (CE) flow.

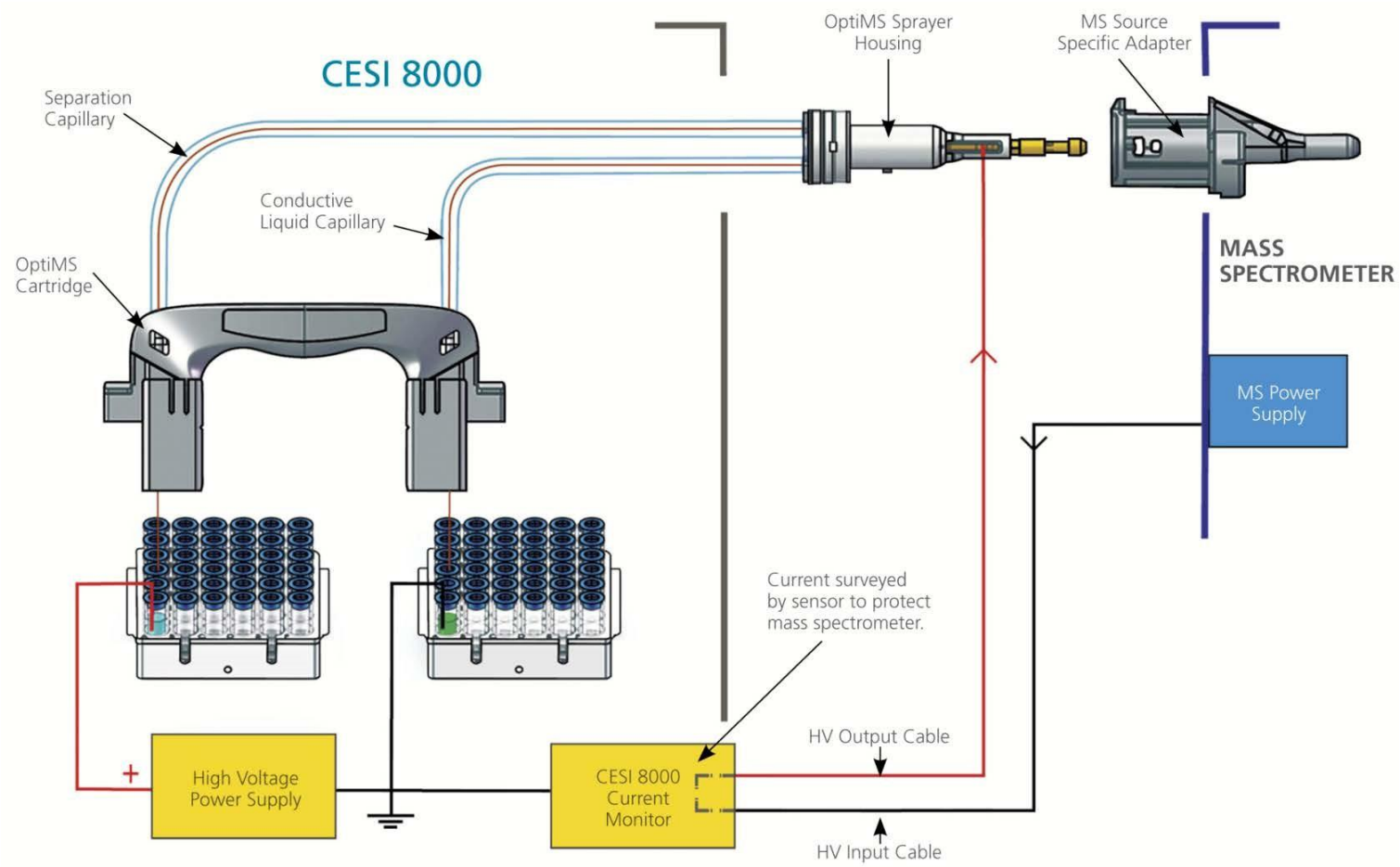

Figure 10 Schematic of the CESI 8000 and the mass spectrometry (MS) source adapter featuring the OptiMS cartridge and the configuration of the separation capillary and conductive liquid capillary, the sprayer housing and the mass spectrometer source adapter [67]

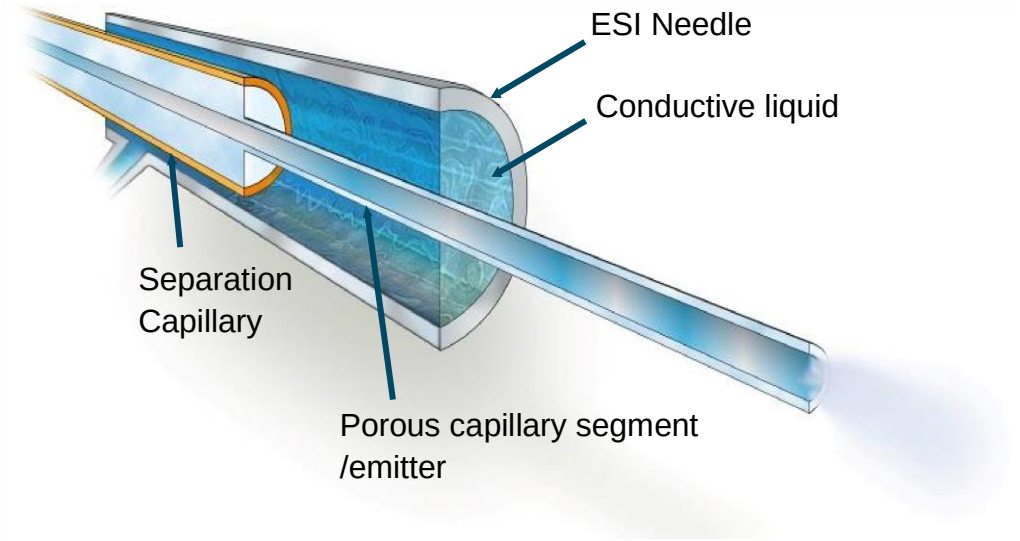

Figure 11 Schematic of the OptiMS adapter showing the sheathless design that allows the application of the ionspray voltage (ISV) via the conductive liquid, which also allows the completing of the circuit required to produce the separation current. The application of the ISV to the conductive liquid induces droplet formation (spray) and ionisation [67].

2.1.3 Current applications of CE-MS

CE-MS is rapidly becoming a key techniques for use in bio-omic applications (e.g. proteomics, metabolomics and genomics) [87]. The use of CE-MS for the analysis bio-molecules, no matter their origin, has increased due to the consistent migration patterns observed for analytes in complex biological samples [88]. CE-MS is now being used in a variety of areas such as metabolite profiling, biomarker identification and analysis [89]. It is also used in peptide centric analysis, the bottom-up approach to the analysis of biotherapeutics; for example mAbs, creating peptides maps for characterisation giving 100 % coverage in a single injection [90]. The analysis of intact proteins is an area where CE can provide significant impact compared to HPLC techniques which struggle when the size of an analyte increases above 50 kDA. Indeed, CE-MS has also being used to successfully separate

and characterise intact proteins [91] and has been used in the characterisation of mAbs and antibody-drug conjugates (ADCs) [92]. Analysis of post translational modifications, also lends itself to CE-MS whether this be again a bottom up approach or at an intact level [93], PTMs including aspartic acid isomerisation, asparagine deamidation, methionine oxidation, C-terminus glutamic acid cyclization and site specific glycosylation have all be successfully analysed with CE-MS [94-96].

CE-MS and LC-MS are orthogonal techniques offering separation based on different attributes of an analyte. In many respects the techniques can be thought of complementary to one another, indeed the use of CE in peptide mapping can increase protein sequence coverage in the region 20 % [97]. When there is overlap between the two techniques there will still be differences e.g. elution order which is related to the analyte's physicochemical properties. This also means the techniques offer different selectivity. To achieve a change in selectivity in LC a change of stationary phase is often required i.e. column chemistry, whereas with CE changes in selectivity can be achieved by simply changing the pH of the BGE. CE-MS can also offer an advantage in the analysis of hydrophilic compounds which are traditionally poorly retained on LC systems. CE-MS and LC-MS both offer advantages and disadvantages over one another, and for the two techniques to be compared head to head might not be the best approach when selecting one technique over the other. Instead the prudent approach would be to determine which method gives the desired outcome, whether that be resolution, peak shape, sensitivity, peptide coverage or identification of PTMs.

2.2 High Performance Liquid Chromatography

High performance liquid chromatography, HPLC, is a separation technique used to determine analytes in complex samples and is most commonly used as a hyphenated

technique coupled to a mass analyser [98, 99]. HPLC can be characterised by the type of chromatography used and/or the method of interaction with the stationary phase and the analyte. Four key categories used to describe this process are normal phase, reversed phase, size exclusion or ion exchange chromatography (Figure 12).

- Normal phase operation is characterised by the use of a stationary phase e.g. bare silica, cyano, diol or amino banded phases that is more polar when compared to the nature of the mobile phase. In a normal phase system, the more polar components of a sample have a stronger interaction with the stationary phase c.f., less polar components, and are therefore retained longer. The types of mobile phases commonly used in normal phase chromatography include, hexane, methylene chloride chloroform or diethyl ether. Due to the nature of these solvents e.g. their low polarity and their inability accept or donates protons, which unfortunately make the eluate unsuitable for use with ESI-MS.
- Size exclusion HPLC separates analytes based on their molecular size with larger molecules travelling faster through the stationary phase compared to smaller molecules. In this system the stationary phase contains pores which exclude larger molecules (hence their rapid movement over the stationary phase) and although this technique is not widely used for quantitative bioanalysis [98], it may have a role to play in the measurement of some biotherapeutics.
- Ion exchange chromatography uses ionic mobile phases of varying pH and ionic strength to control the elution time of analytes passing over a charged resin based stationary phase. An anionic stationary phase can be used to separate cations, that are attracted to the surface of the stationary phase by electrostatic interaction and a cationic stationary phase is used to separate anions.

- Reversed phase chromatography is arguably the most well used method of chromatography in industrial and research applications. In this system the stationary phase is less polar than the mobile phase and so less polar analytes are retained longer than polar ones due to the increased strength of interaction with the non-polar stationary phase. In reversed phase chromatography, the use of polar mobile phases e.g. acetonitrile or methanol make this technique compatible with mass spectrometry [100], and as such the subcategories and applications of this system will be discussed further.

A further adaptation of reverse phase chromatography that gives greater retention of more polar analytes is known as hydrophilic interaction chromatography (HILIC), which pairs a normal phase silica stationary phase with mobile phases that better enables the separation of non-polar analytes [101, 102]. Reversed phase chromatography is commonly could with mass spectrometry for bioanalytical applications , particularly when coupled to triple quadrupole mass spectrometers employing either ESI or atmospheric pressure chemical ionisation (APCI) (see section 2.3) [103]. Hence further information on this analytical technique is given below. Note that HPLC is also a widely used tool in other fields such as metabolomics, proteomics and lipidomics for biomarker research [104, 105].

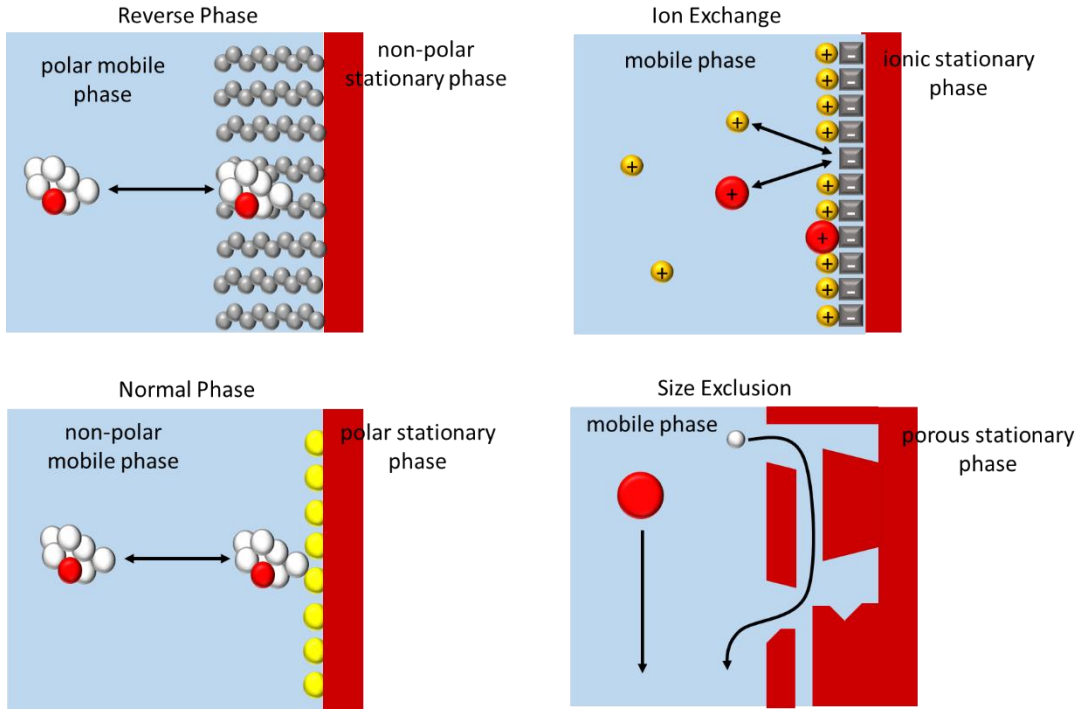

Figure 12 Representation of the four key categories of high performance liquid chromatography (HPLC): normal phase, reverse phase, size exclusion and ion exchange chromatography. Reverse phase exploits the interaction of less polar molecules with the non-polar stationary phase. In normal phase, the polar components have a strong interaction with the polar stationary phase. In ion exchange chromatography, ionic mobile phases control the elution of analytes. Size exclusion chromatography uses a porous stationary phase to slow the travel of smaller molecules through the column.

Non-polar or hydrophobic stationary phases are created by covalently bonding alkyl chains to silanol groups present on the surface of the silica particles. Normally octadecyl carbon (C_{18}) chains are grafted onto the surface of the stationary phase although shorter chain length alkyl groups area also used to alter separation selectivity, such as C_8, and C_4 [106], as are cyano, phenyl or pentafluorophenyl (PFP) groups.

The final stationary phase surface is modified to suit the type of chromatography required. The surface coverage of alkyl chains is far from 100 % and is commonly around 15 – 20 %. This free silanol groups on the surface of the stationary phase have the potential to cause secondary interactions with analytes, including ionic and hydrogen bonding. In the extreme, this can often lead to irreversible interactions between analytes and stationary phase, leading to a reduction in column performance. A process called end capping may be

used to add low molecular weight alkyl groups (*via* a silylating agent like trimethylchlorosilane) to 'cover' the free silanol groups on the surface of the stationary phase therefore limiting any unwanted bonding interactions [107].

2.2.1 Chromatographic parameters used to measure performance

There are several chromatographic parameters that can be calculated and used to characterise the interaction of an analyte with the chromatographic system and hence chromatographic performance. The parameters include the peak asymmetry factor (As), capacity or retention factor (K'), resolution factor (Rs), selectivity factor (α) and chromatographic efficiency (N). The peak asymmetry factor is used to describe the shape of a peak shape (e.g. whether it is Gaussian, fronting or tailing). In reality, it is rare that a HPLC generated peak would be perfectly Gaussian, and more often the peak symmetry, calculated by $A_S = \frac{b}{a}$ (where a and b are the distance from the midpoint, perpendicular from the highest point of the peak to the edge when measured at 10 % peak height), indicates a tailing peak (if the A_s value >1), or a fronting peak (if the A_s value is <1). A_s values resulting between 0.9 and 1.1 indicate reasonably acceptable symmetrical peaks. where a and b are the distance from the midpoint (perpendicular from the highest point of the peak) to the edge when measured at 10 % peak height. The capacity (or retention) factor (K') measures the strength of interaction of an analyte with the stationary phase. The larger the K' value the stronger the interaction and the more highly retained the compound will be. The term K' is calculated by $K' = \frac{(t_R - t_0)}{t_0}$ (where t_0 is equal to the retention of the solvent front or a compound that has no retention e.g. uracil and where t_R is the retention time of the analyte) and is used to compare the performance of different chromatographic system because it is not affected by column dimension or small changes

to the mobile phase flow rate. The resolution equation $R = \frac{t_{R2} - t_{R1}}{0.5(W_1 + W_2)}$ (where t_{R1} and t_{R2} are the retention times for each peak and W_1 and W_2 are the width of each peak at the base) gives a measure of the extent of separation between two adjacent peaks and can be particularly useful when separating complex mixtures. The resolution equation gives a numerical indication of how much the peaks overlap. A R_s value of 1.5 indicates optimal resolution between two adjacent peaks, as this gives an overlap of 0.15 %, values greater than 1.8 indicate that separation is not optimal and the base-line separation is too large and that the run time should be reduced. A R_s value of 1 equates to a 2.3 % overlap between adjacent and peaks (Figure 13) and values less than 1 indicates that adjacent peaks are not sufficiently resolved.

The selectivity factor, α, calculated by $\alpha = \frac{k_2}{k_1} = \frac{(t_{R2} - t_0)}{(t_{R1} - t_0)}$ is also used as an indication of peaks separation and is a ratio of the two peaks' capacity factors. If two peaks have an equal value of α (that is the selectivity factor equals 1, the two peaks will have the same retention time and cannot be resolved. Ideally α values range between 1.05 and 2.0.

The chromatographic, or column, efficiency is used to indicate the number of theoretical plates (N) in the chromatographic system; it is a measurement value that has been 'borrowed' from the fractional distillation industry [108]. Efficiency is a measurement based on the peak's retention time and width, with the general equation for efficiency shown by $N = x\left(\frac{t_R}{\sigma}\right)^2$. However, the terms σ and x are both dependent on where the width of the peak is measured. If the peak width is measured at the base of the peak, x = 16 and giving the equation $N = 16\left(\frac{t_R}{w_b}\right)^2$, and if the peak is measured at half peak height it will be 5.54

giving $N = 5.54\left(\frac{t_R}{w_h}\right)^2$. Note that both the equations for *N* (at the base and at half height) would only produce the same number for efficiency if a peak was Gaussian.

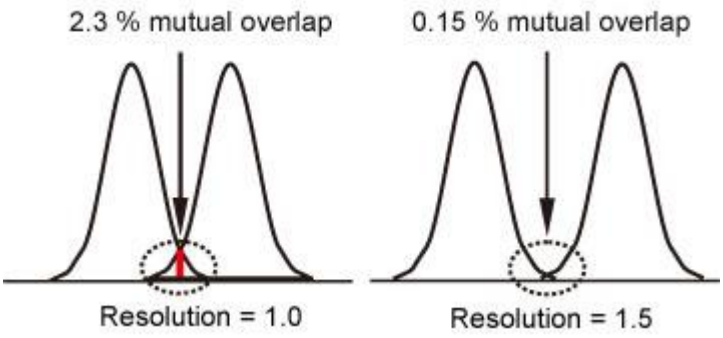

Figure 13 Resolution and peak separation resolution (Rs) values of 1.5 signify optimal resolution between 2 peaks and Rs values of ≤1.0 indicate that two adjacent peaks are not significantly resolved [109].

2.3 Mass Spectrometry

The technique of mass spectrometry can be used to provides both quantitative and qualitative data (depending on the instrument used) allowing the accurate measurement (quantification) or the identification of analytes (structural characterisation). In the broadest terms MS analysis involves

- conversion of analytes to gaseous ions, with or without fragmentation,
- transfer to a high vacuum region to avoid scattering between of ions during transit from formation to detection
- acceleration and focusing of the ion packet to facilitate their transit through the instrument
- separation of different ions according to their respective mass-to-charge ratios. This is achieved by applying electric and or magnetic fields (Figure 14) [110, 111].

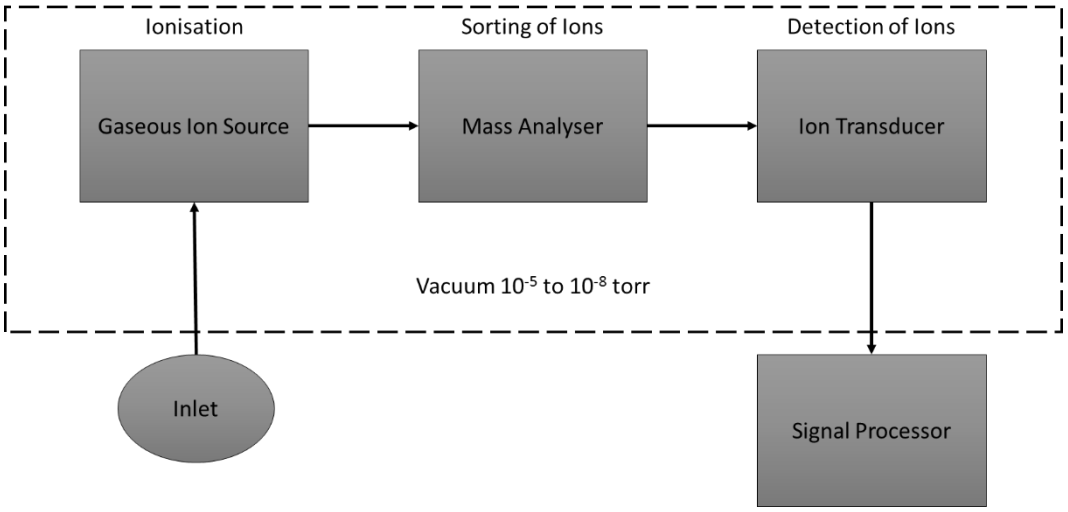

Figure 14 Basic schematic of a mass spectrometer (MS), showing the major components: inlet (e.g. high-performance liquid chromatography or capillary electrophoresis), ion source, mass analyser, ion transducer and signal processor.

Ionisation is the process of forming charged ions from molecules that are in a neutral state, this occurs by either exciting the neutral molecule causing it to eject an electron and form a radical cation (M^+) or the production of and adduct (MH^+) through ion-molecule reactions. Ionisation techniques include electron impact ionisation (EI), chemical impact ionisation (CI), ESI and MALDI [112, 113]. These methods of ionisation can then be subdivided into hard and soft ionisation, where soft ionisation generally produces ionisation of the molecular ion and hard ionisation induces a degree of in-source fragmentation. EI and CI fall into the hard category and ESI and MALDI into the soft.

Looking at ESI (Figure 15), as the technique employed in this thesis, the initial sample starts in the liquid phase, with the formation of charged droplets with the application of high voltage at the tip of a capillary through which the eluate from the inlet system is travelling. The application of such a voltage causes the solution to form an aerosol of charged droplets. These charged droplets then undergo desolvation which results in the production of a Taylor cone [114], from the tip of which other smaller highly charged droplet are formed, this process continues until the droplets contain a single charged molecule. The desolvation process is assisted by the introduction dry nitrogen (N_2) around the capillary

which both helps the formation of the aerosol and directing it towards the mass spectrometer, a second gas is also used to assist with the desolvation and reduce droplet size [113, 115-117].

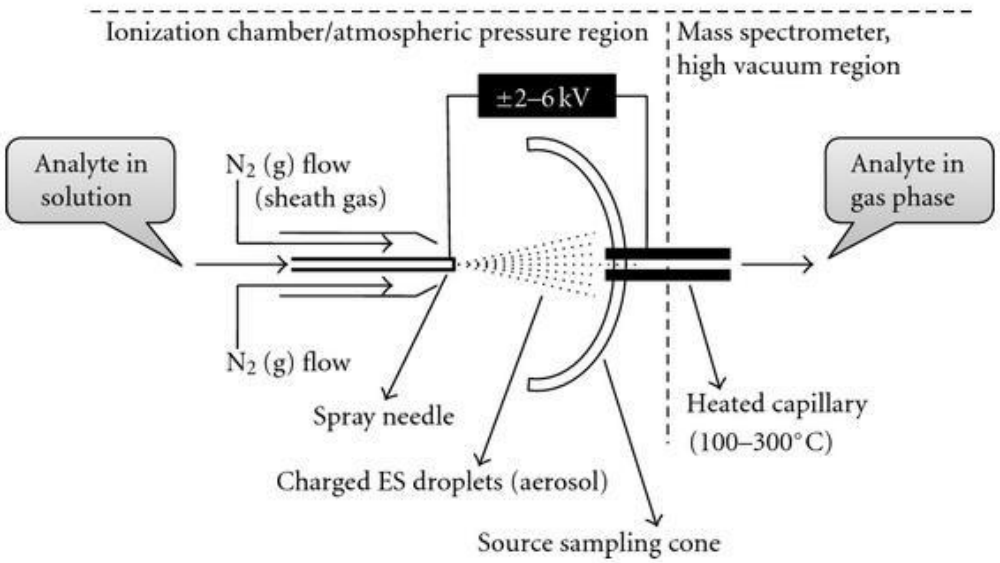

Figure 15 A schematic of an electrospray ionisation (ESI) ion source, depicting the spray needle and the application of voltage and sheath gas to induce charged droplets [116].

Ions are then accelerated by an electric field and enter the mass analyser, the function of which is to separate according to their mass to charge ratio (*m/z)*. There are multiple types of mass analysers, that offer different; resolutions (the amount of separation between two ions), mass ranges, scan rates and detection limits, all are governed by Lorentz force law and Newtons second law of motion [116].

Mass analysers can be used to obtain information about the precursor ion, or fragment, ions. With MS/MS, the precursor ion must first be selected then undergo fragmentation prior to either separation of the product ions or in the case of multiple reaction monitoring (MRM) a second selection based on m/z and subsequently detection. Two or more types of mass analysers may be combined to give differences in the resolution, mass range and the experiments that can be performed. [113]. Mass analysers can be described as either

continuous or pulse, continuous include quadrupole filters and magnetic sector while pulsed mass analysers include time of flight (TOF) quadrupole ion trap (Q-trap).

Quadrupole mass analysers are among the most common [112], this type of mass analyser generally acts as a mass filter, combining direct current (DC) and radio frequency (rf) potentials, the manipulation of these two parameters can be used to select for ions of desired *m/z*. The DC and RF potentials applied to each pair of rods cause the ions to travel in an oscillating motion with those only those ions that that have a stable trajectory transmitted through the mass filter (Figure 16). Quadrupoles can also be used as ion guides with broad *m/z* ranges by applying only a rf potential to the rods. These rf only quadrupoles are employed in triple quadrupole mass spectrometers as the collisions cell (Figure 17).

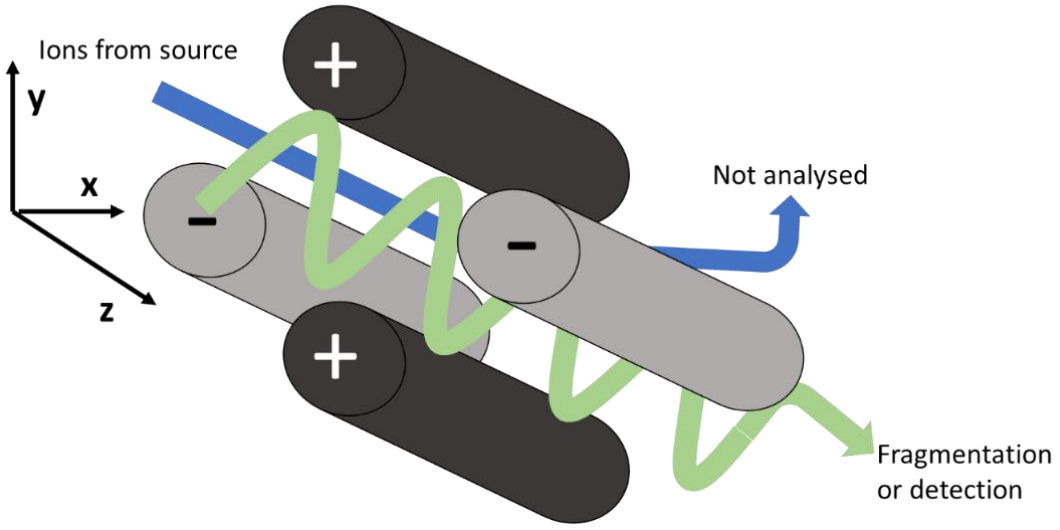

Figure 16 Representation of a quadrupole mass filter, with ions travelling in the direction of z. By adjusting the voltages applied to quadrupoles, ions can be selectively transmitted, with ions not of interest either impacting on the quadrupoles or travelling in different directions and not transmitted.

Quadrupole mass spectrometers, despite having many advantages such as fast scan rates, and high transmission efficiency, as well as practical advantages like their relatively small size and the need for only a modest vacuum. However, quadrupole mass spectrometers do have limitations with respect to both resolution and *m/z* ranges restriction. The resolution of the quadrupole mass spectrometers is limited to that of unit resolution, which in practical terms means the mass analyser can only distinguish between ions that are separated by 1 *m/z* or more [112].

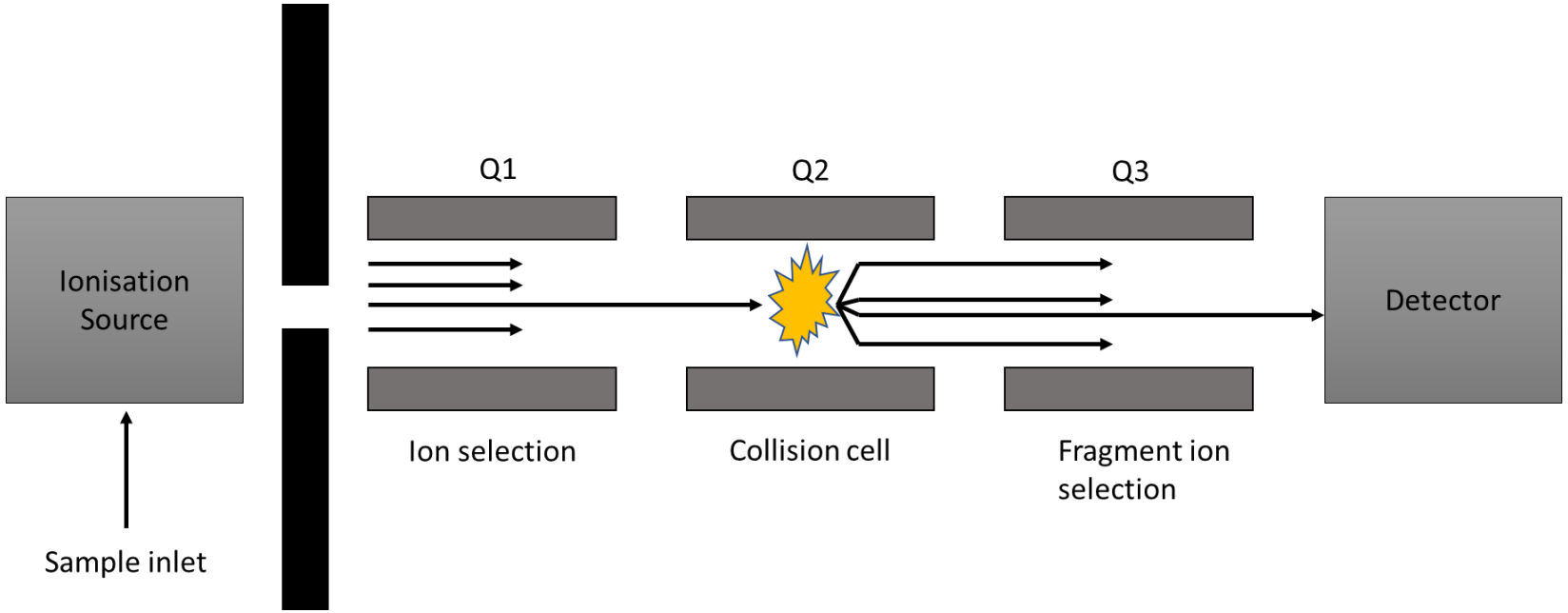

Figure 17 Schematic of a triple quadrupole mass spectrometer being used to perform multiple reaction monitoring (MRM), the technique commonly used for quantification in bioanalytical laboratories. Selection of the precursor ion in quadrupole 1 (Q1) is based on mass to charge ratio (m/z), which then undergoes fragmentation by collision induced dissociation (CID) in the collision cell or quadrupole 2 (Q2) before a further m/z selection in quadrupole 3 (Q3) and subsequent detection.

2.3.1 High resolution mass spectrometry

HRMS can be thought of as any type of mass spectrometry where the exact mass of a molecular ion is determined, and not the nominal mass. HRMS requires sharply focused peaks and, a high resolving power of >10,000. When working with small molecules increased precision (with respect to analyte *m/z*) can reduce uncertainty in metabolite identification and in proteomics. Identification of fewer amino acid combinations are possible with increased precision, potentially leading to the identification of PTMs. The main types of high resolution mass spectrometers include TOF, sector mass spectrometers (SECTOR), Fourier transform-ion cyclotron resonance-mass spectrometer (FT-ICR-MS) and Fourier transform Orbitrap (FT Orbitrap). With the addition of a second mass analyser, tandem high-resolution mass spectrometry (THRMS) has increased the power of the technique with many manufactures producing instruments with combined detectors such as quadrupole time of flight (Q-TOF), ion trap time of flight (IT-TOF), LTQ-Orbirap and Q Exactive-Orbitrap [118, 119]. High resolution mass spectrometers supplied from different instrument manufacturers will have different attributes e.g. resolution, *m/z* range and acquisition speed, as well the differences between the mass analysers e.g Q-TOF, IT-TOF, Q Exactive etc.

2.3.2 Quadrupole time of flight mass spectrometers

A Q-TOF mass spectrometer can be thought of as being a triple quadrupole system, where the third of the three detectors is a reflecting TOF mass analyser (Figure 18). The instrument can be used in two ways, as a TOF-MS where quadrupole 1 (Q1) (refer to Q1 in Figure 18) is used to transmit ions using rf signals only. This allows the production of a high resolution spectrum. In MS/MS mode, Q1 acts as a mass filter at unit mass resolution to transmit only the precursor ion(s) of interest. Then quadrupole 2 (Q2) (refer to Q2 in Figure 18) is used as a collision cell where ions undergo collision-induced dissociation (CID). There is a benefit of having a low collision energy (<10 eV) in Q2 even when using TOF-MS as this adds some collisional focusing while avoiding fragmentation [120, 121]. After leaving Q2 the ions enter the TOF analyser, a pulsed electric field is then applied to make the ions change direction and enter the free drift space [122].

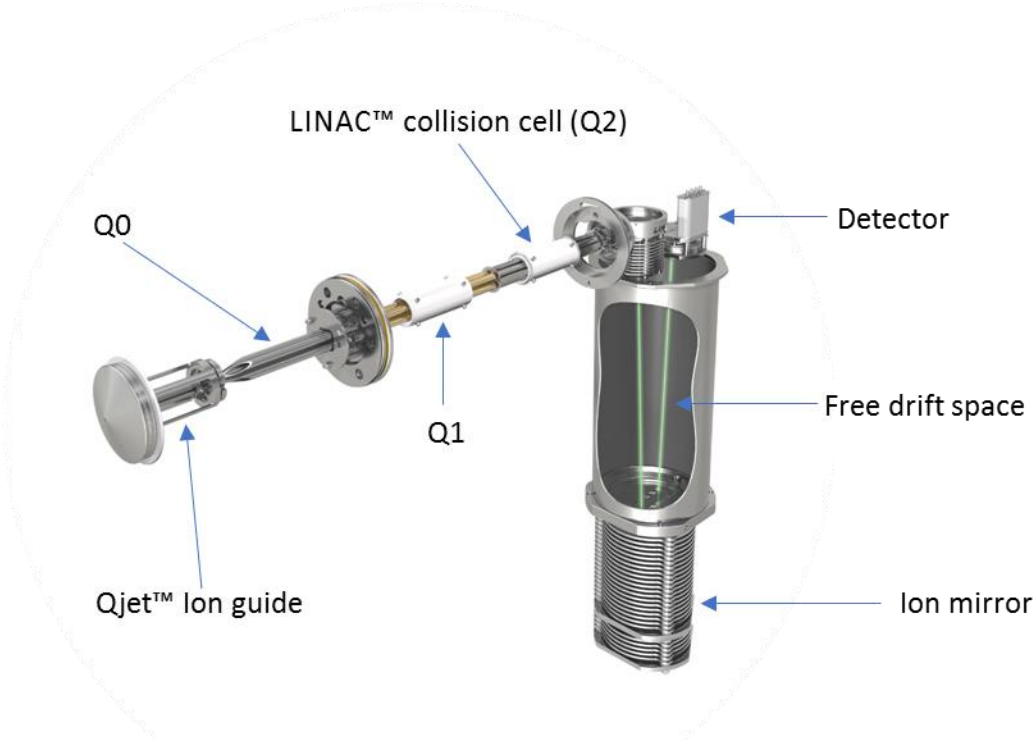

Figure 18 Schematic of the internal components of a Sciex 6600 TripleTOF mass spectrometer (MS) [89]. Q0 is a focusing quadrupole confining the ion beam in the direction of travel through the MS, Q1 provides the mass filter for precursor ions, collision cell or Q2 is where collision induced dissociation (CID) or fragmentation to product ions take place, with the ions then moving into the drift space [123].

TOF-MS is based on the principle that if ions start at the same point and are accelerated by applying the same kinetic energy to a detector then the time of flight is related to *m/z*. This can be described by the equation $TOF = d\sqrt{0.5zeV}\sqrt{m/z}$ where d = distance to detector, zeV = kinetic energy applied and m/z = mass to charge, as this expression contains constants it can then be further derived, to $TOF = k\sqrt{m/z}$, where k is a proportionality constant [124].

To improve the resolution of a TOF mass spectrometer a reflectron can be incorporated, which is used to correct the kinetic energy distribution in the direction of ion flight. Without this correction, not all ions of the same *m/z* will arrive at the detector at the same time because ions are not formed with zero kinetic energy (e.g. at a standstill) and at exactly the same point. As ions of the same m/z ratio (but a spread of kinetic energies) enter the reflectron, those with higher kinetic energies penetrate deeper into the reflectron whereas those with lower kinetic energies take a slightly longer

path (Figure 19). The net result is that a packet of ions, which was spherical initially, is flattened to a disc and it is this disc-like packet of ions that hits the flat surface of the detector at the same time; this is sometimes referred to as TOF focus. A secondary advantage of this arrangement is that the flight path can be can doubled in any given space [125, 126].

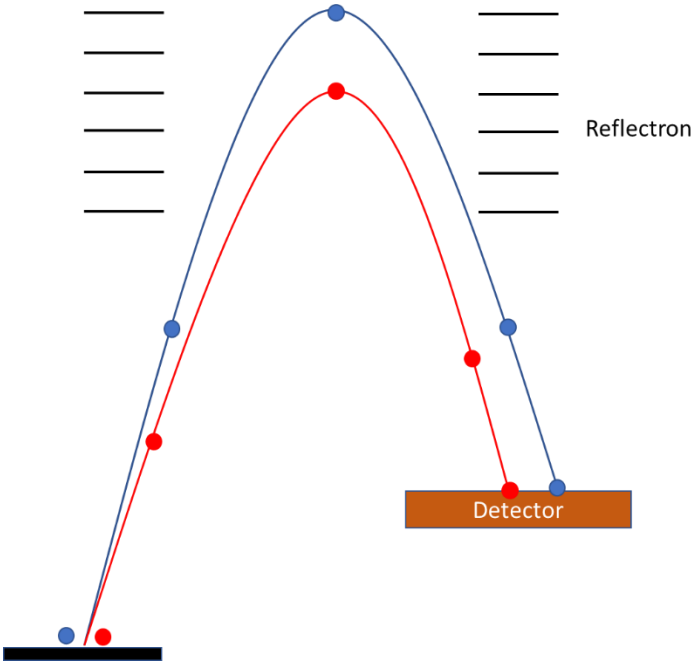

Figure 19 Reflectron schematic. Ions that enter the drift of a time of flight (TOF) mass spectrometer (MS) do not have the same kinetic energies even if they are of the same mass to charge ratio (m/z). The ions that have higher kinetic energies travel further into the reflectron than ions with lower kinetic energy meaning that ions of the same m/z are now travelling at the same speed and hit the detector at the same time. This arrangement also has the advantage of doubling the length of the drift space.

3 Experimental

3.1 Materials and Reagents

Table 2 Table of materials and reagents, function and supplier.

Equipment/Material	Function	Supplier
BupH^{tm} 50 mM sodium carbonate-biocarbonate buffer, pH 9.4	Coating buffer salt	ThermoFisher Scientific, Waltham, MA, USA
Passive coating plates (white, 96-Well)	Solid phase	
SuperBlock®T20 (PBS)	Blocking buffer	
20x phosphate Buffered saline buffer (PBS)	Wash buffer salt	
Tween 20	Wash detergent	
Opima® grade acetonitrile	Extract organic modifier	
Opima® grade methanol	CE solution	
Isopropyl alcohol	CE solution	
Bovine serum albumin (BSA)	Assay buffer protein	Sigma-Aldrich, St. Louis, MO, USA
1 M Dithiothreitol (DTT)	Reducing agent	
Glacial acetic acid	Acidifying reagent	
Formic acid	Acidifying reagent	
Hydrochloric acid (HCl)	Capillary rinse	
IdeZ protease	Digestion Enzyme	Promega, Madison, WI, USA
Human plasma	Standard/QC/ Blank matrix	GSK, Stevenage, UK
mAb	Reference material	
Non-neutralizing idiotypic antibody	Capture antibody	
mAb-2	Internal standard	
Mineral oil	Evaporation limiter	Sciex, Warrington, UK
TripleTOF 6600™	Mass spectrometer	
CESI 8000	Capillary electrophoresis	
Nano spray MS source fitted with OptiMS adapter	Mass spectrometer ion source	
OptiMS neutral cartridge	CE Capillary	
EL X 405	Plate washer	Bio-Tek instruments inc., Winooski, VT, USA

3.2 Preparation of Digested Neat mAb

A neat digest of mAb was prepared from the 10 mg/mL reference material, which was diluted to 50 µg/mL with phosphate buffered saline (PBS) (prepared by diluting 50 mL 20X PBS with 950 mL of ultra-pure water). 500 µL of the 50 µg/mL was added to a 1.5 mL protein LoBind™ Eppendorff tube with 500 µL (50 unit/mL) IdeZ protease enzyme and the mixture was incubated while shaking at 37 °C for 30 min to achieve cleavage at the hinge region of the Hc. Reduction of the disulphide bonds was carried out by adding 100 µL of 50 mM Dithiothreitol (DTT) followed by incubation at 65 °C for 45 min whilst shaking. The sample was then allowed to come to room temperature before 100 µL of neat glacial acetic acid was added and the resultant solution gently mixed. This gave a final total mAb solution concentration of 20.8 µg/mL, containing the Fc, Fd and Lc fragments. A 25 µL aliquot of the digested, reduced, neat mAb solution was placed into individual tubes and stored frozen at -80 °C for use throughout the development of the CE methods in this research project. Prior to injection onto the CE-MS system, a 25 µL aliquot was thawed and allowed to come to room temperature before 75 µL of acetonitrile was added and the solution gently mixed. 100 µL of the neat extract was added to a PCR vial insert and a single drop of mineral oil added to limit solution evaporation.

3.3 Preparation of Reduced Neat mAb

To determine the viability of removing the digestion with IdeZ protease, a solution of reduced neat mAb was prepared as follows. A 50 µg/mL solution was prepared as in section 3.2, 500 µL of the 50 µg/mL was added to a 1.5 mL protein LoBind™ Eppendorff tube and mixed with 500 µL of water (in place of the IdeZ protease solution). A 100 µL aliquot of 50 mM DTT was then added prior to incubation while shaking at 65 °C for 45 min; this solution was then allowed to come to room temperature before the addition of 100 µL glacial acetic acid. Again, this gave a concentration of 20.8 µg/mL in terms of the intact mAb, in the form of Lc and Hc present in the sample, prior to injection onto the CE-MS system. Here, a 25 µL aliquot of the reduced mAb solution was combined with 75 µL of acetonitrile in a PCR vial insert together with a single drop of mineral oil.

3.4 Preparation of Human Plasma Extracts

To assess the CE-MS method, extracts were generated using a 'pull down' approach with an idiotypic antibody to remove the mAb of interest from the plasma. A solution of coating buffer was prepared by adding 50 µL of non-neutralizing idiotypic antibody (2.4 mg/mL) to 10 mL of 50 mM sodium carbonate-bicarbonate buffer, pH 9.4 and mixing. A 100 µL aliquot was then added to each well of a 96 well passive coating plate, which was then sealed and incubated whilst shaking at 4 °C for at least 18 h to allow binding to take place. With the idiotypic antibody bound to the surface of the plate, the plate was washed with PBS containing Tween 20 (0.1 % v/v), through 5 cycles, on the automated plate washer in order to remove any excess coating buffer and therefore any unbound idiotypic antibody. The next step was to block any free binding sites that remained on the plate to prevent nonspecific binding; this was achieved by adding 100 µL of SuperBlock®T20 (PBS) to each well, the plate was then sealed and incubated for 30 min at 37 °C whilst shaking. During this step human plasma was spiked with reference material and diluted to 10, 25, 50, 100, 250, 500, 1000, 2500, 5000 or 10000 ng/mL. Each concertation then underwent a 10-fold dilution with PBS containing Tween 20 (0.1 % v/v) and Bovine serum albumin (BSA) (0.1 % v/v). After washing the plate (as before) 100 µL of the human plasma samples diluted with PBS mixture was added to each well, again the plate was sealed and incubated at 37 °C for 2 h. Then plate was then washed as before prior to the manual addition of 200 µL of PBS to each well. The process was repeated 4 times to ensure no surfactants remained. The reducing agent was then added, 20 µL of 50 mM DTT containing 4.75 µg/mL of mAb-2 (as internal standard), the plate sealed and incubated for 45 min whilst shaking at 65 °C. After reduction had taken place and the plate had cooled to room temperature, 5 µL of neat glacial acetic acid was added to stop the reaction and elute the mAb from the plate. At this point the plate was either sealed and stored at 4 °C if more samples had been generated than the 48-sample capacity of the CESI 8000, or a 75 µL aliquot of acetonitrile was added to each well and mixed before being transferred to a PCR vial insert with a single drop of mineral oil ready for injection.

3.5 Initial CE Conditions

Table 3 Initial CE separation conditions as provided by Sciex.

Separation Condition/Parameter	Buffer	CESI Setting	Duration
BGE	10% Acetic acid	-	-
Injection	-	10 kV	99 seconds
Separation	10% Acetic acid	30 kV, 10 psi	20 minutes

3.6 Mass spectrometer method

Analyses were carried out using a Sciex 6600 TripleTOF™ mass spectrometer, with a nano spray source fitted with an OptiMS cartridge adapter (Figure 20). The MS method was operated in TOFMS mode over the range 800 to 3000 *m/z* with an accumulation time of 750 ms, curtain gas set to 5 psi, ionspray voltage (ISV) between 1700 and 2000 (depending on capillary), collision energy of 15, time bins to sum at 64 and an acquisition time of 17 min.

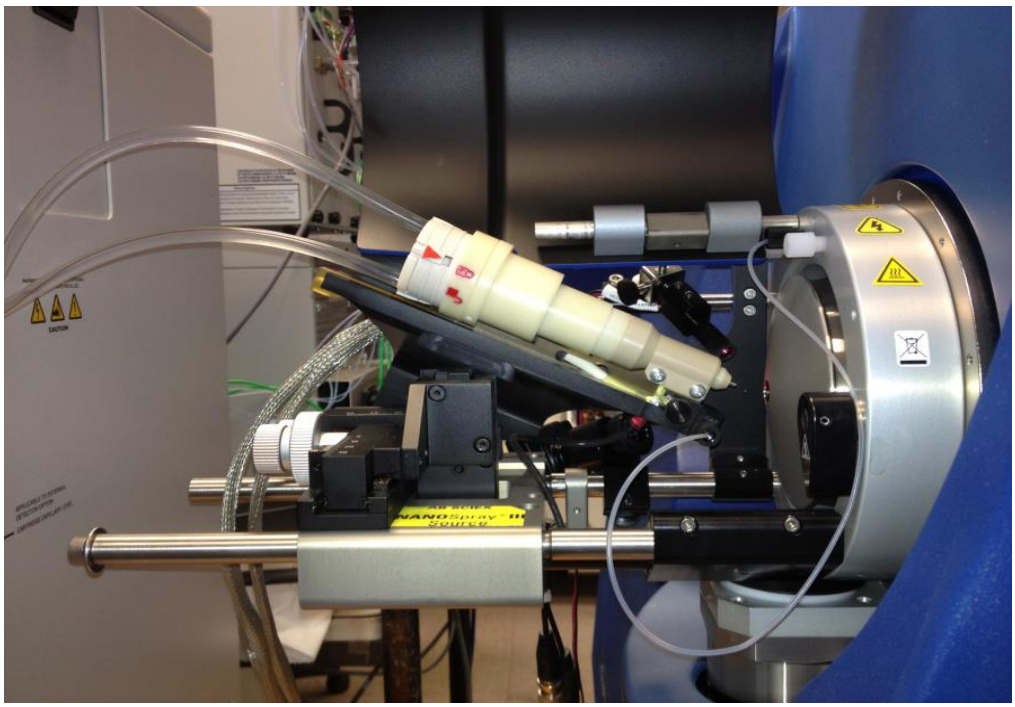

Figure 20 A Sciex nano spray source fitted with OptiMS adapter, with an OptiMS cartridge in place, the source has had the housing removed to show the adapter and cartridge more clearly [67].

3.7 CE and OptiMS Cartridge Set-up

3.7.1 OptiMS cartridge conditioning

Prior to use, the OptiMS cartridge required rehydration conditioning, which consisted of rinsing the separation capillary with 0.1 M hydrochloric acid (HCl) at 100 psi for 5 min followed by rinsing the conductive line with water for 3 min at 100 psi, followed by rinsing the separation line with water at 100 psi for 30 min. Once the flow was visually checked the emitter tip was placed into a tube containing water to prevent it from drying out. The final step in the conditioning process, was a low flow (5 psi) water rinse of the separation capillary for a minimum of 18 h (preferably longer and rinse times of up to 66 h were used over the weekend). The capillary was then ready for use. Alternatively, a shorter electrical conditioning procedure was used only after the cartridge has been previously used and stored correctly. This process also used the same initial 0.1 M HCl and water rinses, but the low pressure water rinse was replaced and instead both lines were filled with 50 mM ammonium acetate pH 3 for 3 min at 100 psi (after fitting the OptiMS sprayer housing into the source adapter). A 30 kV separation voltage was then applied with the flow of 50 mM ammonium acetate pH at 5 psi on both lines, the cartridge was then ready for use.

3.7.2 Spray evaluation

The sprayer must be adjusted to achieve the best position and spray stability, this was done using several different commercially available compounds, or by using one that was more compatible with the application. Sciex offer 2 compounds for spray evaluation: a peptide mix known as “pI 9.5 peptide” or a protein test mix. In this case a stored IdeZ digestion of neat material was used, however the process outlined below would be the same even if the commercially available material was used. The conductive line was rinsed at 100 psi for 2 min with acetic acid (10 %, v/v), the separation line was filled with IdeZ digest, prepared by diluting the 25 µL stored aliquot (section 3.2) with 75 µL acetic acid (10 %, v/v). A separation voltage of 30 kV was applied with a pressure of 1.5 psi to achieve a continuous infusion of material. Firstly, the ion spray voltage (ISV) was adjusted by

manually increasing the voltage from 1000 V in 100 V increments until the best ISV was achieved in terms of intensity of signal and spray stability (assessed by monitoring baseline fluctuation), usually an ISV of between 1500 and 2000 gave the best results, although the ISV was noted to vary between cartridges and sometimes alter the cartridge was stored. Second, the spray position was adjusted in three positions, proximity to the MS orifice, height in relation to the orifice and laterally, again the goal here was to achieve maximum intensity and spray stability over the parameters studied.

4 Results

Throughout this section the terms optimise, or optimisation of conditions will be used, these terms will be will be used to describe the selection of the best single method condition obtained in this study and does not refer to use of the term 'optimisation' as normally applied in multivariant analyses.

As shown in section 4.1 the initial starting CE conditions used (given in Table 3, section 3.5) to analyse mAb, (prepared as described in Section 3.2) did not produce an optimal electropherogram and attempts were made to improve the electropherogram for the quantification of mAb. When considering the optimal electropherogram produced by the CE method there were 3 main considerations: peak shape; analyte response in terms of peak intensity and run time. Absolute peak separation, or resolution, was not considered in the optimisation experiments due to the ability of the high-resolution mass spectrometer (Sciex 6600 TripleTOF) to separate mAb fragments on the basis of differing mass-to-charge ratios. When considering peak shape several experimental parameters were assessed to improve the electropherogram; EK injection (which can permit 'stacking' in a discontinuous buffer system (section 2.1.1)), pressure and BGE. These parameters will also contribute to the analyte response and migration time. Optimisation of the method may involve a compromise between these three parameters in order to achieve the best all round separation method.

4.1 Optimisation of the Capillary Electrophoresis Method

To establish and test a CE-MS method for the quantification of this mAb, sample extracts were obtained by digesting neat reference material or after the mAb underwent a 'pull down' from human plasma using an anti-idiotypic antibody as a capture antibody. The experimental methods are given in sections 3.2, 3.3 and 3.4. Initially, digested neat reference material samples were used to optimise the CE method as these samples did not include additional complicating factors such as

matrix effects from human plasma components. In later experiments, as the method development was refined, immunocapture of the mAb from human plasma was introduced to evaluate the performance of the method in as this was the physiologically relevant matrix.

The reference material was supplied at a mAb concentration of 10 mg/mL and was diluted to 50 µg/mL in a solution of PBS and 0.1 % Tween 20. Digestion with IdeZ was performed to cleave the mAb at its hinge region, followed by disulphide bond reduction. This procedure yielded 3 mAb fragments Fc, Fd or Lc regions (all approximately 25 kDa in mass), see Figure 1, and typical spectra are shown in Appendix 1, Appendix 2 or Appendix 3, respectively with the deconvoluted spectra (shown in Appendix 4) confirming the identity of each fragment. The digest mixture was divided into 25 µL aliquots and stored at -80 °C for use across the method optimisation experiments. An aliquot of the digest was thawed and diluted with 75 µL of acetonitrile which also contained 5 % acetic acid. The presence of acetonitrile and acetic acid was to facilitate the use of EK injection as a means of introducing the sample to the CE separation system. As mentioned in section 2.1.1, EK injection involves applying a constant voltage to the sample, in this case 10 kV for 99 s, which allowed the sample to migrate into the capillary. The initial data were collected over 17 min, with the fragments migrating between 11 and 13 min. Accounting for capillary loading, injection and wash steps the total cycle time was approximately 25 min.

The preliminary CE method was provided by Sciex and had been generated for an instrument demonstration of the CESI 8000 instrument. This method showed that the three expected mAb fragments (Fc, Fd and Lc) were generated and that m/z values of electropherogram peaks were consistent with the amino acid sequences. However, the peaks obtained were poor (with respect to peak shape and height) as shown in the reconstructed electropherogram in Figure 21. Here, a single charge state for each fragment was plotted using *m/z* 1260 Da, 1282 Da or 1301 Da, for the Fc, Fd or Lc, respectively). Peak shape was extremely poor particularly for the Fc fragment with peak splitting evident confirming that further improvement of the CE method was required. It was theorised that

the peak shape observed was poor due to band broadening either as a result of the pressure applied during the separation resulting in parabolic flow within the capillary or due to diffusion of the sample as it migrated through the capillary over the relatively long injection time of 99 s; which was chosen to maximise the loading amount of analyte.

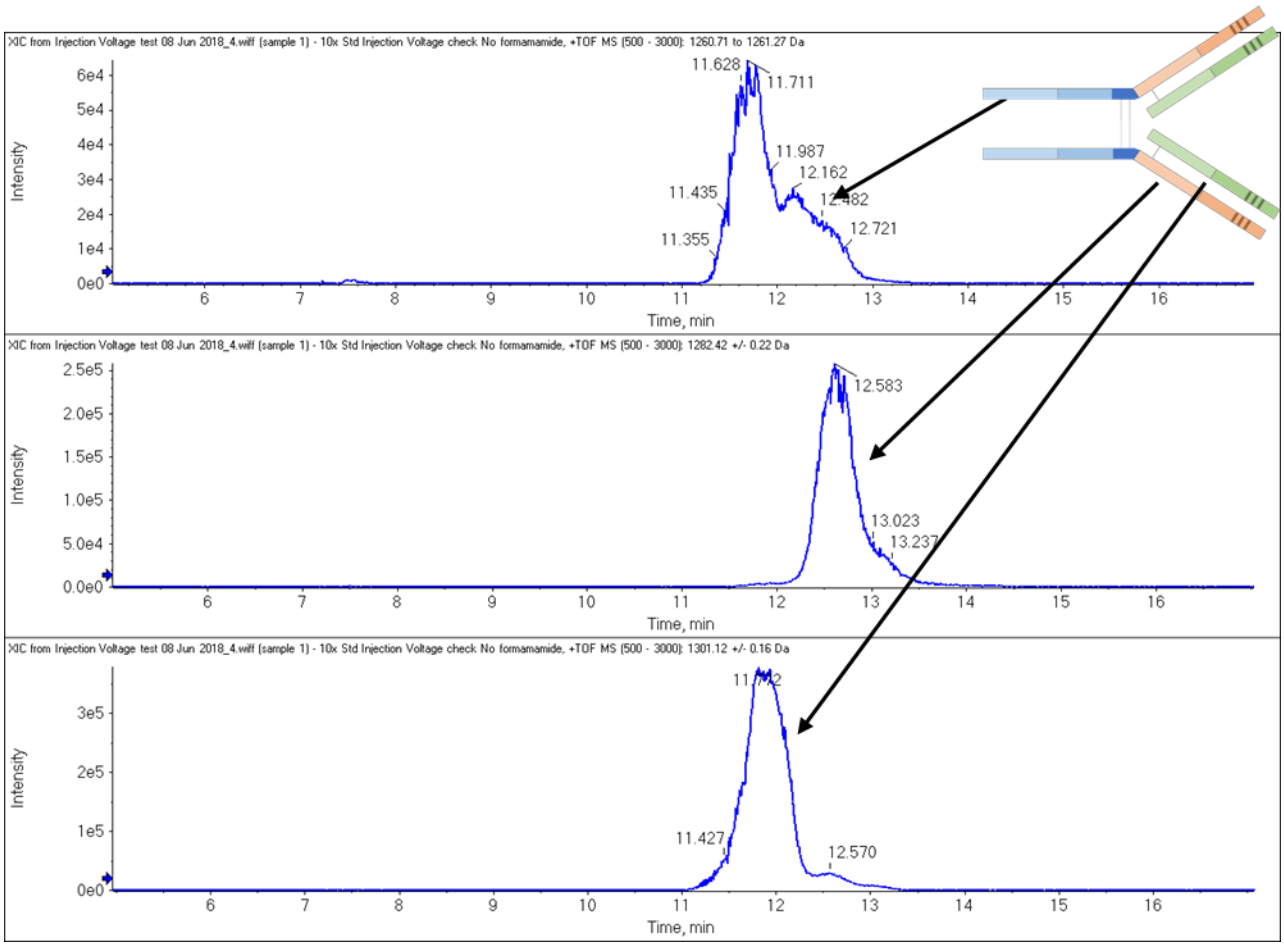

Figure 21 Electropherogram generated with starting conditions showing the three fragments of the mAb following digestion with immunoglobulin degrading enzyme (IdeZ). Top to bottom: Fragment crystallisable (Fc), heavy chain portion of the fragment antigen binding (Fab) region (Fd) and light chain (Lc).

4.1.1 Introduction and optimisation of a discontinuous buffer system

A discontinuous buffer system was introduced to improve peak shape by influencing changes in conductivity (and pH). A change in conductivity meant that the mAb fragments would migrate at a different rate, when compared to injecting directly into the BGE, leading to the phenomenon known sample stacking (section 2.1.1). This discontinuous buffer system was achieved by the introduction of an ammonium acetate plug prior to EK sample injection. Furthermore, it was necessary to introduce a two-stage pressure approach so that the parabolic flow profile caused by the application

of pressure did not override the 'stacking' effects of the ammonium acetate plug. Initially, a plug of 0.5 M ammonium acetate at native pH (20 s at 1 psi) was inserted prior to the introduction of the mAb digest along with a 30 kV separation. The two stages of pressure were applied as follows: 1 psi for the first 8 min then 10 psi for a further 8 min. These initial conditions were chosen to give an injection plug of sufficient size and to provide different conductivities without generating sample plugs with increased viscosity (which can be a problem at high concentrations of ammonium acetate).

Introduction of the ammonium acetate plug, along with the two-stage pressure injection resulted in much improved peak shapes (see Figure 22) and peak symmetry was markedly better for the Fd and Lc fragments. However, the Fc fragment still exhibited some tailing indicating that band broadening was still occurring and therefore further improvement of method was required. Options to improve the Fc electropherogram included: alteration of the concentration and/or size of the ammonium acetate plug with the goal of increasing the stacking effect; or optimisation of the two-stage pressure step in order to limit the effects of the application of pressure. There was the possibility, however, that altering these two parameters would not lead to an improved peak shape because of conformational flexibility in solution of the Fc fragment, exhibiting differing degrees of folding. In this instance, two or more conformers would be migrating differently in the buffer system within the capillary as mobility is dependent of the mass-to-size ratio.

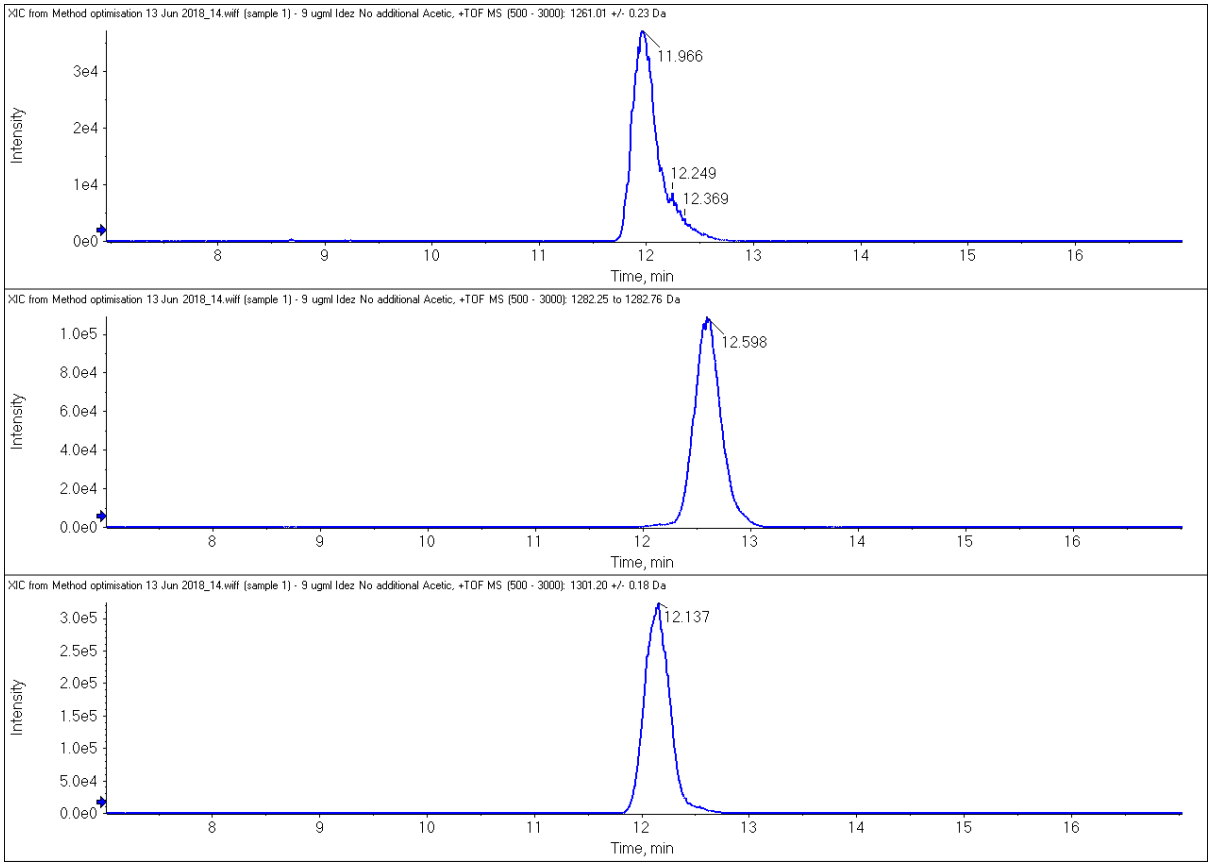

Figure 22 Electropherogram showing the three Immunoglobulin degrading enzyme (IdeZ) induced fragments, fragment crystallisable (Fc) (top), heavy chain portion of the fragment antigen binding (Fab) region (Fd) (middle) and light chain (Lc) (bottom) after introduction of an ammonium acetate plug and two stage pressure separation, allowing for stacking and a reduction in band broadening.

Altering the concentration and volume of the ammonium acetate plug was assessed first to further improve the separation process. Injections of digested mAb solution were introduced into buffer systems containing plugs of 0.5 M, 1 M, 2.5 M or 5 M ammonium acetate (Figure 23). As shown, increasing the concentration of ammonium acetate had an effect on migration times of each fragment while decreasing resolution, but had very little effect on the peak shape. An increase in concentration directly correlated with an increase in migration time as higher acetate concentrations lead to lower conductivities and hence smaller electric fields.

Increasing the concentration of the ammonium acetate plug also decreased peak resolution of the three mAb fragments. With 1 M ammonium acetate (Figure 23 top), Fd and Lc peaks showed signs of resolution (Rs = 0.55, see Appendix 5 for calculation) but as the ammonium acetate concentration increased to 5 M (Figure 23, bottom) they almost co-migrate (Rs = 0.40, see Appendix 5 for calculation). In summary, the use of an ammonium acetate plug improved peak shape for all three

fragments when compared to direct injection into the BGE. However, there was no improvement in peak shape when acetate concentrations greater than 1 M were used, and so this concentration was chosen to provide the best separation with respect to migration time, peak shape and resolution.

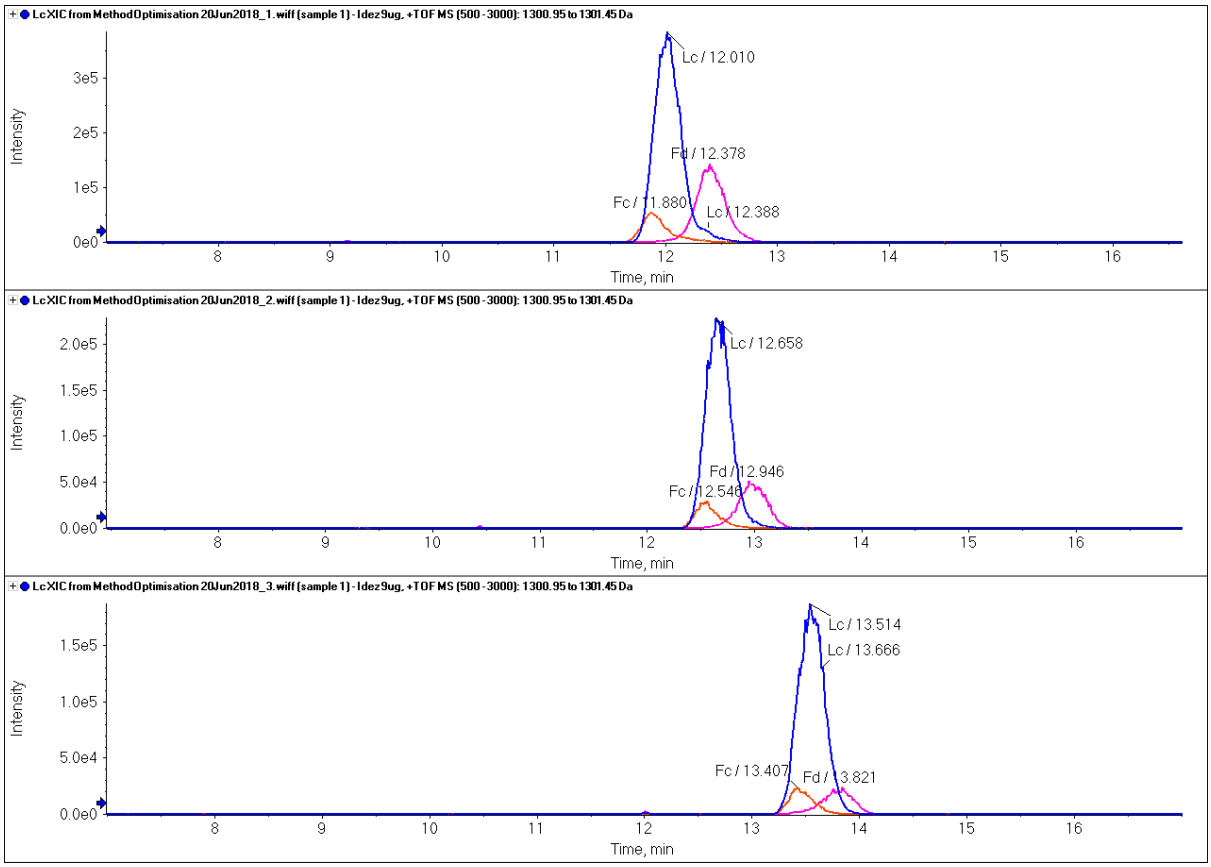

Figure 23 Electropherograms showing the effect of increasing the concentration of the ammonium acetate plug prior to introduction of sample, 1 M (top), 2.5 M (middle) and 5 M (bottom) concentrations on the fragment crystallisable (Fc) (orange), heavy chain portion of the fragment antigen binding (Fab) region (Fd) (pink) and light chain (Lc) (blue) mAb fragments.

It should be noted that an increase in ammonium acetate concentration also inversely influences the MS signal intensity generated. Table 4 lists the Lc fragment peak heights where a 2-fold decrease in sensitivity was observed for an ammonium acetate concentration increase from 1 to 2.5 M, which is a notable increase. When considering this in the context of the application of this method, lower peak sensitivity leads to higher detection limits, ultimately meaning less well-defined PK for the mAb. This was a second reason to choose a 1 M ammonium acetate plus for further experiments.

Table 4 The effect of concentration of the ammonium acetate plug on peak height of the Lc fragment.

Concentration of Ammonium Acetate Plug (M)	MS Response (peak height) of LC Fragment (ion counts per second)
1	5.0e5
2.5	2.5e5
5	2.1e5

Following selection of the ammounium acetate plug concentration, attention was turned to varying the pressure used to inject the plug or the duration of the injection. Since increasing the duration of the injection contributes to the cycle time, changes to the size of the plug were achieved by adjusting the pressure. A series of injections of the digest solution were carried out by introducing the 1 M ammonium acetate plug at 0.5, 1, 3, 5, 7, 9, 11, 15, 17 or 20 psi. Using the Lc fragment as in an indicator of peak performance, Figure 24 illustrates the steady increase in migration time observed with increasing pressure; similar to the trend observed when increasing ammonium acetate concentration. Again, the size of the injected plug had little or no effect on peak shape. There was, however, a slight impact on MS response when injection pressures above 3 psi were used. A reduction in signal intensity (peak height) was observed. Overall these experiments were used to select conditions that used a 1 M ammonium acetate plug injected at a pressure of 1 psi for 20 s.

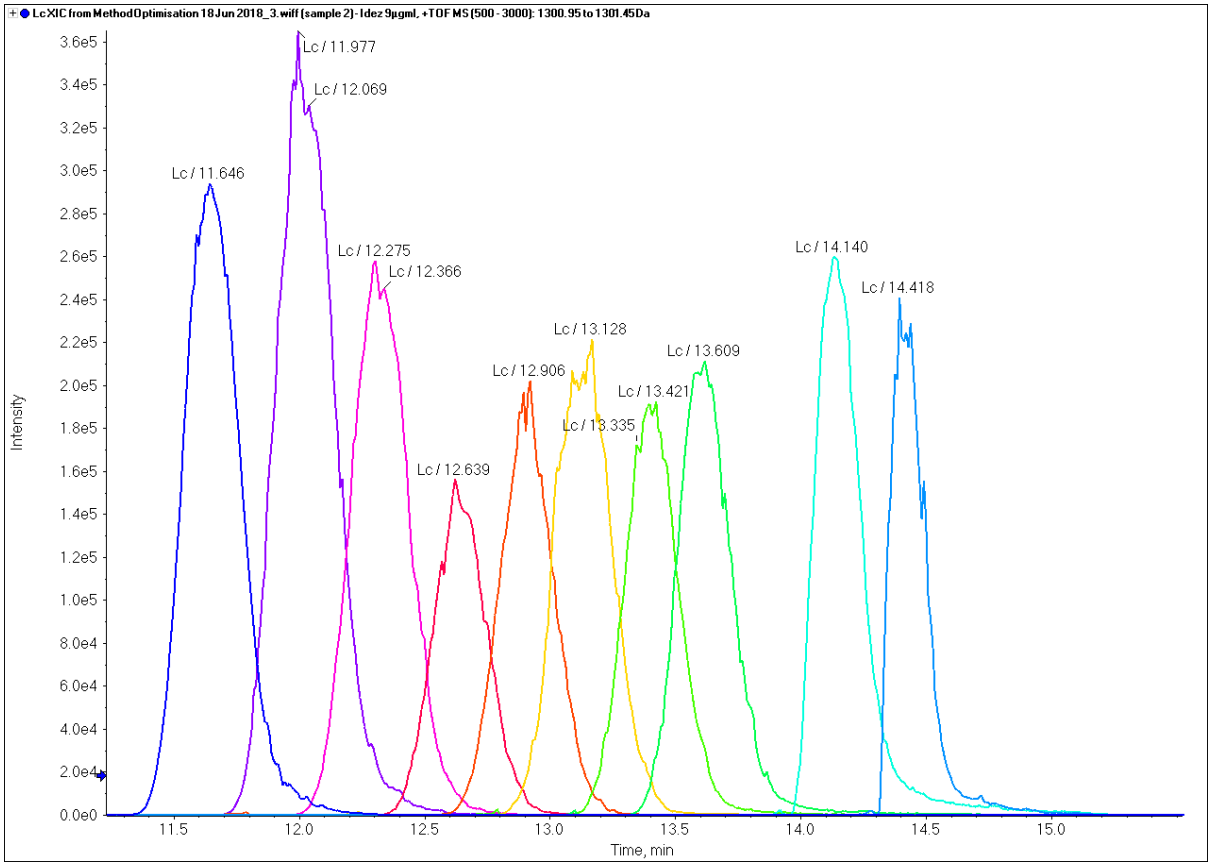

Figure 24 Overlaid electropherograms of the light chain (Lc) fragment after varying the size of the ammonium acetate plug by adjusting the pressure at which the plug is injected. The overlaid electropherograms from the Lc fragment left to right represent plug sizes 0.5, 1, 3, 5, 7, 9, 11, 15, 17 or 20 psi.

In order to use the discontinuous buffer system and take advantage of the stacking effects of the ammonium acetate plug, a small amount of conductive electrolyte solution must be injected prior to EK injection. This is due to the low conductivity of the plug impeding a voltage-based injection. This allowed further opportunity for method optimisation of 3 different electrolyte solutions: acetic acid at 1 % and 15 % (which is the BGE) or 1% formic acid. Higher levels of formic acid were not considered because of higher viscosity of this acid compared to acetic acid. Acetic acid and formic acid were selected for investigation as they are compatible with mass spectrometry.

The effects of modifying the injection plug with acetic or formic acid were minimal (Figure 25), however, 1 % formic acid was shown to give minor advantages when compared to 1 % acetic acid or BGE of 15 % acetic acid in terms of peak shape, MS response and resolution. Minor differences in migration time were also observed between the 3 electrolyte solutions. Based on the observed results, the conditions selected for a discontinuous buffer system were: a pre-injection plug of 1 M

ammonium acetate at 1 psi for 20 s, followed by injection of 1 % formic acid at 1 psi for 20 s. This system resulted in good peak shape for both the Lc and Fd fragments, the Fc fragment did continue to exhibit tailing, but showed some improvement over the initial conditions assessed in Section 4.1.

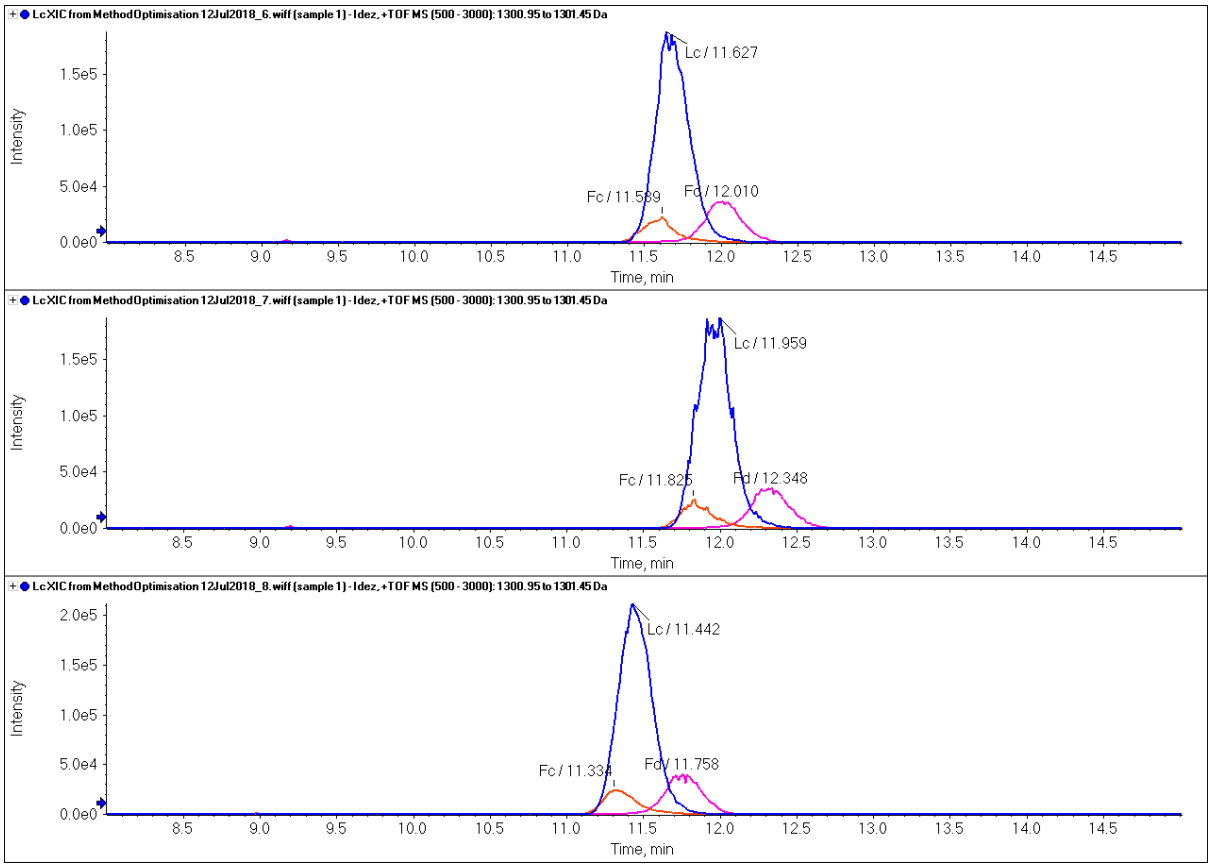

Figure 25 Effect of the composition of the injection plug 15 % acetic acid (top), 1 % acetic acid (middle) and 1 % formic acid (bottom) on the 3 mAb fragments, fragment crystallisable (Fc) in orange, heavy chain portion of the fragment antigen binding (Fab) region (Fd) in pink and light chain (Lc) in blue.

4.1.2 Optimisation of the two-stage pressure separation

Pressure is applied to the capillary to create flow, with greater pressure there will be higher flow rates. This has several consequences, including the possibility of creating a parabolic flow profile, band broadening and poor peak shape. With increased pressure also comes reduced migration times resulting in less time for the analyte to resolve. However, pressure helps to generate a consistent, steady spray at the emitter tip and therefore provides a more reproducible MS response. A two-stage pressure separation takes advantage of the benefits of applying pressure while limiting the drawbacks; this means applying low pressure at the start of the CE method allowing separation

to occur on the basis of molecular properties (charge-to-size ratio of the analytes). Ions that may cause suppression to the MS response, like excessive amounts of ammonium acetate from the plug, will travel faster through the capillary and co-elute with the analytes of interest, and for some separations this will also increase resolution between analytes. Once the desired separation has been achieved the pressure can be increased, both speeding up osmotic flow through the capillary and improving spray from the emitter tip; this would reduce the overall run time whilst maintaining the integrity of the capillary separation.

When determining the best conditions for a two-stage separation, the pressure and duration of each stage must be considered. For stage one (application of low pressure) the key factor was found to be time (Figure 26). A pressure of 1 psi was selected as the lowest for practical use and the duration was assessed over 2, 4, 6 or 8 minutes (Figure 26). For stage two (application of higher pressure) the pressures assessed were 5, 10 or 15 psi (Figure 27). The electropherograms indicated that a combination of 1 psi for 8 min followed by 15 psi for 6 min provided a good balance between peak shape, resolution of the three mAb fragments, MS response and overall run time per injection. The resolution between the Lc and Fd fragments remained stable with varying the pressure in stage two at approximately 0.5 at both 5 and 15 psi, 10 psi showed lower resolution (0.36), largely caused by the fronting observed with Fd fragment, see Appendix 6. Longer migration times were noted when the pressure application in stage 1 was held at 1 psi for longer, which was due to lower osmotic flow through the capillary (the migration of analyte heavily relies on its EOM to move towards the cathode). For stage two the migration time reduced with increasing flow rate as analytes are carried in the moving BGE.

There are now two final parameters to consider, the effect of varying the BGE on the separation, and lastly the effect of the injection voltage.

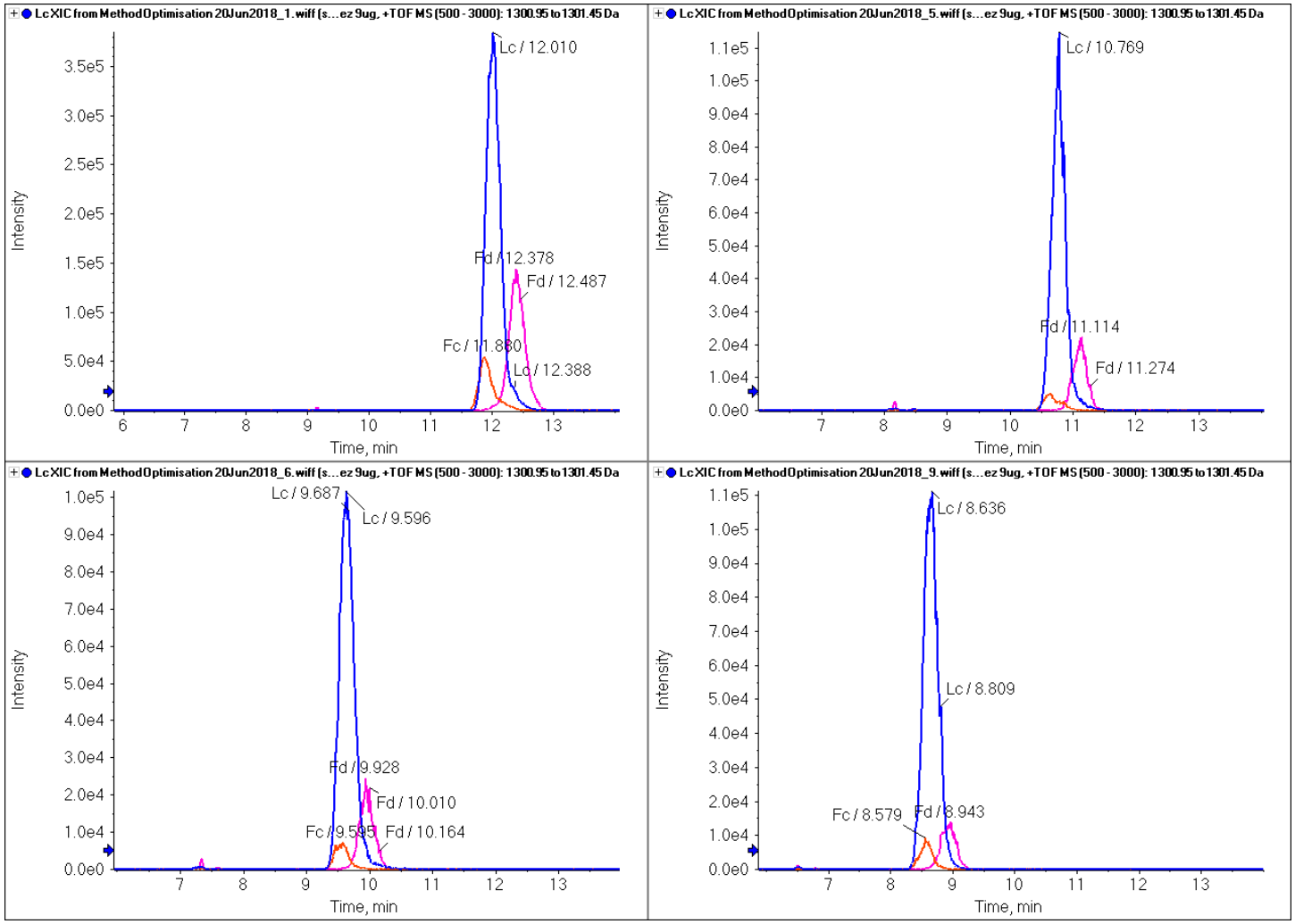

Figure 26 The impact of varying the duration of the 1 psi stage (first) of the separation. 8 min (top left), 6 min (top right), 4 min (bottom left) and 2 min (bottom right) on the 3 mAb fragments, fragment crystallisable (Fc) in orange, heavy chain portion of the fragment antigen binding (Fab) region (Fd) in pink and light chain (Lc) in blue.

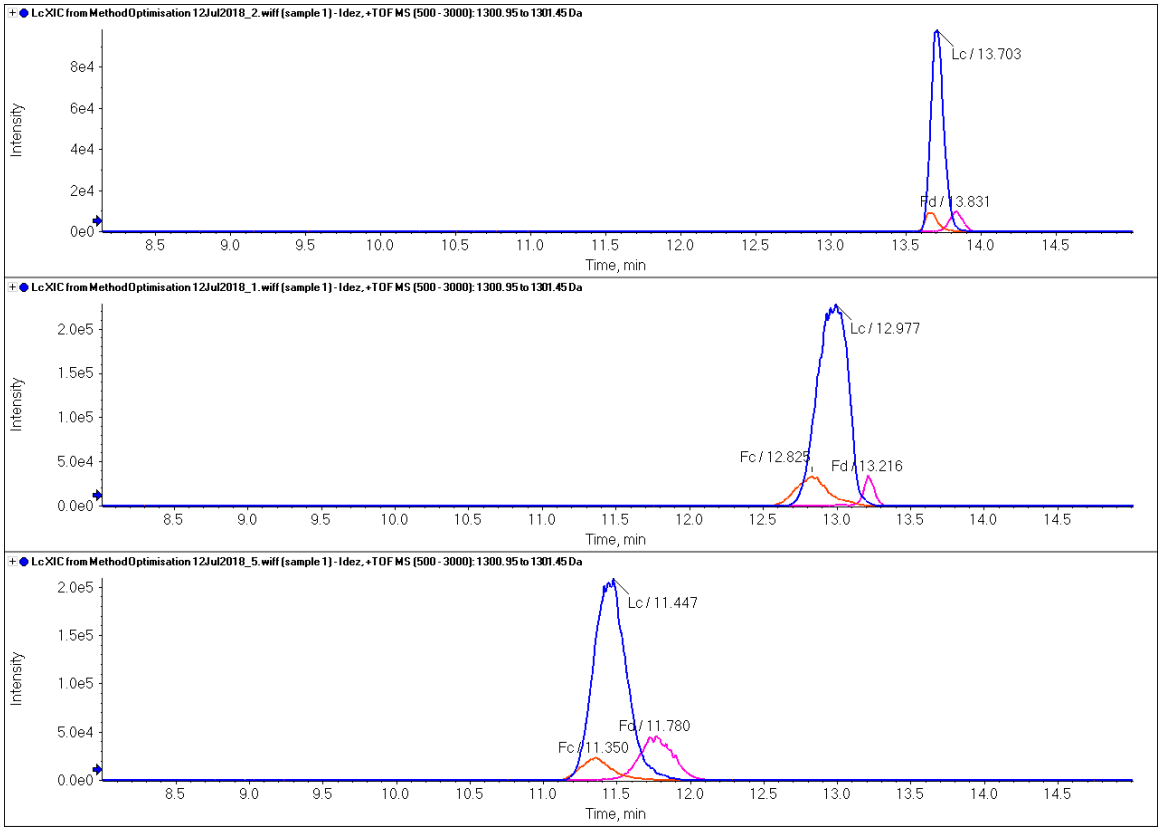

Figure 27 The effect of varying the pressure used as stage 2 of the separation, 5 psi (top) 10 psi (middle) and 15 psi (bottom) on the 3 mAb fragments, fragment crystallisable (Fc) in orange, heavy chain portion of the fragment antigen binding (Fab) region (Fd) in pink and light chain (Lc) in blue.

4.1.3 Optimisation of the background electrolyte

The BGE is key to achieving good peak shape and may give rise to increases in sensitivity for the three mAb analytes. Injections were carried out to evaluate six different BGE conditions, 1, 2, 5, 15 or 20 % (v/v) acetic acid along with a mixture of formic acid (1 %, v/v) and isopropyl alcohol (IPA, 10 %, v/v). As mentioned previously, organic solvents such as IPA are important to reduce the viscosity of the BGE in order to maintain acceptable normal pressures within the capillary. The higher levels of acetic acid, 15 and 20 % (v/v) in the BGE, realised the most favourable conditions and provided the most improved all-round response (Figure 28). There was minimal difference in peak shape, migration time and separation of fragments with 15 % or 20 % acetic acid, although at 15 % acetic acid, the MS response (peak height) was greater. Acetic acid concentrations of 5 % and below in the BGE reduced the quality of the peaks shape and reduced the MS response. Observation of resultant

data (see Figure 28) indicated that there was some improvement when using the formic acid/IPA mixture over 1 % acetic acid, but the peak shape and migration time did not improve significantly enough to match results obtained with higher acetic acids concentrations.

As there was little difference in the data obtained with the BGE when using 15 % or 20 % v/v acetic acid, 15 v/v % was used in future analyses. Moreover, use of 20 % acetic acid in the BGE increased the viscosity of the solution to a point where there may have been issues with the capillary.

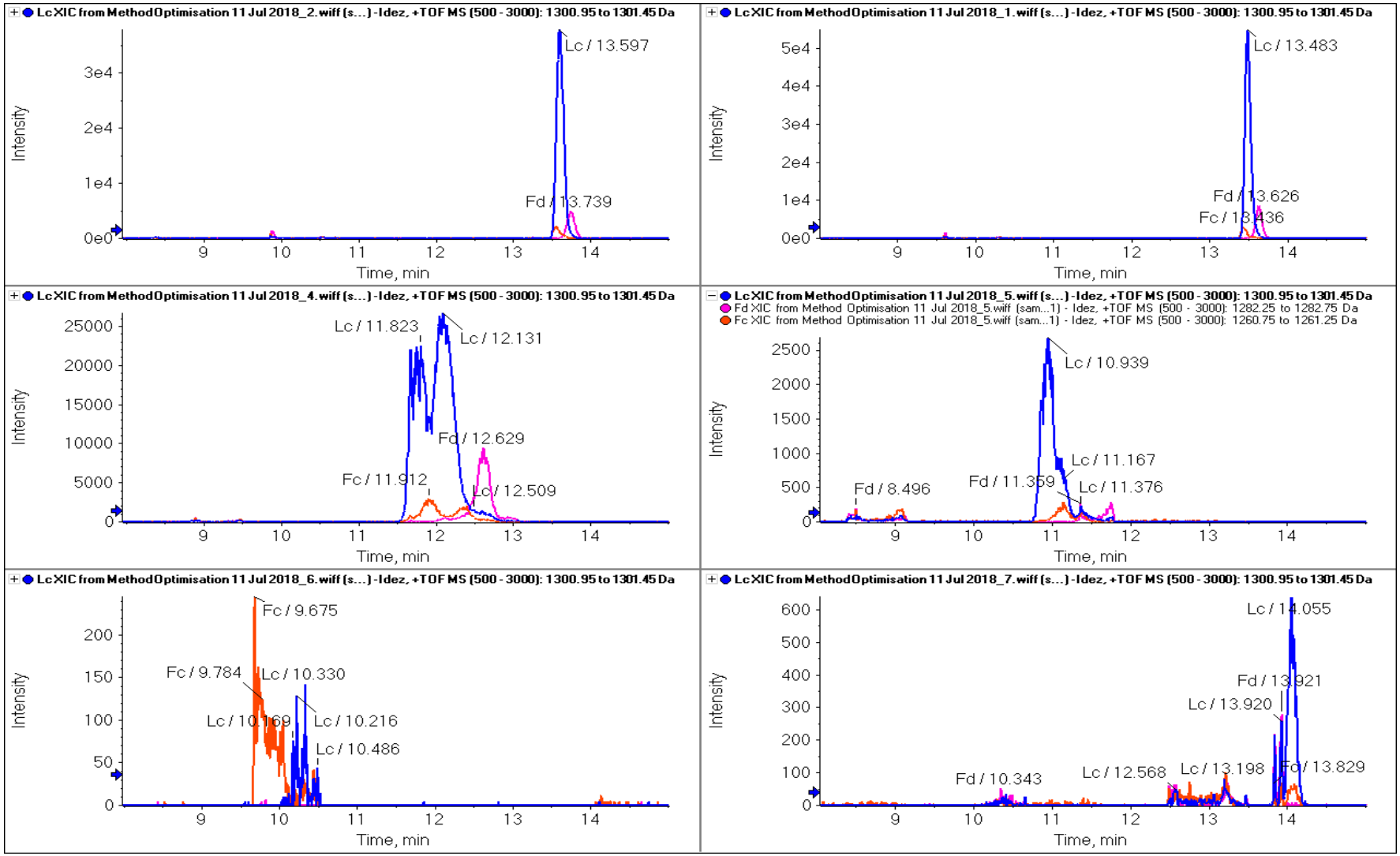

Figure 28 Effect of background electrolyte composition on the separation, response and migration of the three mAb fragments; BGE composition 20% acetic acid (top left), 15% acetic acid (top right), 5% acetic acid (middle left), 2% acetic acid (middle right), 1% acetic acid (bottom right) and 1% formic acid plus 10% IPA (bottom right).

4.1.4 Effect of varying the voltage used for sample introduction

There are two ways that the EK injection can be altered; by varying the voltage or by varying the time that voltage is applied. The EK injection of the sample was altered by adjusting the voltage applied to the sample only. Three EK injection voltages were assessed, 1, 5 or 10 kV. As expected, the voltage had a direct impact on the MS response with an injection voltage of 10 kV giving the greatest signal in terms of peak height (Figure 29). Increasing the voltage negatively impacted peak shape, with 10kV also giving rise to peak fronting, particularly for the Fc fragment. However, it was concluded that the increase in MS response with a 10kV injection was of more importance than the slight deterioration in peak shape.

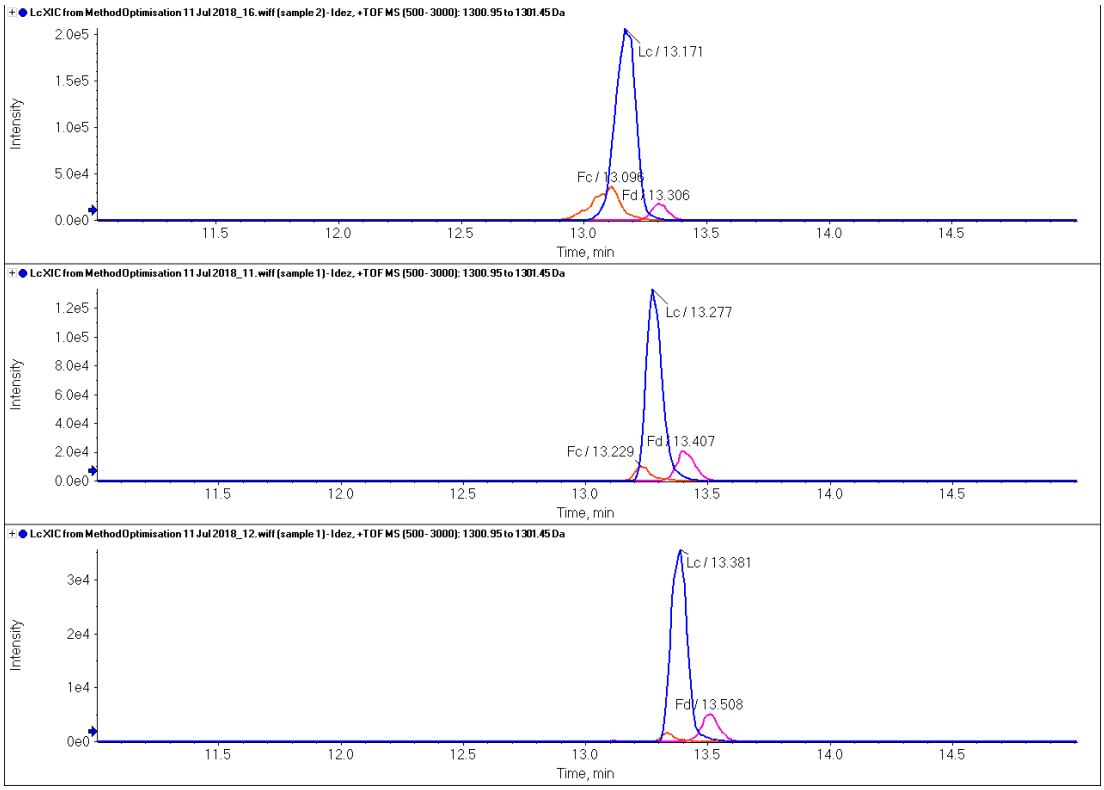

Figure 29 Effect of injection voltage on response and separation of the three mAb fragments. Injection voltage 10 kV (top), 5 kV (middle) and 1 kV bottom.

4.1.5 The final separation method

Table 5 lists the final method parameters after adjustment of all the operating conditions. The electropherogram (

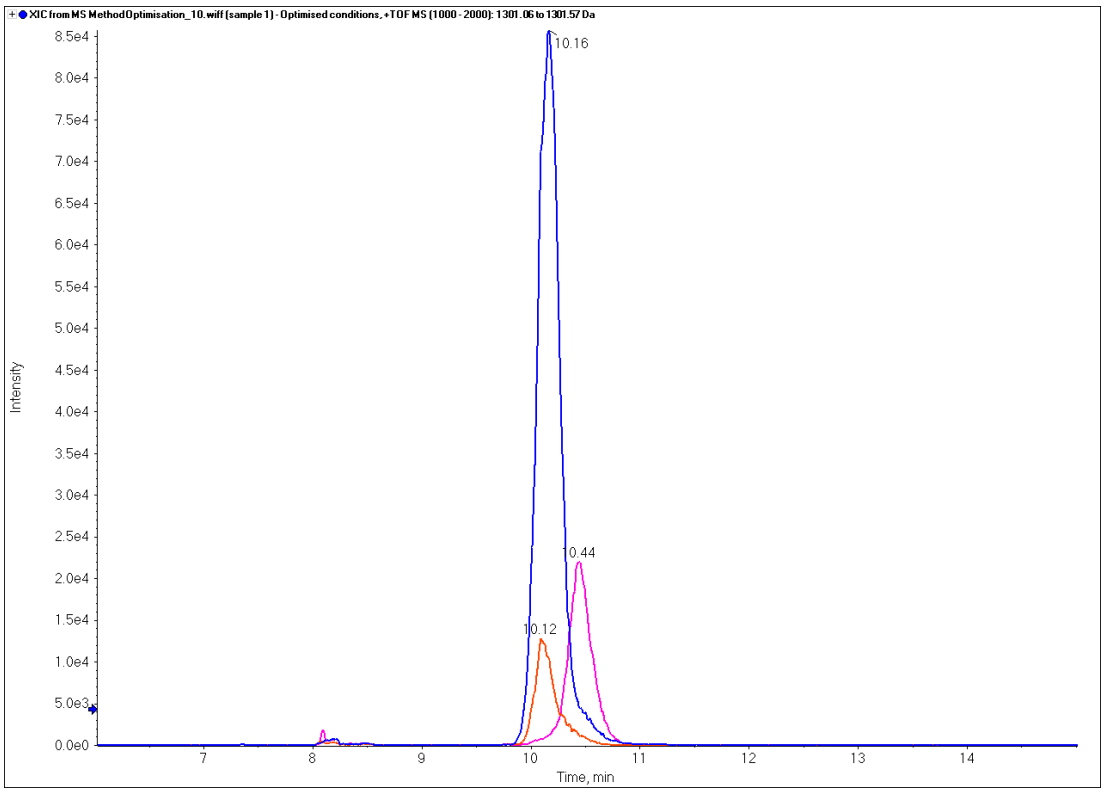

Figure *30*) exhibited good peak shape (albeit with some tailing on the Fc fragment), good MS response (peak height) and migration times of less than 11 min for all 3 mAb fragments. Implementation of the discontinuous buffer system with 1 M ammonium acetate plug followed an injection plug of 1 % formic acid (v/v) was an effective means of inducing sample stacking and reducing band broadening during the sample introduction. Dividing the application of pressure into two stages during the separation phase was also effective at minimising band broadening, thereby providing a degree of resolution between the mAb fragments while inducing sufficient flow through the capillary for a steady spray at the emitter tip. BGE of 15 % acetic acid (v/v) provided good peak shape, resolution and sensitivity and maintaining a sample injection voltage of 10 kV maximised the sample loading and therefore the MS response, meaning the lowest possible limit of quantification.

Table 5 Final optimised separation condition/parameters.

Separation Condition/Parameter	Buffer	CESI Setting	Duration
BGE	15% Acetic acid	-	-
Pre-injection plug	1 M ammonium acetate	1 psi	20 seconds
Injection plug	1% formic acid (v/v)	1 psi	20 seconds
Injection	-	10 kV	99 seconds
Separation	-	30 kV, 1 psi	8 minutes
		30 kV, 15 psi	6 minutes

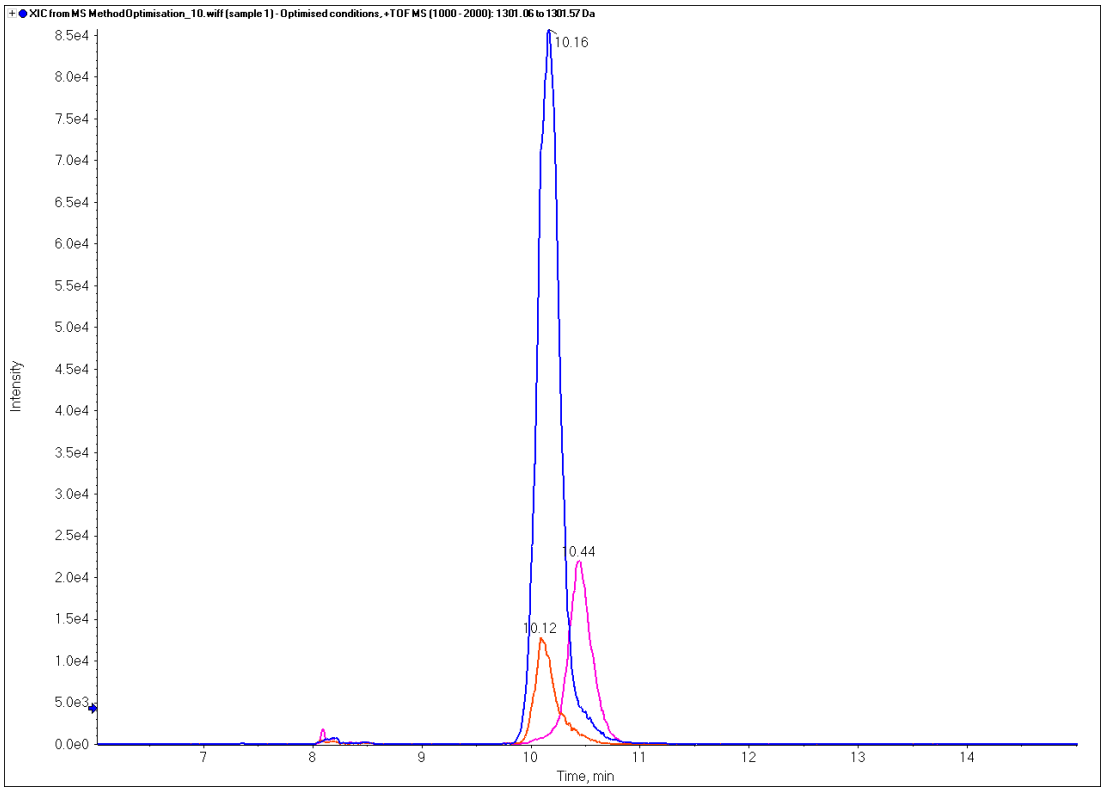

Figure 30 Electropherogram of the three mAb fragments using the final CESI separation method.

4.1.6 Simplification of the sample preparation

Having established the optimal condition for the CE separation further improvements were investigated with the sample preparation. IdeZ cleaves the Hc at the hinge and after disulphide reduction with DTT giving rise to the three mAb fragments. As already seen previous figures, the Fc fragment performs the most poorly both in terms of MS response

and CE separation, making it very difficult to use in a quantitative mass spec assay for the determination of PK profiles.

If the IdeZ cleavage step could be removed then there would be potential advantages, simplifying the sample preparation and reducing the sample preparation time by 30 min. A further advantage would be pre-concentration as the total volume of the extract would be reduced. Removal of the IdeZ digestion and moving straight to disulphide reduction would mean that the Fd and Fc fragments would remain connected, or in other words, the Hc would remain intact. This would result in 2 (Lc and Hc) fragments rather than 3 (Lc, Fd and Fc) and should have no effect on the Lc. However, method performance for the resulting Hc fragment would need to be assessed in terms of MS response and CE separation. Figure 31 illustrates an electropherogram generated using the final optimised CE separation method (Table 5) of the Lc and Hc as well as a deconvoluted MS spectra (the charge envelopes can be seen in Appendix 8 and Appendix 9, respectively). The Lc fragment gives the greatest MS response while the Hc signal is comparable to that of the Fd fragment. The two peaks are still not resolved, however, although it would have been preferable to achieve electrophoretic resolution it would mean too much of a compromise in terms of run time and potentially peak shape. Absolute resolution is not considered a major issue, given the resolution of the TripleTOF 6600™. The spectral resolution in terms of mass-charge-ratio allows for the either peak to be used for quantification.

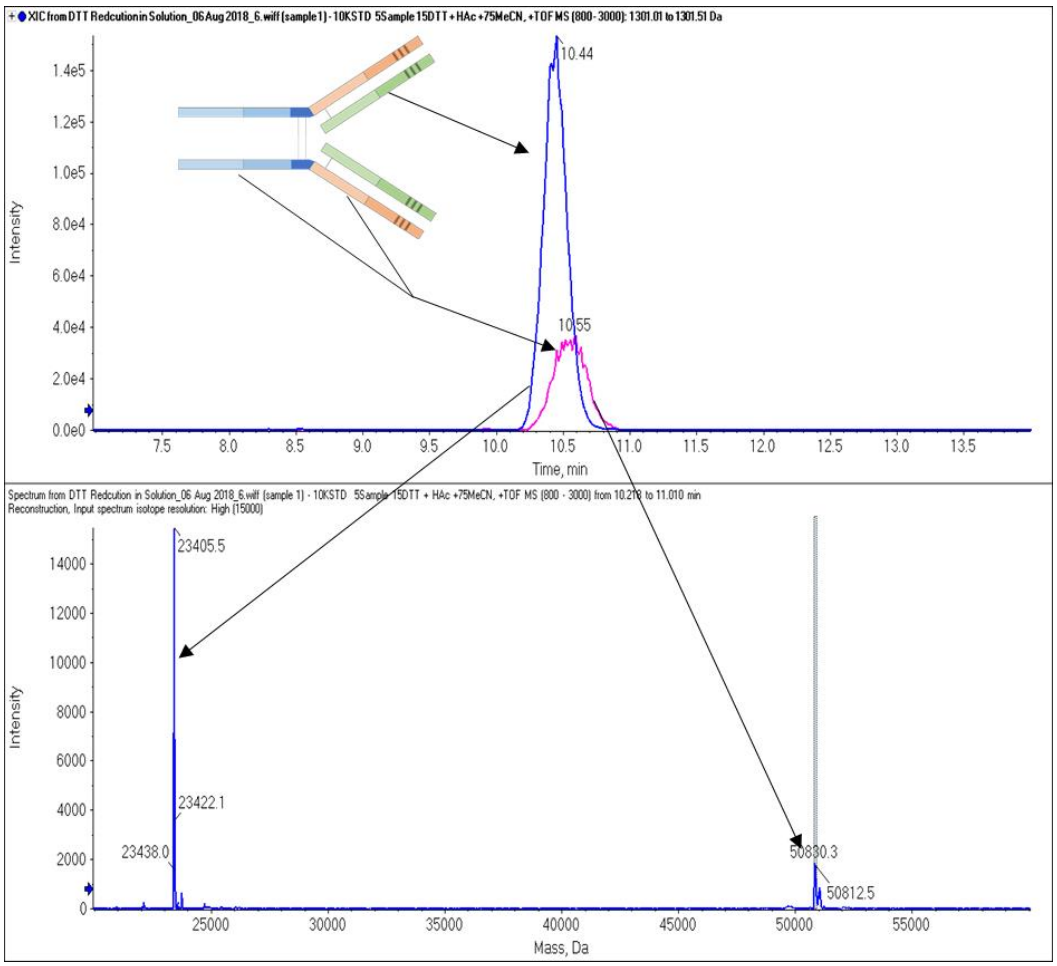

Figure 31 Top: reconstructed electropherogram for both light chain (Lc), and heavy chain (Hc). Bottom: a deconvoluted spectrum showing the mass of the reduced Lc and Hc of the mAb.

4.2 Assessment of the Performance of the Developed CESI-MS Method for the Quantification a mAb

After completion of the method improvements using the reference material digest, the ability of the method to be used for the quantification of the mAb in human plasma needed to be assessed, in terms limit of quantification, linearity over a concentration range, injection to injection reproducibility and stability of migration time. These parameters were evaluated using spiked human plasma spiked with mAb followed by 'pull down' extraction as outlined in section 3.4.

To assess the limit of quantification and linearity, a calibration curve for the mAb was prepared in human plasma over the range of 10 to 10,000 ng/mL in human plasma and samples prepared according the method in section 3.4 and analysed using the CE and MS methods in sections 4.1.5 and 3.6, respectively. At this point a second mAb with a different amino acid sequence was included at the reduction step to act as an internal standard and aid reliable quantification. When considering the lower limit of quantification for a viable analytical method in a regulated environment any response in blank plasma needs to be less than 20 % of the response of the analyte. Table 6 shows data for generated from the analysis of the human plasma calibration curve after quantification using Sciex processing software Multiquant™ and the IQ4 algorithm to generate peak areas, calculated concentrations and accuracies with quantification based on the single most abundant charge state (≈1301 *m/z*). The two lowest concentrations 10 and 25 ng/mL were not acceptable as there was a significant peak observed in the samples from blank plasma. Therefore, the lower limit of quantification for this method was 50 ng/mL in human plasma (Figure *32*) with associated signal-to-noise ratio of approximately 20:1. There is potential for improvement in the quantification limit by removal of the peaks in blanks, which was most likely caused by carryover from the outside of the capillary. Inclusion of additional dip steps could potentially remove this.

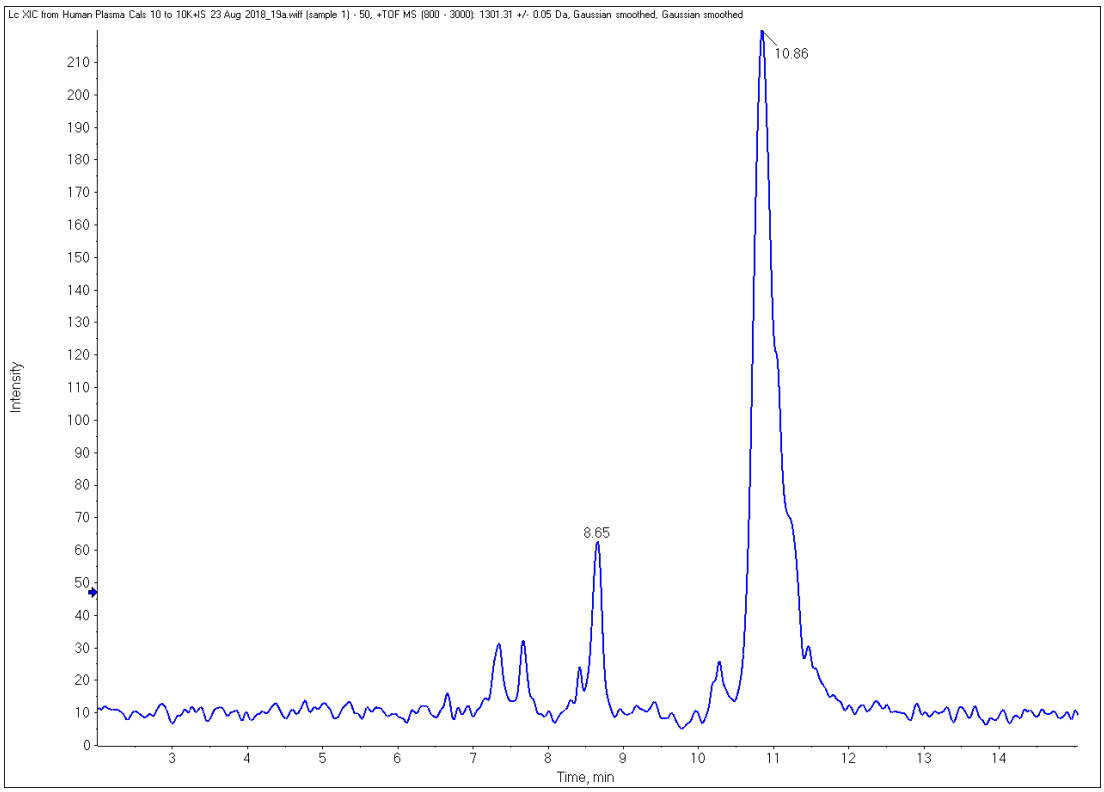

Figure 32 Electropherogram of 50 ng/mL in human plasma after immuno capture. This reconstructed electropherogram is based on a single chart state of the light chain (Lc) at m/z 1301.3, generating a signal to noise ratio of 20:1

Although the standard curve generated from the experiment was not linear (Figure 33), there was good agreement with the back-calculated and nominal concentrations utilising quadratic fit and with a 1/x weighting. Indeed, over the range 50 to 10,000 ng/mL the back-calculated concentrations range between accuracies of 85 % to 111 %, which were within the +/- 15 % limits of regulated LC-MS based methods.

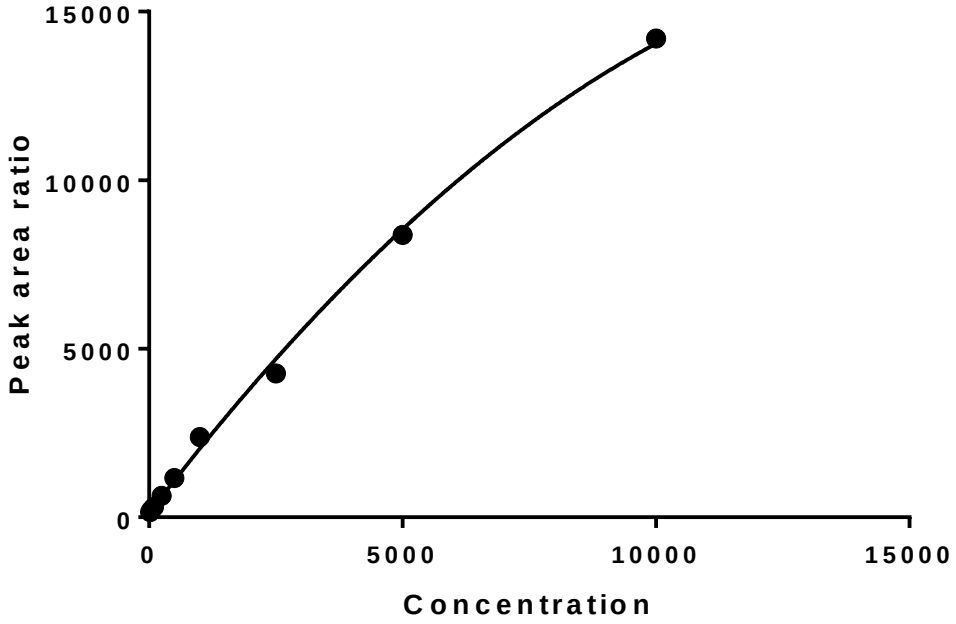

Figure 33 A single representative calibration curve, from extracted human plasma samples, based on peak area ratio of a single, most abundant charge state (≈1301 m/z) of the light chain (Lc) with a 1/x weighting applied.

Table 6 Area and accuracy of a standard line from 10 to 10,000 ng/mL in human plasma after immuno capture and CESI-MS analysis for a single charge state of the Lc. Data generated using Sciex Multiquant™ and IQ4 peak integration algorithm.

mAb Concentration in Human Plasma (ng/mL)	Calculated mAb Concentration (ng/mL)	Accuracy (%)	Peak Area for Lc Single Charge State
10	N/A	N/A	N/A
25	2615.00	10460.01	1423.86
50	46.12	92.24	4586.58
100	85.00	85.00	5304.39
250	270.32	108.13	10959.06
500	553.99	110.80	14539.03
1000	1067.06	106.71	34932.30
2500	2616.07	104.64	61317.75
5000	4444.70	88.89	121494.06
10000	10758.33	107.58	192400.64

Without compensation by the internal standard the variability between injections was high. The coefficient of variation (CV) (equation in Appendix 7) was greater than 37 % (Table 7) over 12 injections (6 each from 2 vials). In contrast, the CVs were down to less than 8 % including compensation by the mAb internal standard (Table 7) and was within acceptable

bioanalytical limits. Improved CVs with internal standardisation when quantifying Lc from a single charge state in the MS spectra or the sum of multiple charge states. The charge envelopes can be seen in Figure 34, with the individual charge states for the Lc and Hc of mAb and mAb-2 present and identifiable. The migration times were also consistent across multiple injections as can be seen in Figure 35, were for 9 injections of the calibration line the migration times varied between 10.80 and 10.96 min (equating to a variance of less than 10 s over a total run time of 3 h). The migration time does not move progressively earlier or later but maintains in this region from injection to injection.

Table 7 Reproducibility of repeat injection by electrokinetic injection of CESI 8000. Peak area ratios calculated from the peak area of the light chains (Lc) of mAb (m/z ≈ 1301) and of mAb-2 (m/z ≈ 1289) for the single charge state and the light chains (Lc) of mAb (sum of charge states m/z ≈ 1115, 1171, 1232, 1301, 1377, 1463 and 1561) and of mAb-2 (sum of charge states m/z ≈ 1221, 1289, 1365, 1450 and 1547) for the sum of multiple charge states.

	Single Charge State		**Sum Multiple Charge States**	
Rep	**Peak Area**	**Peak Area Ratio**	**Peak Area**	**Peak Area Ratio**
1	6.56E+05	2.21	2.05E+06	6.89
2	1.67E+06	1.89	5.27E+06	5.97
3	1.93E+06	1.88	6.17E+06	5.99
4	2.52E+06	1.64	8.17E+06	5.31
5	1.55E+06	1.81	4.90E+06	5.73
6	1.61E+06	1.95	5.18E+06	6.27
7	1.73E+06	2.14	5.60E+06	6.92
8	3.74E+05	1.97	1.14E+06	6.01
9	1.14E+06	1.94	3.66E+06	6.21
10	1.10E+06	2.04	3.51E+06	6.51
11	1.30E+06	1.81	4.13E+06	5.76
12	1.90E+06	2.10	6.15E+06	6.81
Mean	1529418.18	1.92	4897090.91	6.13
SD	554388.42	0.14	1810057.32	0.48
%CV	**36.3**	**7.4**	**37.0**	**7.8**

Rep 1 excluded from calculations due to a poor electropherogram

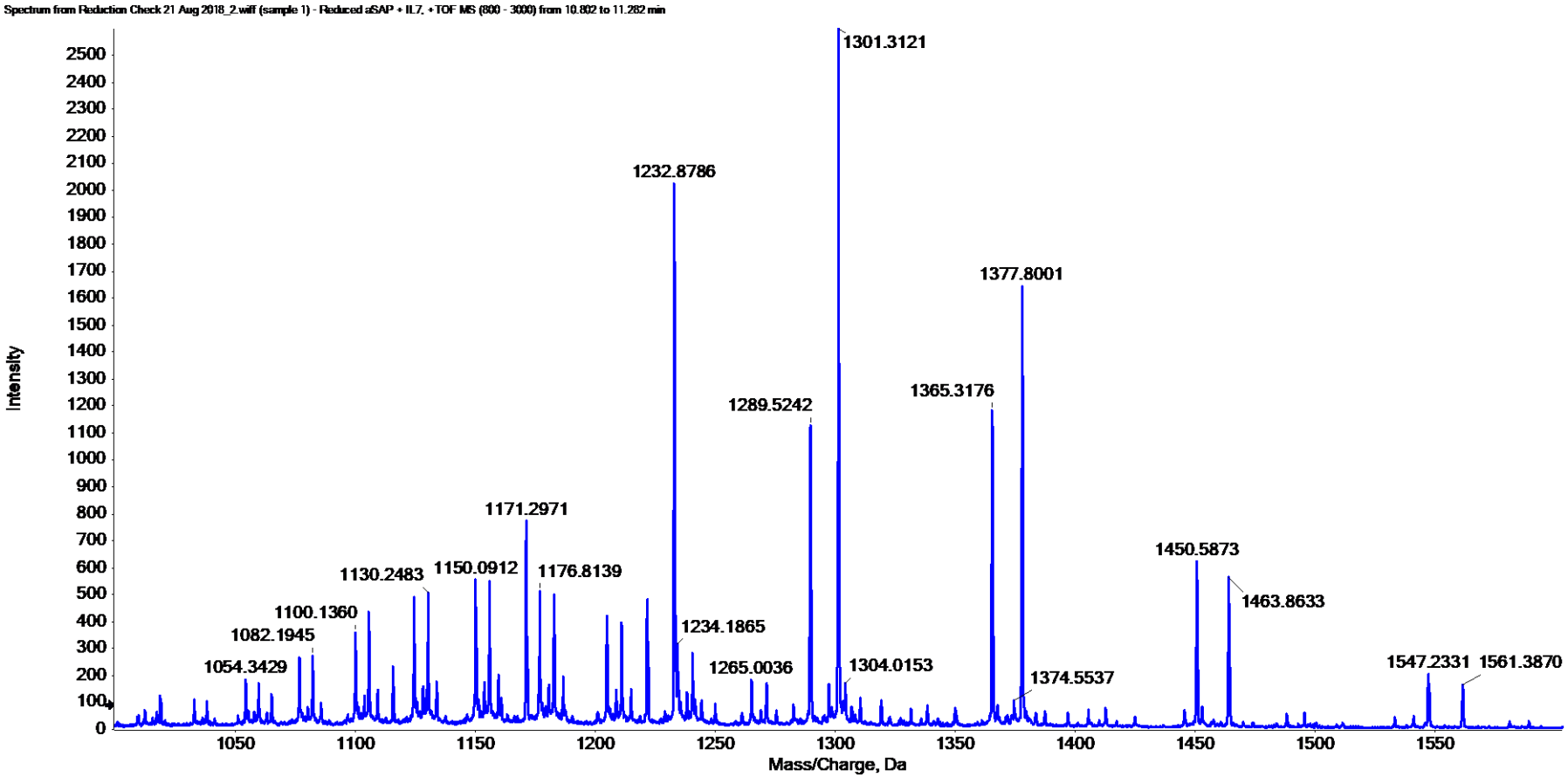

Figure 34 Spectrum generated from the reduction of mAb and mAb-2 showing the charge envelopes for the light and heavy chains of both. Key m/z for mAb light chain are 1115, 1171, 1232, 1301, 1377, 1463 and 1561 and for mAb-2 are 1221, 1289, 1365, 1450 and 1547, which are used for quantitation and reconstruction of electropherograms.

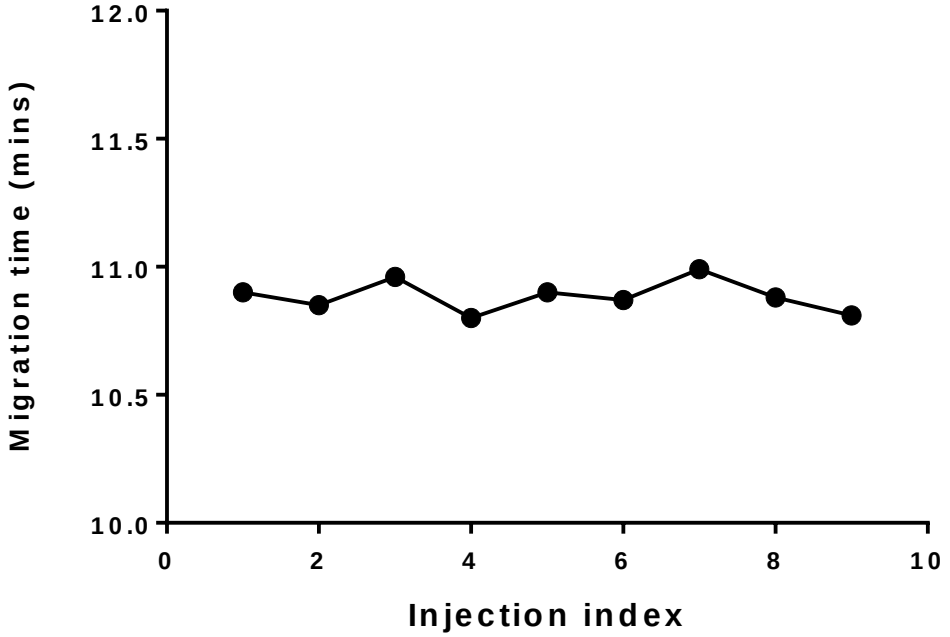

Figure 35 Plot showing the consistency of migration time, for the mAb in extracted human plasma samples. The migration times vary between 10.80 and 10.96 min, less than 10 s over the 3 hours of the run.

4.3 Conclusions

A novel CE-HRMS method was developed for the quantification of a mAb in human plasma using a middle down proteomics approach, where large mAb fragments e.g. Fd, Fc, Lc or Hc regions infer the concentration of the intact mAb. The CE separation used a discontinuous buffer system comprising a BGE of 15 % (v/v) acetic acid, a 1 M ammonium acetate stacking plug, an injection plug of 1 % (v/v) formic acid and a two-stage pressure separation with a voltage of 30 kV. Sample introduction was achieved *via* EK injection by applying a voltage of 10 kV to the sample for 99 s. The method was used to quantify the mAb, to concentrations of approximately 50 ng/mL in human plasma and has the potential, with minor modifications, to remove or decrease carry over. The inclusion of an internal standard vastly improved the injection to injection reproducibility to within limits that would be

acceptable for a validated regulatory method. Over the range of 50 to 10000 ng/mL the calibration curve required a quadratic fit with a 1/x weighting. Truncation of the calibration range would be necessary if a linear fit were deemed appropriate, or alternatively further work could be initiated to determine the reason for nonlinearity. Possibilities might include (1) MS detector saturation because too many Lc ions are hitting the detector simultaneously and therefore some do not register, (2) the recovery time MS detector is affected by very highly charged proteins ions and hence some do not register or (3) at concentrations approaching 10000 ng/mL the EK injection is becoming saturated, although the migration times across on a single capillary and batch of buffers are consistent (over the course of a 9 point calibration curve the migration times are within 10 s).

5 Discussion

The purpose of this project was to determine whether a CE-MS system could provide an effective method for quantification of mAb in the growing area of biotherapeutics in the pharmaceutical industry. Furthermore, the question of whether this method could be used as an orthogonal technique to LC-MS providing TK and PK data using a middle down approach, rather than the established 'bottom up' methods, was addressed. Essentially the middle down approach could overcome concerns that 'bottom up' methods potentially lead to loss of information during the digestion process and that inferred circulating concentrations of the intact molecule (interpolated from a small peptide fragment) may lead to inaccuracies in the data generated. In the course of this work a combined CE-MS method has been developed for the quantification of a mAb in human using a CESI 8000 to provide electrophoretic separation, coupled with a TripleTOF 6600 high resolution mass spectrometer to provide detection. The final method for quantification based on reduction of the mAb disulphide bonds to give rise to the Lc and Hc which were then used for quantification.

5.1 Electrophoretic Separation System

The separation system developed for the quantification of mAb fragments utilises a discontinuous buffer system, the result of which is a pre-concentration effect known as sample stacking, as first demonstrated by Quirino and Terabe (1998) [127], who showed that peak sharpening can be achieved by building different areas of conductivity within the capillary. In essence, the analyte moves faster through areas of low conductivity, which is then dramatically slowed on transition to the adjacent region of high conductivity [128, 129]. In the separation system developed in this thesis the zone of low conductivity was the

1 M ammonium acetate plug and the high conductivity BGE was acetic acid (15% v/v), which overall vastly improved the peak shape of the mAb fragments versus from the initial starting method. Equally the application of pressure in stages greatly helped ameliorate peak shape, by flattening parabolic flow that afflicts pressure driven separation systems.

Although the EOM associated with a CE separation naturally counteracts parabolic band broadening [74], the application of some pressure is required due to acidic nature of the buffers being used. Indeed, without application of pressure the EOF would be very low. The application of pressure at 1 psi stage one should not yield a parabolic flow profile [130] and therefore the combined EOF and EOM drive the separation. However, it was necessary to increase the pressure towards then end of the separation (prior to the migration time of the mAb fragments) in order to achieve a steady eluent spray at the emitter tip. This was necessary to achieve a good MS response with the added advantage of reducing the overall cycle time. One disadvantage of the pressure increase was the potential to reduce the resolution between the mAb fragments, however, this was not of significant due the use of HRMS as the detection system. Since the inclusion HRMS introduces selectivity based of mass discrimination, baselines resolution is not a perquisite when the components under study differ in molecular weight (strictly mass-to-charge ratio). So, although it may have been possible to fully resolve the peaks particularly for the Lc and Hc this was not pursued, but could be included in further work, which may extend the applicability to other protein constructs.

The use of EK injection allows for selective introduction of the analyte (from the aliquot on the autosampler) into the separation system because different ions in solution migrate at different rates in a given electric field. In contract hydrodynamic injection introduces a set amount of sample, and therefore the same amount of all ions contained in the sample

[131]. Contrasting these two approaches optimisation of the EK conditions, leads to fewer background ions being introduced, which in turn has the potential to reduce ion suppression and increase the signal to noise ratio ultimately meaning that lower limits of quantification can be achieved. A lower limit of quantification of 50 ng/mL was achieved, with the potential to go lower by removal of some carryover from the external surfaces of the capillary. There have been questions raised over the injection-to-injection reproducibility of EK injection as a means of sample introduction as part of a quantitative analysis, i.e. this means of sample introduction leads to large percent CVs, although internal standardisation could correct for this [132]. This was certainly the case for the quantification of the mAb in this study, with improvements in CV from approximately 40% down to in the region of 8% over the course of 12 repeat injections by inclusion of a second reference mAb alongside the reducing agent.

The OptiMS cartridge provides a plug and play approach to interfacing CE with MS, and the neutral coated capillary produces a robust and reliable connection, with more than 500 injections completed throughout this method development and evaluation on a single OptiMS cartridge with consistent migration times.

The CESI 8000 and OptiMS cartridge operate a sheathless CE-MS interface. Sheath flow has been the more common approach and is considered to be a robust technique, but has the several drawbacks such as eluent dilution as well as the potential for the sheath liquid to adversely impact MS ionisation [133]. Haselberg *et al.* 2013, [134] showed that a sheathless approach was viable for profiling of pharmaceutical proteins and this work in this thesis showed that the approach was also suitable for the quantification of biotherapeutics.

5.2 HRMS

In this work it has been shown that HRMS and in particular Q-TOF technology can be used for quantification of mAbs, but there still needs to be further work to fully validate the method. Quantitative analysis has been dominated by triple quadrupole mass spectrometers, with HRMS being predominately applied in areas such as metabolite identification, metabonomics and proteomics [135]. The use of HRMS for combined quantitative and qualitative is a major attraction, and with the current generation of HRMS instruments this is becoming a more realistic proposition. HRMS instruments also have a greater mass range than the common quadrupole analyser making them suitable for intact or middle down analysis. In the development of this method the Sciex 6600 TripleTOF mass spectrometer was operated in TOF-MS mode, and as such, the molecule did not undergo fragmentation within the mass spectrometer and therefore quantification was based on the mass of the mAb fragments injected (or strictly speaking from the multiple charge states ionised) ultimately the Lc and Hc only. Quantification can be achieved using a single charge state or by summing multiple charge states of the individual fragments with the most appropriate method varying between molecules. The approach chosen for the quantitation will depend on the signal to noise ratio that the different charge states or the use of multiple charge states generate. A further consideration when carrying out the post-acquisition data processing is the mass extraction window (MEW) that is to be used [136] and this again will vary between molecule and the resolution achieved.

Based on the findings presented here HRMS is capable of being used for the quantitative analysis of mAbs. However, to be used for the generation of TK and PK data in a regulated environment the *a priori* definition of the post-acquisition data processing parameters will be necessary for the quantification of the circulating concertation of the unmodified mAb.

5.3 Impact of this Methodology on the Quantification of mAbs

This study successfully demonstrates that combining CE with HRMS with for the quantification of this mAb can be successful. CE using EK injection employing a discontinuous buffer system and 2 stage application of pressure provided a reproducible (with the use of an internal standard) and sensitive technique for both sample introduction and separation. This is complemented by the tripleTOF 6600 QTOF MS providing the sensitivity and selectivity required, particularly when combined with the post-acquisition processing options for accurate full scan mass data. One further advantage of full scan HRMS is enabling the assessment qualitative aspects within the same analysis. Certain PTMs will detectable by mass shifts even if not resolved by the separation. Certain PTMs like aspartate isomerism, however, will not able distinguishable because there is no mass difference and hence the separation system will need to provide the analytical fidelity in this instance.

In terms of validating for use on a regulated study, as already stated the method still needs full characterisation, although the work does indicate that it would meet the criteria outlined by Jenkins *et al.* [137] and by Duggan *et al*. [138] for acceptance criteria for LC-MS/MS analysis of bio-therapeutics using a bottom up, peptide approach. At this point this would be the most appropriate criteria to assess this method.

This method demonstrates that there is potential for the use of CE-MS for the quantification of mAbs, and as such gain greater confidence in establishing circulating concentrations of intact mAbs and in addition to generate further information that is not currently available with analysis with ELISA or peptide based/bottom up approaches. Furthermore, the CE separation method developed for the analysis of the particular mAb used in this study would be able to be used with very little alteration, for a variety of other

mAbs as demonstrated with the in inclusion of a second mAb as an internal standard. Taking into consideration the MS method used has very little optimisation of parameters and has a wide and acquires over a wide *m/z* range, the entire CE-MS method could be classed as a generic method for the analysis of mAbs, with the specifics coming from the post-acquisition processing.

5.4 Future Work and Further Applications of CE-MS Quantification

As mentioned in section 4.2, the method did exhibit carryover from sample to sample, the likely source of this is from the mAb fragments adhering to the outside of the capillary during the injection cycle. The is scope to reduce this as a part of the method, during this development a single water dip step was used after injection to clean the outside of the capillary, it is likely that this is insufficient. The inclusion of additional dip steps, using different solvents and/or solvents at differing pHs. The inclusion of further dip steps would have no impact on the separation, as the solvents used do not enter the capillary. Characterising these cleaning steps may allow the lowering of the lower limit of quantification. Another area that it would be ideal to explore to fully assess the full potential is to look at the injection cycle in further detail, the CESI 8000 has the potential to carry out multiple injections in one cycle. It would be interesting to explore the possibility of reducing the injection time, currently at 99 seconds but have 2 injections of 60 seconds for example. This approach may help load more mAb fragment into the capillary therefore increase the MS response without an impact on peak shape due to the stacking effects of the discontinuous buffer system. This double injection approach may also be used to confirm the quadratic nature of the calibration curve is a result of the saturating the injection or saturating the MS detector. It would also be an advantage to investigate minor changes to the sample preparation to ensure the recovery from plate is optimal and any dilution of the final extract to produce a sample of a composition that is suitable for CE

analysis. Once these final experiments had been completed, as previously stated, a key piece of work would be to validate the method to determine the precision and accuracy over the concentration range as well as characterising any matrix effects and recovery of the mAb.

Another interesting area to explore is the post-acquisition processing, the current method quantifies using a single or multiple charge state, these are highly charged species and form the spectra that can be seen in the appendices. An evolution of this approach may to be use the deconvoluted spectra to reconstruct the chromatogram and quantify on the *m/z* of the entire mAb fragment (Lc or Hc).

Given the ability of this method to quantify the mAbs there is scope for the CE-MS approach to be used for the quantification of other classes of molecule. Methods could be developed for other biotherapeutics, the likes of immunoconjugates, Ig scaffolds and therapeutic peptides all have the potential to be quantified using this approach. Another potential area of use for this technique would be the quantification of naturally occurring molecules that are known as biomarkers, which are also of interest in the pharmaceutical industry. There is also the potential for CE-MS to be used with synthetic compounds like oligonucleotides and even NCEs. Oligonucleotides, although not a large proportion of the work in the bioanalytical lab offer significant challenges. Quantification by LC-MS requiring the use of ion pair reagents the cause ion suppression, these ion pair reagents also take time to remove from the system, often meaning that a dedicated system is required to support this type of analysis. CE is already used it the characterisation of oligonucleotides and such as such CE-MS has potential for use in a quantitative assay.

6 Appendices

Appendix 1 Typical spectra, post IdeZ digest, the deconvoluted spectra of the Lc fragment showing the mass (bottom) and corresponding charge states (marked in red) (top).

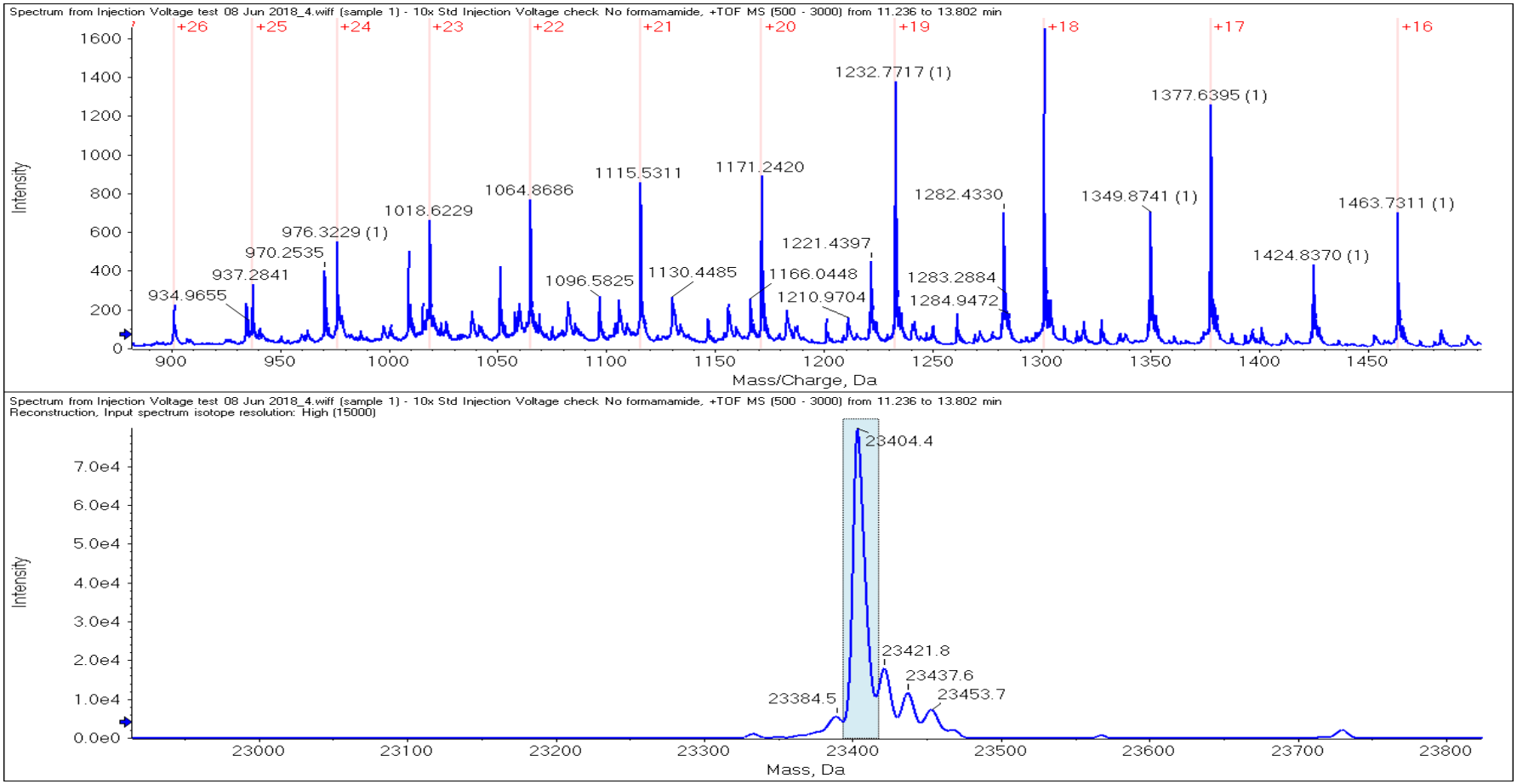

Appendix 2 Typical spectra, post IdeZ digest, the deconvoluted spectra of the Fc showing the mass (bottom) and corresponding charge states (marked in red) (top).

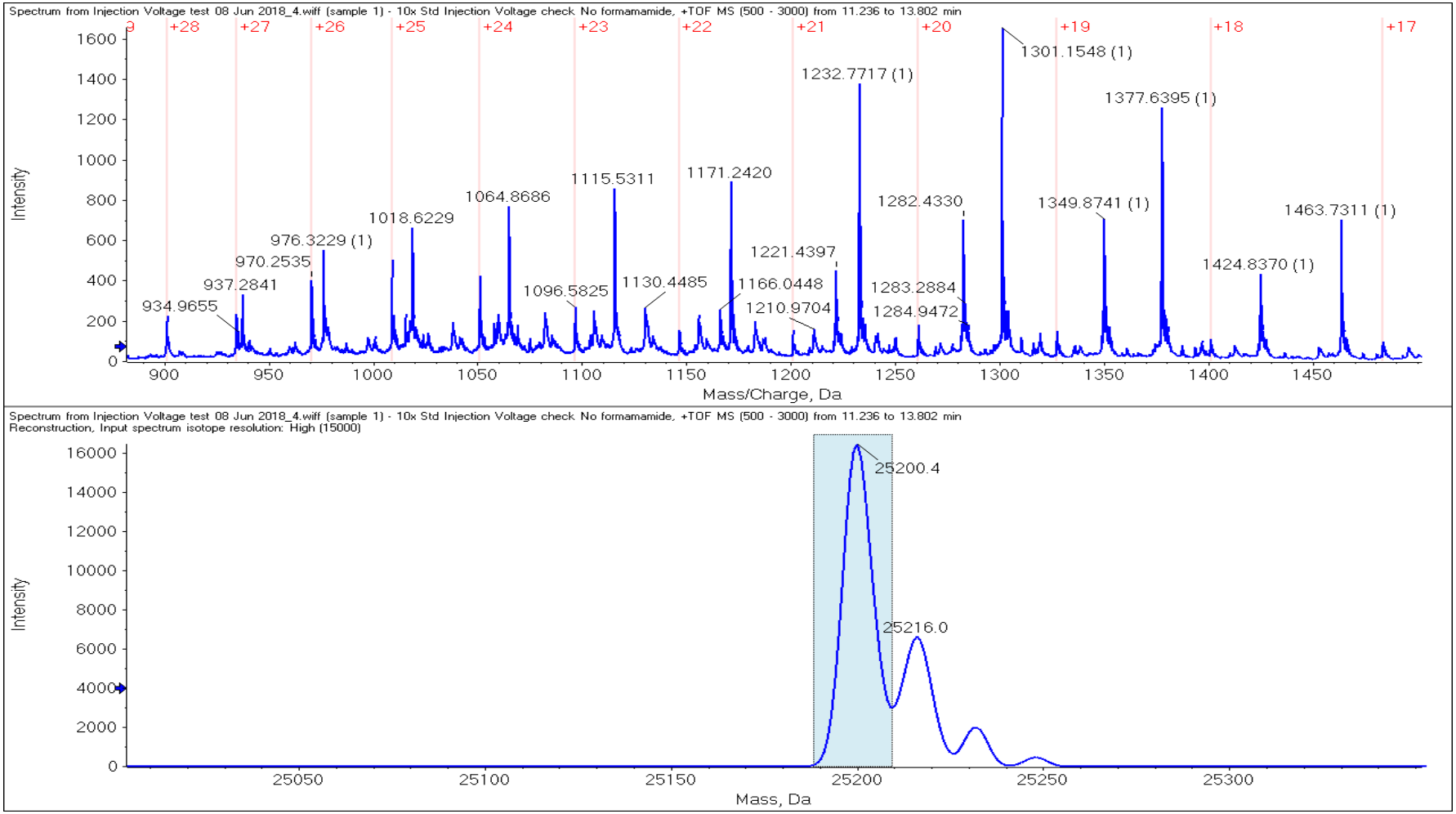

Appendix 3 Typical spectra, post IdeZ digest, the deconvoluted spectra of the Fd fragment showing the mass (bottom) and corresponding charge states (marked in red) (top).

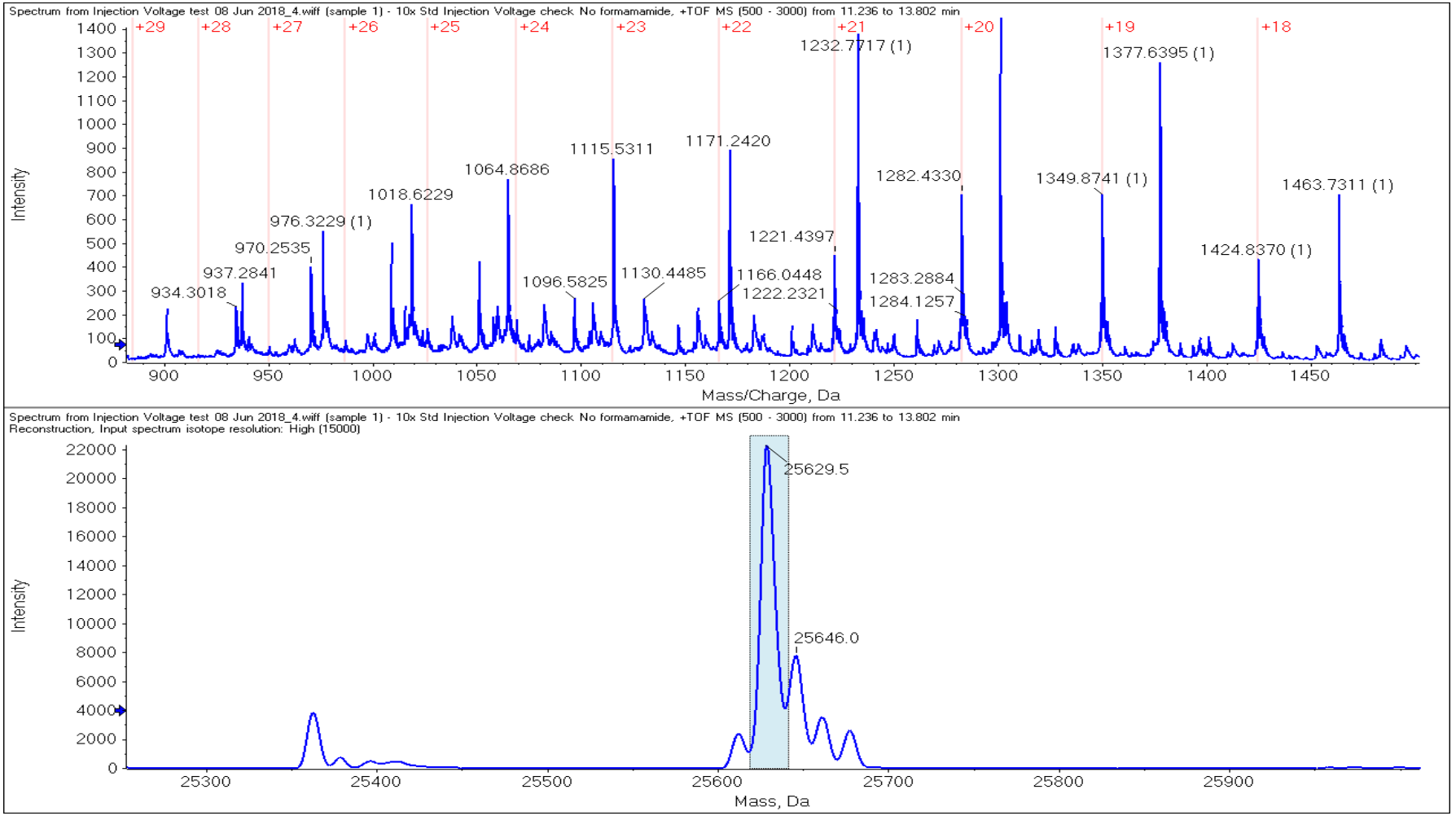

Appendix 4 Typical deconvoluted spectra after IdeZ digest 3 ≈25 kDa fragments (Fc, Fd and Lc).

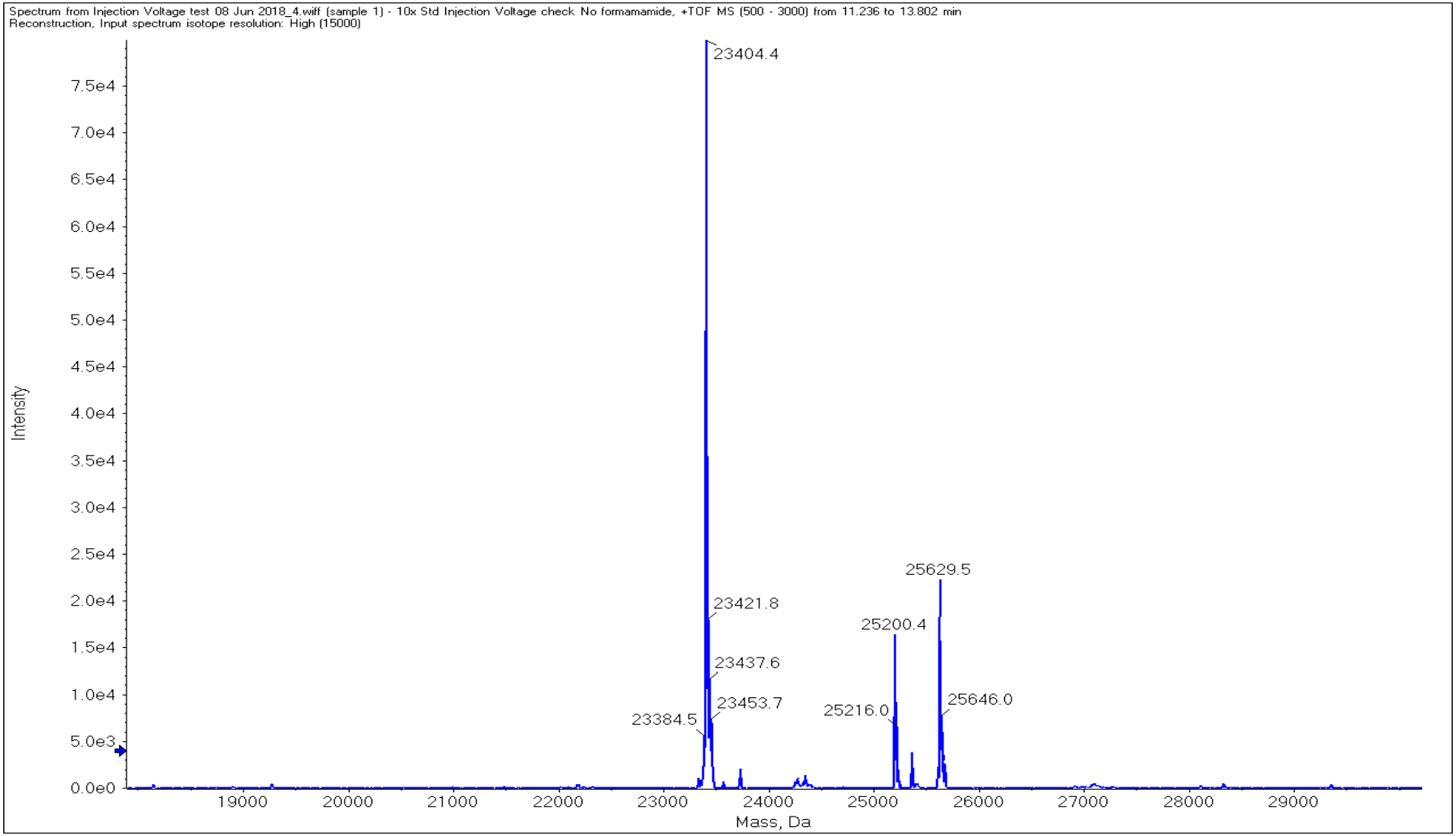

Appendix 5 Calculation of resolution when varying the concentration of the ammonium acetate plug.

1 M ammonium acetate plug

$$\frac{12.378 - 12.100}{0.5(0.684 + 0.633)} = 0.55$$

5 M ammonium acetate plug

$$\frac{13.821 - 13.514}{0.5(0.734 + 0.784)} = 0.40$$

Appendix 6 Calculation of resolution when varying the pressure of stage two of the CE separation.

5 psi

$$\frac{13.831 - 13.703}{0.5(0.252 + 0.0.249)} = 0.51$$

10 psi

$$\frac{13.216 - 12.977}{0.5(0.566 + 0.730)} = 0.36$$

15 psi

$$\frac{11.780 - 11.447}{0.5(0.648 + 0.667)} = 0.51$$

Appendix 7 Equation for the calculation of the coefficient of variance.

$$\%CV = \left(\frac{SD}{\bar{X}}\right) \times 100$$

where SD = Standard deviation

$\bar{X}$ = Mean

Appendix 8 Typical spectra, post disulphide reduction, the deconvoluted spectra of the Lc, showing the mass (bottom) and corresponding charge states (marked in red) (top).

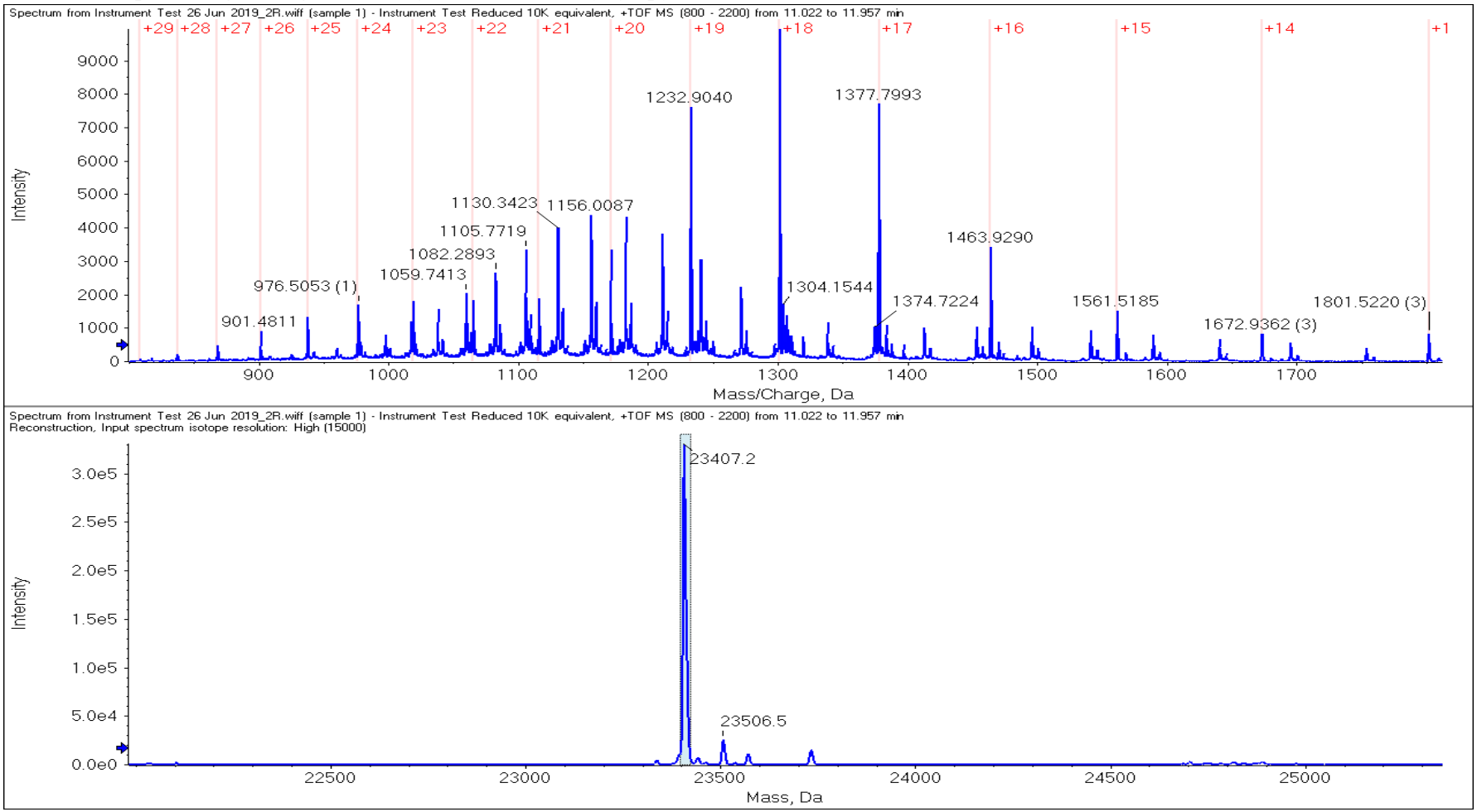

Appendix 9 Typical spectra, post disulphide reduction, showing the deconvoluted spectra of the Hc and corresponding charge states.

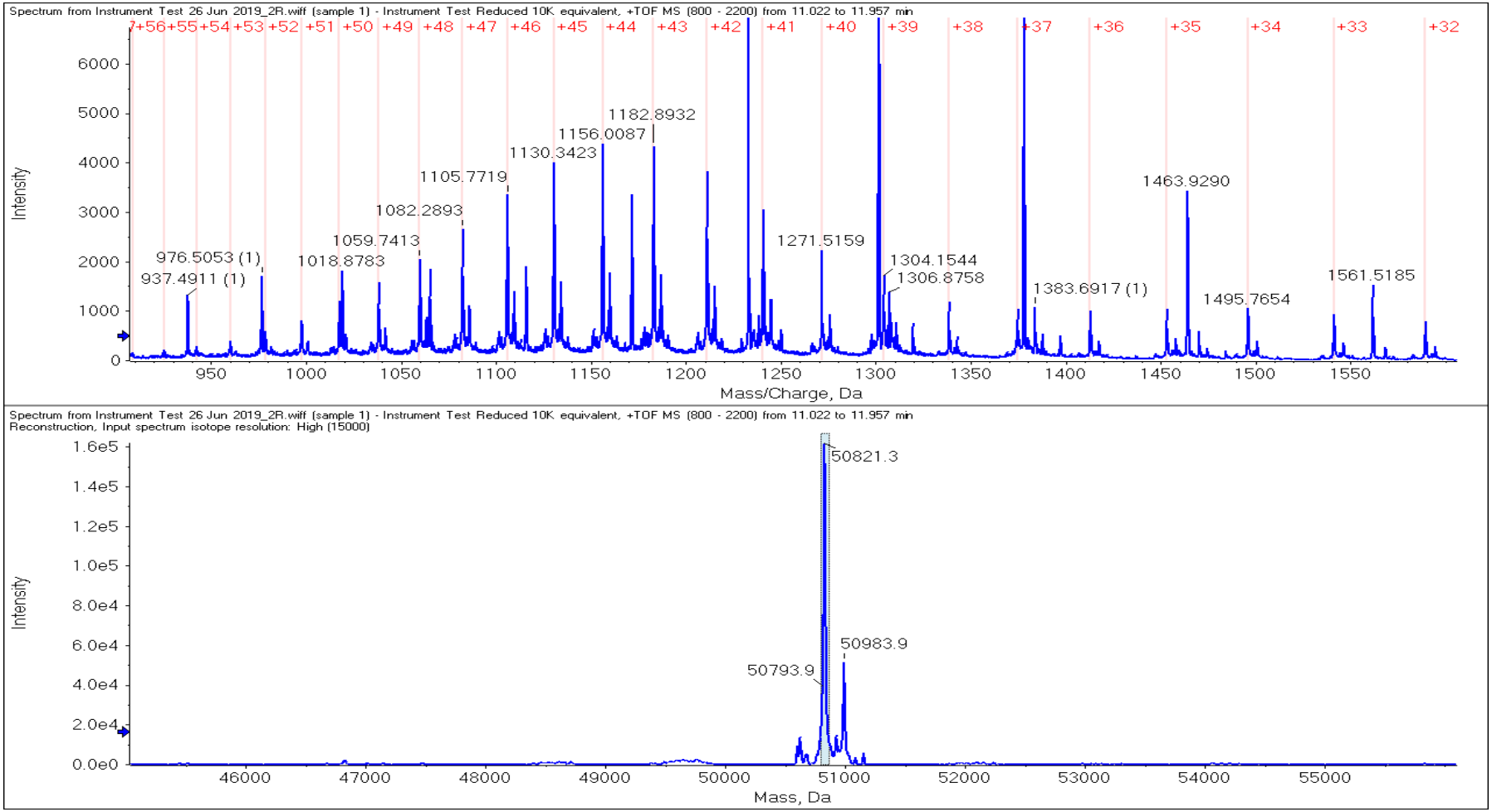

7 References

1. G de la Torre, B. and F. Albericio, *The pharmaceutical industry in 2018. An analysis of FDA drug approvals from the perspective of molecules.* Molecules, 2019. **24**(4): p. 809.
2. Navarra, P., *The process of drug discovery and the Yin/Yang of small-molecule/biotech option.* Microchemical Journal, 2018. **136**: p. 139-142.
3. Hurst, S. *Biotherapeutics Drug Development*. Bioanalytical Chemistry 2011 [cited 2019 04/06/2019]; Available from: http://web2.uconn.edu/rusling/BioTx%20April%2019%202011%20SHurst.pdf.
4. Giovannetti, G.T. *Biotechnology Report 2016 - Beyond Borders Retruning to Earth*. 2013 [cited 2019 04/06/2019]; Available from: https://www.ey.com/Publication/vwLUAssets/EY-beyond-borders-2016/$FILE/EY-beyond-borders-2016.pdf.
5. Mullard, A., *Biotech R&D spend jumps by more than 15%.* Nature Reviews Drug Discovery, 2016. **15**: p. 447.
6. Worsley, A. *Biotherapeutics – a new funding scheme for research*. 2014; Available from: ttps://scienceblog.cancerresearchuk.org/2014/10/21/biotherapeutics-a-new-funding-scheme-for-research/.
7. *Biotherapeutic medicines: Grasping the new generation of treatments*, I.F.o.P.M. Associations, Editor. 2012.
8. Reichert, J.M., *Antibodies to watch in 2017.* mAbs, 2017. **9**(2): p. 167-181.
9. *BIOLOGICAL DRUGS - information sheet*, in *www.crohnsandcolitis.org.uk*, C.a.C. UK, Editor.
10. AlDeghaither, D., B.G. Smaglo, and L.M. Weiner, *Beyond peptides and mAbs--current status and future perspectives for biotherapeutics with novel constructs.* Journal of clinical pharmacology, 2015. **55 Suppl 3**(0 3): p. S4-S20.
11. Ecker, D.M., S.D. Jones, and H.L. Levine, *The therapeutic monoclonal antibody market.* mAbs, 2014. **7**(1): p. 9-14.
12. Wang, X., T.K. Das, S.K. Singh, and S. Kumar. *Potential aggregation prone regions in biotherapeutics: a survey of commercial monoclonal antibodies*. in *MAbs*. 2009. Taylor & Francis.
13. Ratanji, K.D., J.P. Derrick, R.J. Dearman, and I. Kimber, *Immunogenicity of therapeutic proteins: influence of aggregation.* Journal of immunotoxicology, 2014. **11**(2): p. 99-109.
14. Adams, G.P. and L.M. Weiner, *Monoclonal antibody therapy of cancer.* Nature biotechnology, 2005. **23**(9): p. 1147.
15. Chames, P., M. Van Regenmortel, E. Weiss, and D. Baty, *Therapeutic antibodies: successes, limitations and hopes for the future.* British journal of pharmacology, 2009. **157**(2): p. 220-233.
16. Review, A., *What are Antibody-drug Conjugates?* ADCREVIEW, Journal of Antibody-drug conjugates, 2019.
17. Birrer, M.J., K.N. Moore, I. Betella, and R.C. Bates, *Antibody-Drug Conjugate-Based Therapeutics: State of the Science.* JNCI: Journal of the National Cancer Institute, 2019.

18. Bross, P.F., J. Beitz, G. Chen, X.H. Chen, E. Duffy, L. Kieffer, S. Roy, R. Sridhara, A. Rahman, and G. Williams, *Approval summary: gemtuzumab ozogamicin in relapsed acute myeloid leukemia.* Clinical Cancer Research, 2001. **7**(6): p. 1490-1496.
19. Pasche, N. and D. Neri, *Immunocytokines: a novel class of potent armed antibodies.* Drug Discovery Today, 2012. **17**(11): p. 583-590.
20. List, T. and D. Neri, *Immunocytokines: a review of molecules in clinical development for cancer therapy.* Clinical pharmacology : advances and applications, 2013. **5**(Suppl 1): p. 29-45.
21. Gutbrodt, K.L. and D. Neri, *Immunocytokines.* Antibodies, 2012. **1**(1): p. 70-87.
22. Vazquez-Lombardi, R., B. Roome, and D. Christ, *Molecular engineering of therapeutic cytokines.* Antibodies, 2013. **2**(3): p. 426-451.
23. Kontermann, R.E., *Antibody–cytokine fusion proteins.* Archives of Biochemistry and Biophysics, 2012. **526**(2): p. 194-205.
24. Sterjova, M. and E. Janevik-Ivanovska, *Anticancer monoclonal antibodies and their radioimmunoconjugates-gateway to the more successful therapy.* Knowledge-International Journal, Scientific Papers, 2019. **30**(4): p. 725-731.
25. Chanier, T. and P. Chames, *Nanobody Engineering: Toward Next Generation Immunotherapies and Immunoimaging of Cancer.* Antibodies, 2019. **8**(1): p. 13.
26. Jank, L., C. Pinto-Espinoza, Y. Duan, F. Koch-Nolte, T. Magnus, and B. Rissiek, *Current Approaches and Future Perspectives for Nanobodies in Stroke Diagnostic and Therapy.* Antibodies, 2019. **8**(1): p. 5.
27. Duggan, S., *Caplacizumab: First Global Approval.* Drugs, 2018. **78**(15): p. 1639-1642.
28. Van Roy, M., C. Ververken, E. Beirnaert, S. Hoefman, J. Kolkman, M. Vierboom, E. Breedveld, B. 't Hart, S. Poelmans, L. Bontinck, A. Hemeryck, S. Jacobs, J. Baumeister, and H. Ulrichts, *The preclinical pharmacology of the high affinity anti-IL-6R Nanobody® ALX-0061 supports its clinical development in rheumatoid arthritis.* Arthritis Research & Therapy, 2015. **17**(1): p. 135.
29. Roopenian, D.C. and S. Akilesh, *FcRn: the neonatal Fc receptor comes of age.* Nature Reviews Immunology, 2007. **7**: p. 715.
30. Choi, H.S., W. Liu, P. Misra, E. Tanaka, J.P. Zimmer, B. Itty Ipe, M.G. Bawendi, and J.V. Frangioni, *Renal clearance of quantum dots.* Nature biotechnology, 2007. **25**(10): p. 1165-1170.
31. Kovaleva, M., L. Ferguson, J. Steven, A. Porter, and C. Barelle, *Shark variable new antigen receptor biologics – a novel technology platform for therapeutic drug development.* Expert Opinion on Biological Therapy, 2014. **14**(10): p. 1527-1539.
32. Spiess, C., Q. Zhai, and P.J. Carter, *Alternative molecular formats and therapeutic applications for bispecific antibodies.* Molecular Immunology, 2015. **67**(2, Part A): p. 95-106.
33. Sedykh, S.E., V.V. Prinz, V.N. Buneva, and G.A. Nevinsky, *Bispecific antibodies: design, therapy, perspectives.* Drug design, development and therapy, 2018. **12**: p. 195-208.
34. Thakur, A. and L.G. Lum, *"NextGen" Biologics: Bispecific Antibodies and Emerging Clinical Results.* Expert Opinion on Biological Therapy, 2016. **16**(5): p. 675-688.
35. Kontermann, R. and U. Brinkmann, *Bispecific Antibodies*. Vol. 20. 2015.
36. Fosgerau, K. and T. Hoffmann, *Peptide therapeutics: current status and future directions.* Drug Discovery Today, 2015. **20**(1): p. 122-128.
37. Lau, J.L. and M.K. Dunn, *Therapeutic peptides: Historical perspectives, current development trends, and future directions.* Bioorganic & Medicinal Chemistry, 2018. **26**(10): p. 2700-2707.

38. Slominsky, P.A. and M.I. Shadrina, *Peptide Pharmaceuticals: Opportunities, Prospects, and Limitations.* Molecular Genetics, Microbiology and Virology, 2018. **33**(1): p. 8-14.
39. Hopfgartner, G. and E. Bourgogne, *Quantitative high-throughput analysis of drugs in biological matrices by mass spectrometry.* Mass Spectrometry Reviews, 2003. **22**(3): p. 195-214.
40. Lee, M.S. and E.H. Kerns, *LC/MS applications in drug development.* Mass Spectrometry Reviews, 1999. **18**(3-4): p. 187-279.
41. Xu, R.N., L. Fan, M.J. Rieser, and T.A. El-Shourbagy, *Recent advances in high-throughput quantitative bioanalysis by LC-MS/MS.* J Pharm Biomed Anal, 2007. **44**(2): p. 342-55.
42. Ji, Q.C., E.M. Gage, R. Rodila, M.S. Chang, and T.A. El-Shourbagy, *Method development for the concentration determination of a protein in human plasma utilizing 96-well solid-phase extraction and liquid chromatography/tandem mass spectrometric detection.* Rapid Commun Mass Spectrom, 2003. **17**(8): p. 794-9.
43. Oran, P.E., J.W. Jarvis, C.R. Borges, N.D. Sherma, and R.W. Nelson, *Mass spectrometric immunoassay of intact insulin and related variants for population proteomics studies.* Proteomics Clin Appl, 2011. **5**(7-8): p. 454-9.
44. Gucinski, A.C. and M.T. Boyne, 2nd, *Evaluation of intact mass spectrometry for the quantitative analysis of protein therapeutics.* Anal Chem, 2012. **84**(18): p. 8045-51.
45. Lequin, R.M., *Enzyme immunoassay (EIA)/enzyme-linked immunosorbent assay (ELISA).* Clin Chem, 2005. **51**(12): p. 2415-8.
46. Kuang, B., L. King, and H.F. Wang, *Therapeutic monoclonal antibody concentration monitoring: free or total?* Bioanalysis, 2010. **2**(6): p. 1125-40.
47. Lee, J.W., M. Kelley, L.E. King, J. Yang, H. Salimi-Moosavi, M.T. Tang, J.F. Lu, J. Kamerud, A. Ahene, H. Myler, and C. Rogers, *Bioanalytical approaches to quantify "total" and "free" therapeutic antibodies and their targets: technical challenges and PK/PD applications over the course of drug development.* Aaps j, 2011. **13**(1): p. 99-110.
48. Ahene, A.B., *Application and interpretation of free and total drug measurements in the development of biologics.* Bioanalysis, 2011. **3**(11): p. 1287-95.
49. Thway, T.M., I. Magana, A. Bautista, V. Jawa, W. Gu, and M. Ma, *Impact of anti-drug antibodies in preclinical pharmacokinetic assessment.* Aaps j, 2013. **15**(3): p. 856-63.
50. De Simone, A., J. Fiori, M. Naldi, A. D'Urzo, V. Tumiatti, A. Milelli, and V. Andrisano, *Application of an ESI-QTOF method for the detailed characterization of GSK-3β inhibitors.* Journal of Pharmaceutical and Biomedical Analysis, 2017. **144**: p. 159-166.
51. Zhang, Y., B.R. Fonslow, B. Shan, M.-C. Baek, and J.R. Yates, 3rd, *Protein analysis by shotgun/bottom-up proteomics.* Chemical reviews, 2013. **113**(4): p. 2343-2394.
52. Becker, J.O. and A.N. Hoofnagle, *Replacing immunoassays with tryptic digestion-peptide immunoaffinity enrichment and LC–MS/MS.* Bioanalysis, 2012. **4**(3): p. 281-290.
53. Kellie, J.F., J.R. Kehler, and M.E. Szapacs, *Application of high-resolution MS for development of peptide and large-molecule drug candidates.* Bioanalysis, 2016. **8**(3): p. 169-177.
54. Compton, P.D., N.L. Kelleher, and J. Gunawardena, *Estimating the Distribution of Protein Post-Translational Modification States by Mass Spectrometry.* Journal of Proteome Research, 2018. **17**(8): p. 2727-2734.

55. Wohlschlager, T., C. Regl, C.G. Huber, and K. Sandra, *Monitoring of oxidation in biopharmaceuticals with top-to-bottom high performance liquid chromatography-mass spectrometry methodologies: A critical check.* LC-GC Europe, 2018. **31**(6): p. 326-331.
56. Zhang, L., L.A. Vasicek, S. Hsieh, S. Zhang, K.P. Bateman, and J. Henion, *Top-down LC-MS quantitation of intact denatured and native monoclonal antibodies in biological samples.* Bioanalysis, 2018. **10**(13): p. 1039-1054.
57. Casado-Vela, J., A. Cebrián, M.T. Gómez Del Pulgar, E. Sánchez-López, M. Vilaseca, L. Menchén, C. Diema, S. Sellés-Marchart, M.J. Martínez-Esteso, N. Yubero, R. Bru-Martínez, and J.C. Lacal, *Lights and shadows of proteomic technologies for the study of protein species including isoforms, splicing variants and protein post-translational modifications.* Proteomics, 2011. **11**(4): p. 590-603.
58. Breuker, K., M. Jin, X. Han, H. Jiang, and F.W. McLafferty, *Top-Down Identification and Characterization of Biomolecules by Mass Spectrometry.* Journal of the American Society for Mass Spectrometry, 2008. **19**(8): p. 1045-1053.
59. Greer, S.M., S. Sidoli, M. Coradin, M. Schack Jespersen, V. Schwämmle, O.N. Jensen, B.A. Garcia, and J.S. Brodbelt, *Extensive Characterization of Heavily Modified Histone Tails by 193 nm Ultraviolet Photodissociation Mass Spectrometry via a Middle-Down Strategy.* Analytical Chemistry, 2018. **90**(17): p. 10425-10433.
60. Cannon, J., K. Lohnes, C. Wynne, Y. Wang, N. Edwards, and C. Fenselau, *High-throughput middle-down analysis using an orbitrap.* Journal of proteome research, 2010. **9**(8): p. 3886-3890.
61. Moradian, A., A. Kalli, M.J. Sweredoski, and S. Hess, *The top-down, middle-down, and bottom-up mass spectrometry approaches for characterization of histone variants and their post-translational modifications.* Proteomics, 2014. **14**(4-5): p. 489-97.
62. Wu, C., J.C. Tran, L. Zamdborg, K.R. Durbin, M. Li, D.R. Ahlf, B.P. Early, P.M. Thomas, J.V. Sweedler, and N.L. Kelleher, *A protease for 'middle-down' proteomics.* Nature Methods, 2012. **9**(8): p. 822-824.
63. Fornelli, L., D. Ayoub, K. Aizikov, A. Beck, and Y.O. Tsybin, *Middle-Down Analysis of Monoclonal Antibodies with Electron Transfer Dissociation Orbitrap Fourier Transform Mass Spectrometry.* Analytical Chemistry, 2014. **86**(6): p. 3005-3012.
64. Nowak, C., R. Patel, and H. Liu, *Characterization of recombinant monoclonal IgG2 antibodies using LC-MS and limited Lys-C digestion.* Journal of Chromatography B: Analytical Technologies in the Biomedical and Life Sciences, 2018. **1092**: p. 15-18.
65. Li, S.F.Y., *Capillary electrophoresis: principles, practice and applications*. Vol. 52. 1992: Elsevier.
66. Pontillo, C., S. Filip, D.M. Borràs, W. Mullen, A. Vlahou, and H. Mischak, *CE-MS-based proteomics in biomarker discovery and clinical application.* PROTEOMICS – Clinical Applications, 2015. **9**(3-4): p. 322-334.
67. Lößner, C., *CESI training*, R. Snell, Editor. 2018.
68. Kemp, G., *Capillary electrophoresis: a versatile family of analytical techniques.* Biotechnology and applied biochemistry, 1998. **27**(1): p. 9-17.
69. Altria, K.D., *Capillary electrophoresis guidebook: principles, operation, and applications*. Vol. 52. 1996: Springer Science & Business Media.
70. Lee, C.S., W.C. Blanchard, and C.T. Wu, *Direct control of the electroosmosis in capillary zone electrophoresis by using an external electric field.* Analytical Chemistry, 1990. **62**(14): p. 1550-1552.

71. Huang, X., M.J. Gordon, and R.N. Zare, *Current-monitoring method for measuring the electroosmotic flow rate in capillary zone electrophoresis.* Analytical chemistry, 1988. **60**(17): p. 1837-1838.
72. Hayes, M.A., I. Kheterpal, and A.G. Ewing, *Effects of buffer pH on electroosmotic flow control by an applied radial voltage for capillary zone electrophoresis.* Analytical chemistry, 1993. **65**(1): p. 27-31.
73. Taylor, J.A. and E.S. Yeung, *Imaging of hydrodynamic and electrokinetic flow profiles in capillaries.* Analytical Chemistry, 1993. **65**(20): p. 2928-2932.
74. James, N., *Capillary electrophoresis.* 1995.
75. Rathore, A.S., *Joule heating and determination of temperature in capillary electrophoresis and capillary electrochromatography columns.* Journal of Chromatography A, 2004. **1037**(1-2): p. 431-443.
76. Knox, J.H. and K.A. McCormack, *Temperature effects in capillary electrophoresis. 1: Internal capillary temperature and effect upon performance.* Chromatographia, 1994. **38**(3-4): p. 207-214.
77. Gobie, W.A. and C.F. Ivory, *Thermal model of capillary electrophoresis and a method for counteracting thermal band broadening.* Journal of Chromatography A, 1990. **516**(1): p. 191-210.
78. Rush, R.S., A.S. Cohen, and B.L. Karger, *Influence of column temperature on the electrophoretic behavior of myoglobin and. alpha.-lactalbumin in high-performance capillary electrophoresis.* Analytical chemistry, 1991. **63**(14): p. 1346-1350.
79. Albin, M., P.D. Grossman, and S.E. Moring, *Sensitivity enhancement for capillary electrophoresis.* Analytical Chemistry, 1993. **65**(10): p. 489A-497A.
80. Schwer, C. and F. Lottspeich, *Analytical and micropreparative separation of peptides by capillary zone electrophoresis using discontinuous buffer systems.* Journal of Chromatography A, 1992. **623**(2): p. 345-355.
81. Gebauer, P., W. Thormann, and P. Boček, *Sample self-stacking in zone electrophoresis: Theoretical description of the zone electrophoretic separation of minor compounds in the presence of bulk amounts of a sample component with high mobility and like charge.* Journal of Chromatography A, 1992. **608**(1-2): p. 47-57.
82. Stutz, H., *Advances in the analysis of proteins and peptides by capillary electrophoresis with matrix-assisted laser desorption/ionization and electrospray-mass spectrometry detection.* Electrophoresis, 2005. **26**(7-8): p. 1254-1290.
83. Gaspar, A., M. Englmann, A. Fekete, M. Harir, and P. Schmitt-Kopplin, *Trends in CE-MS 2005–2006.* Electrophoresis, 2008. **29**(1): p. 66-79.
84. Zamfir, A.D., *Recent advances in sheathless interfacing of capillary electrophoresis and electrospray ionization mass spectrometry.* Journal of Chromatography A, 2007. **1159**(1-2): p. 2-13.
85. Pattky, M. and C. Huhn, *Advantages and limitations of a new cationic coating inducing a slow electroosmotic flow for CE-MS peptide analysis: a comparative study with commercial coatings.* Analytical and bioanalytical chemistry, 2013. **405**(1): p. 225-237.
86. Belder, D., A. Deege, H. Husmann, F. Kohler, and M. Ludwig, *Cross-linked poly (vinyl alcohol) as permanent hydrophilic column coating for capillary electrophoresis.* Electrophoresis, 2001. **22**(17): p. 3813-3818.
87. Stalmach, A., A. Albalat, W. Mullen, and H. Mischak, *Recent advances in capillary electrophoresis coupled to mass spectrometry for clinical proteomic applications.* Electrophoresis, 2013. **34**(11): p. 1452-1464.

88. Zhao, S.S., X. Zhong, C. Tie, and D.D. Chen, *Capillary electrophoresis-mass spectrometry for analysis of complex samples.* Proteomics, 2012. **12**(19-20): p. 2991-3012.
89. Pontillo, C., S. Filip, D.M. Borràs, W. Mullen, A. Vlahou, and H. Mischak, *CE-MS-based proteomics in biomarker discovery and clinical application.* PROTEOMICS–Clinical Applications, 2015. **9**(3-4): p. 322-334.
90. Gahoual, R., J.-M. Busnel, A. Beck, Y.-N. François, and E. Leize-Wagner, *Full antibody primary structure and microvariant characterization in a single injection using transient isotachophoresis and sheathless capillary electrophoresis–tandem mass spectrometry.* Analytical chemistry, 2014. **86**(18): p. 9074-9081.
91. Marie, A.-L., C. Przybylski, F. Gonnet, R. Daniel, R. Urbain, G. Chevreux, S. Jorieux, and M. Taverna, *Capillary zone electrophoresis and capillary electrophoresis-mass spectrometry for analyzing qualitative and quantitative variations in therapeutic albumin.* Analytica chimica acta, 2013. **800**: p. 103-110.
92. Redman, E.A., J.S. Mellors, J.A. Starkey, and J.M. Ramsey, *Characterization of intact antibody drug conjugate variants using microfluidic capillary electrophoresis–mass spectrometry.* Analytical chemistry, 2016. **88**(4): p. 2220-2226.
93. Sarg, B., K. Faserl, L. Kremser, B. Halfinger, R. Sebastiano, and H.H. Lindner, *Comparing and combining capillary electrophoresis electrospray ionization mass spectrometry and nano–liquid chromatography electrospray ionization mass spectrometry for the characterization of post-translationally modified histones.* Molecular & cellular proteomics, 2013. **12**(9): p. 2640-2656.
94. Gahoual, R., A. Beck, Y.N. François, and E. Leize-Wagner, *Independent highly sensitive characterization of asparagine deamidation and aspartic acid isomerization by sheathless CZE-ESI-MS/MS.* Journal of mass spectrometry, 2016. **51**(2): p. 150-158.
95. Said, N., R. Gahoual, L. Kuhn, A. Beck, Y.-N. François, and E. Leize-Wagner, *Structural characterization of antibody drug conjugate by a combination of intact, middle-up and bottom-up techniques using sheathless capillary electrophoresis–Tandem mass spectrometry as nanoESI infusion platform and separation method.* Analytica chimica acta, 2016. **918**: p. 50-59.
96. Gahoual, R., M. Biacchi, J. Chicher, L. Kuhn, P. Hammann, A. Beck, E. Leize-Wagner, and Y.N. François. *Monoclonal antibodies biosimilarity assessment using transient isotachophoresis capillary zone electrophoresis-tandem mass spectrometry*. in *MAbs*. 2014. Taylor & Francis.
97. Klein, J., T. Papadopoulos, H. Mischak, and W. Mullen, *Comparison of CE-MS/MS and LC-MS/MS sequencing demonstrates significant complementarity in natural peptide identification in human urine.* Electrophoresis, 2014. **35**(7): p. 1060-1064.
98. Kočová Vlčková, H., V. Pilařová, P. Svobodová, J. Plíšek, F. Švec, and L. Nováková, *Current state of bioanalytical chromatography in clinical analysis.* Analyst, 2018. **143**(6): p. 1305-1325.
99. Salvagno, G.L., E. Danese, and G. Lippi, *Preanalytical variables for liquid chromatography-mass spectrometry (LC-MS) analysis of human blood specimens.* Clinical biochemistry, 2017. **50**(10-11): p. 582-586.
100. Howard, G. and A.J. Martin, *The separation of the C12-C18 fatty acids by reversed-phase partition chromatography.* Biochemical Journal, 1950. **46**(5): p. 532.
101. Alpert, A.J., *Hydrophilic-interaction chromatography for the separation of peptides, nucleic acids and other polar compounds.* Journal of chromatography A, 1990. **499**: p. 177-196.

102. Hemström, P. and K. Irgum, *Hydrophilic interaction chromatography.* Journal of Separation Science, 2006. **29**(12): p. 1784-1821.
103. Wu, A.H.B. and D. French, *Implementation of liquid chromatography/mass spectrometry into the clinical laboratory.* Clinica Chimica Acta, 2013. **420**: p. 4-10.
104. Sandra, K. and P. Sandra, *Lipidomics from an analytical perspective.* Curr Opin Chem Biol, 2013. **17**(5): p. 847-53.
105. Gika, H.G., G.A. Theodoridis, R.S. Plumb, and I.D. Wilson, *Current practice of liquid chromatography-mass spectrometry in metabolomics and metabonomics.* J Pharm Biomed Anal, 2014. **87**: p. 12-25.
106. Molnár, I. and C. Horváth, *Reverse-phase chromatography of polar biological substances: separation of catechol compounds by high-performance liquid chromatography.* Clinical Chemistry, 1976. **22**(9): p. 1497-1502.
107. Marshall, D.B., C.L. Cole, and A.D. Norman, *The Use of Trimethylsilylphosphine as an End-Capping Reagent in RP-HPLC.* Journal of Chromatographic Science, 1987. **25**(6): p. 262-266.
108. Barth, H.G., *Chromatography Fundamentals, Part IV: Origin of Theoretical Plates—Fractional Distillation and Countercurrent Distribution Extractions.* LCGC North America, 2018. **36**(8): p. 532-535.
109. Shaimadzu. [cited 2019 20/05/2019]; Available from: https://www.shimadzu.com/an/hplc/support/lib/lctalk/resol-1.html.
110. Scott, R.P.W., *Gas Chromatography - Tandem Techniques*. Chromatography Online.
111. Mellon, F.A., *MASS SPECTROMETRY | Principles and Instrumentation*, in *Encyclopedia of Food Sciences and Nutrition (Second Edition)*, B. Caballero, Editor. 2003, Academic Press: Oxford. p. 3739-3749.
112. Van Bramer, S.E., *An introduction to mass spectrometry.* Lecture Notes, 1997.
113. Demartini, D.R., *A short overview of the components in mass spectrometry instrumentation for proteomics analyses*, in *Tandem mass spectrometry-molecular characterization*. 2013, IntechOpen.
114. Taylor, G.I., *Disintegration of water drops in an electric field.* Proceedings of the Royal Society of London. Series A. Mathematical and Physical Sciences, 1964. **280**(1382): p. 383-397.
115. Wilm, M., *Principles of electrospray ionization.* Molecular & cellular proteomics, 2011. **10**(7): p. M111. 009407.
116. Banerjee, S. and S. Mazumdar, *Electrospray ionization mass spectrometry: a technique to access the information beyond the molecular weight of the analyte.* International journal of analytical chemistry, 2012. **2012**.
117. Gabelica, V. and E. De Pauw, *Internal energy and fragmentation of ions produced in electrospray sources.* Mass Spectrom Rev, 2005. **24**(4): p. 566-87.
118. Biocompare. *High Resolution Mass Spectrometry*. 2007 [cited 2019 20/05/2019]; Available from: https://www.biocompare.com/Editorial-Articles/41598-High-Resolution-Mass-Spectrometry/.
119. Longfei Lin, H.L., Miao Zhang, Xiaoxv Dong, Xingbin Yin, Changhai Qub and Jian Ni *Types, principle, and characteristics of tandem high-resolution mass spectrometry and its applications.* RSC Advances, 2015(130): p. 107192-108066.
120. Douglas, D. and J.B. French, *Collisional focusing effects in radio frequency quadrupoles.* Journal of the American Society for Mass Spectrometry, 1992. **3**(4): p. 398-408.
121. Krutchinsky, A., I. Chernushevich, V. Spicer, W. Ens, and K. Standing, *Collisional damping interface for an electrospray ionization time-of-flight mass spectrometer.* Journal of the American Society for Mass Spectrometry, 1998. **9**(6): p. 569-579.

122. Chernushevich, I.V., A.V. Loboda, and B.A. Thomson, *An introduction to quadrupole–time-of-flight mass spectrometry.* Journal of mass spectrometry, 2001. **36**(8): p. 849-865.
123. *TripleTOF-6600-Flyer*. [cited 2019 22/05/2019]; Available from: https://sciex.com/Documents/brochures/TripleTOF-6600-Flyer.pdf.
124. Marshall, A.G. and C.L. Hendrickson, *High-resolution mass spectrometers.* Annu Rev Anal Chem (Palo Alto Calif), 2008. **1**: p. 579-99.
125. Mamyrin, B., V. Karataev, D. Shmikk, and V. Zagulin, *The mass-reflectron, a new nonmagnetic time-of-flight mass spectrometer with high resolution.* Zh. Eksp. Teor. Fiz, 1973. **64**: p. 82-89.
126. Cotter, R.J., *The New Time-of-Flight Mass Spectrometry.* Analytical chemistry, 1999. **71**(13): p. 445A-451A.
127. Quirino, J.P. and S. Terabe, *On-Line Concentration of Neutral Analytes for Micellar Electrokinetic Chromatography. 5. Field-Enhanced Sample Injection with Reverse Migrating Micelles.* Analytical Chemistry, 1998. **70**(9): p. 1893-1901.
128. Quirino, J.P. and S. Terabe, *On-Line Concentration of Neutral Analytes for Micellar Electrokinetic Chromatography. 3. Stacking with Reverse Migrating Micelles.* Analytical Chemistry, 1998. **70**(1): p. 149-157.
129. Ptolemy, A.S. and P. Britz-McKibbin, *New advances in on-line sample preconcentration by capillary electrophoresis using dynamic pH junction.* Analyst, 2008. **133**(12): p. 1643-1648.
130. Jia, Z., T. Ramstad, and M. Zhong, *Medium-throughput pKa screening of pharmaceuticals by pressure-assisted capillary electrophoresis.* ELECTROPHORESIS, 2001. **22**(6): p. 1112-1118.
131. Dose, E.V. and G. Guiochon, *Problems of quantitative injection in capillary zone electrophoresis.* Analytical Chemistry, 1992. **64**(2): p. 123-128.
132. Lee, T.T. and E.S. Yeung, *Compensating for instrumental and sampling biases accompanying electrokinetic injection in capillary zone electrophoresis.* Analytical Chemistry, 1992. **64**(11): p. 1226-1231.
133. Ramautar, R., J.-M. Busnel, A.M. Deelder, and O.A. Mayboroda, *Enhancing the Coverage of the Urinary Metabolome by Sheathless Capillary Electrophoresis-Mass Spectrometry.* Analytical Chemistry, 2012. **84**(2): p. 885-892.
134. Haselberg, R., G.J. de Jong, and G.W. Somsen, *Low-Flow Sheathless Capillary Electrophoresis–Mass Spectrometry for Sensitive Glycoform Profiling of Intact Pharmaceutical Proteins.* Analytical Chemistry, 2013. **85**(4): p. 2289-2296.
135. Zhang, N.R., S. Yu, P. Tiller, S. Yeh, E. Mahan, and W.B. Emary, *Quantitation of small molecules using high-resolution accurate mass spectrometers – a different approach for analysis of biological samples.* Rapid Communications in Mass Spectrometry, 2009. **23**(7): p. 1085-1094.
136. Xia, Y.-Q., J. Lau, T. Olah, and M. Jemal, *Targeted quantitative bioanalysis in plasma using liquid chromatography/high-resolution accurate mass spectrometry: an evaluation of global selectivity as a function of mass resolving power and extraction window, with comparison of centroid and profile modes.* Rapid Communications in Mass Spectrometry, 2011. **25**(19): p. 2863-2878.
137. Jenkins, R., J.X. Duggan, A.-F. Aubry, J. Zeng, J.W. Lee, L. Cojocaru, D. Dufield, F. Garofolo, S. Kaur, G.A. Schultz, K. Xu, Z. Yang, J. Yu, Y.J. Zhang, and F. Vazvaei, *Recommendations for Validation of LC-MS/MS Bioanalytical Methods for Protein Biotherapeutics.* The AAPS Journal, 2015. **17**(1): p. 1-16.

138. Duggan, J.X., F. Vazvaei, and R. Jenkins, *Bioanalytical method validation considerations for LC–MS/MS assays of therapeutic proteins.* Bioanalysis, 2015. **7**(11): p. 1389-1395.